2010-09-09

Mitochondrial Dysfunction and AKT Isoform-Specific Regulation in 3T3-L1 Adipocytes: A Dissertation

Xiarong Shi

University of Massachusetts Medical School

MITOCHONDRIAL DYSFUNCTION AND AKT ISOFORM-SPECIFIC REGULATION IN 3T3-L1 ADIPOCYTES

A Dissertation Presented

By

XIARONG SHI

Submitted to the Faculty of the

University of Massachusetts Graduate School of Biomedical Sciences, Worcester

in partial fulfillment of the requirements for the degree of

DOCTOR OF PHILOSOPHY

September 9, 2010

INTERDISCIPLINARY GRADUATE PROGRAM

MITOCHONDRIAL DYSFUNCTION AND AKT ISOFORM-SPECIFIC REGULATION IN 3T3-L1 ADIPOCYTES

A Dissertation Presented By

Xiarong Shi

The signatures of the Dissertation Defense Committee signifies completion and approval as to style and content of the Dissertation

_____

Silvia Corvera, M.D., Thesis Advisor

_____

Mary-Elizabeth Patti, M.D., Member of Committee

_____

William Royer, Ph.D., Member of Committee

_____

Fumihiko Urano, M.D., Ph.D., Member of Committee

_____

Yong-Xu Wang, Ph.D., Member of Committee

The signature of the Chair of the Committee signifies that the written dissertation meets the requirements of the Dissertation Committee

_____

Michael Czech, Ph.D., Chair of Committee

The signature of the Dean of the Graduate School of Biomedical Sciences signifies that the student has met all graduation requirements of the School

_____

Anthony Carruthers, Ph.D.
Dean of the Graduate School of Biomedical Sciences

Interdisciplinary Graduate Program
September 9, 2010

ACKNOWLEDGEMENTS

First and foremost, I would like to sincerely thank my mentor, Dr. Silvia Corvera, for her years of guidance and support during my graduate training in her lab. Her insightful advice and incredible intelligence always inspired and guided me through difficult times. She has taught me to become a scientist who can work both independently and collaboratively, which will be a priceless treasure throughout my whole life.

I would like to thank my thesis research committee, Drs., Michael Czech, Yong-Xu Wang, and Heidi Tissenbaum. They have always been supportive and encouraging even during the hardest times. Their insightful advice has kept me on the right path. I would also like to thank Drs., Fumihiko Urano, William Royer and Mary-Elizabeth Patti, for their willingness and dedication to evaluate my work as members of my Dissertation Examination Committee.

I would like to thank the past and present members of the Corvera laboratory, Dr. Akira Hayakawa, Dr. James Young, Dr. Helena Walz, Dr. Deborah Leonard, Dr. Olga Gealikman, Dr. Catherine Bue, Dr. Anil Chawla, and Alison Burkart, My Chouinard, Deanna Navaroli and Khanh-Van Tran. They have been wonderful friends and great colleagues, who have helped me in many ways. Without them, I could not have had such a wonderful time and successfully finished my graduate study and thesis.

I also would like to thank many other laboratories including the Czech lab, Lambright lab, Xu lab, Ip lab, Richter lab, Mello lab, and the Bio-imaging Group, in the Program in Molecular Medicine at University of Massachusetts Medical School, for

sharing their equipment and expertise. I am very grateful that I have worked in such a collaborative and friendly environment.

I couldn’t be more thankful to my parents, Huichu Shi, and Zi’e Shen, for their unconditional love and support through every step of my life. I regret that I could not be around when they went through the hardest times.

I really want to thank my beautiful wife, Fang Chen, for her love, patience and understanding through these years. Without her support, I could not have gone so far.

Last but not least, I would like to thank all the friends in the UMMS community, who have supported and encouraged me during all these years and shared great times with me.

ABSTRACT

Excess food consumption and/or lack of exercise have dramatically contributed to the prevalence of overweight (BMI≥25) and obesity (BMI≥30) in modern society. The obesity epidemic has been linked to the rise in type 2 diabetes. In recent years, evidence has pointed to a close association between mitochondrial dysfunction in white adipose tissue (WAT) and insulin resistance, a key feature of type 2 diabetes. In order to dissect the cause and effect relationship between WAT mitochondrial dysfunction and insulin resistance, we established an *in vitro* cell line system to investigate this issue. We artificially introduced mitochondrial dysfunction in 3T3-L1 adipocytes by depleting the mitochondrial transcription factor A (Tfam) during adipogenesis, without changing the overall adipocyte differentiation program. We found that these Tfam-depleted 3T3-L1 adipocytes showed symptoms of insulin resistance, evidenced by impaired insulin-stimulated GLUT4 translocation and glucose uptake. This result suggested that mitochondrial dysfunction could be a primary contributor to insulin resistance in fat tissue. However, the exact mechanism underlying this finding remains unclear.

As part of a comprehensive understanding of insulin signaling in fat cells, we also investigated the involvement of the endosomal protein WDFY2 in the regulation of Akt isoform-specific effect on glucose uptake. In 3T3-L1 adipocytes, both Akt1 and Akt2 isoforms are expressed, but only Akt2 plays an indispensible role in insulin-stimulated GLUT4 translocation and glucose uptake. Previous studies implied that endosomal proteins may take a part in determining Akt substrate specificity. Here we found that WDFY2 preferentially co-localized with Akt2 and that knockdown of WDFY2 inhibited

insulin-stimulated glucose uptake in 3T3-L1 adipocytes, suggesting that endosomes are involved in this regulation. The effect of WDFY2 knockdown on insulin-stimulated glucose uptake worked through the down-regulation of Akt2, but not Akt1, protein level. We concluded that, endosomal protein WDFY2, by preferentially interacting with Akt2, regulates insulin signaling in glucose uptake in 3T3-L1 adipocytes. Our findings may help to develop specific therapeutic interventions for treatment of insulin resistance and type 2 diabetes.

TABLE OF CONTENTS

LIST OF FIGURES

LIST OF TABLES

COPYRIGHT NOTICE

Parts of this dissertation have appeared in separate publications:

Shi X, Burkart A, Nicoloro SM, Czech MP, Straubhaar J, Corvera S. Paradoxical effect of mitochondrial respiratory chain impairment on insulin signaling and glucose transport in adipose cells. J Biol Chem. 2008;283(45):30658-67

Walz HA[*], **Shi X**[*], Chouinard M, Bue CA, Navaroli DM, Hayakawa A, et al. Isoform-specific regulation of Akt signaling by the endosomal protein WDFY2. J Biol Chem. 2010;285(19):14101-8 (*, These authors contributed equally)

LIST OF ABBREVIATIONS

4E-BP1	eIF4E binding protein 1
5-FOA	5-fluoroorotic acid
Acp6	acid phosphatase 6
AIF	apoptosis inducing factor
Agk	acylglycerol kinase
AGPAT	1-cylglycerol-3-phosphate O-acyltransferase
AMPK	AMP-activated protein kinase
APPL	adaptor protein containing PH-domain, PTB domain, Leucine zipper motif
APS	adaptor protein containing a pleckstrin homology and SH2 domain
aP2	adipocytes P2
AS160	Akt substrate 160 kDa
Atp6	ATP synthase F0 subunit 6
BAT	brown adipose tissue
BMI	body mass index
C/EBP	CCAAT enhancer binding proteins
CAP	c-Cbl associating protein
c-Cbl	c-Casitas b-lineage lymphom
Cox1	cytochrome c oxidase subunit I
Cytb	cytochrome b
DGAT	diacylglycerol O-acyltransferase
EEA1	early endosome antigen 1
eEF	eukaryotic elongation factors
eEF1A	eukaryotic elongation factor 1 alpha
eEF2K	eukaryotic elongation factor 2 kinase
eIF	eukaryotic initiation factor
ERK	extracellular regulated MAP kinase
ETC	electron transport chain
FCCP	carbonyl cyanide-4-(trifluoromethoxy)-phenylhydrazone
FDG-PET	fluorodeoxyglucose positron-emission tomography
FOXO1	forkhead box O1
FYVE	Fab1, YOTB, Vac1, EEA1
GAP	GTPase-activating protein
GEF	guanine nucleotide exchange factor
GLUT4	glucose transporter 4
GPAT	glycerol-3-phosphate acyltransferase

GSK-3	glycogen synthase kinase 3
GST	glutathione S-transferase
HA	hemagglutinin
HFD	high fat diet
IGF-1	insulin-like growth factor 1
IRS	insulin receptor substrate
KEGG	Kyoto Encyclopedia of Genes and Genomes
MCP-1	monocyte chemoattractant protein 1
MEF	mouse embryonic fibroblast
MOI	multiplicity of infection
mtDNA	mitochondrial DNA
mTORC	mammalian target of rapamycin complex
Nd1	NADH dehydrogenase subunit 1
OXPHOS	oxidative phosphorylation
PAI-1	plasminogen activator inhibitor-1
PAS	phospho-Akt substrate
PAS50	phospho-Akt Substrate 50 kDa
PDK	3-phosphoinositide-dependent protein kinase
PEP	phosphoenolpyruvate
PEPCK	phosphoenolpyruvate carboxykinase
PGC-1α	peroxisome proliferator-activated receptor gamma co-activator -1αlpha
PI-3K	phosphatidylinositol 3-kinase
PI3P	Phosphatidylinositol 3-phosphate
PIKfyve	phosphoinositide kinase, FYVE finger containing
PIP_3	phosphatidylinositol (3,4,5)-trisphosphate
PKC	protein kinase C
PPARγ	peroxisome proliferator-activated receptor gamma
PRDM16	PRD1-BF1-RIZ1 homologous domain containing 16
PTB	phosphotyrosine binding domains
PTEN	phosphatase and tensin homolog
RBP4	retinol binding protein 4
RNAi	RNA interfering
ROS	reactive oxygen species
rpS6	ribosomal protein S6
S6K	ribosomal protein S6 kinase
TBC1D1	TBC1 domain family member 1
TCA	tricarboxylic acid
Tfam	transcription factor A, mitochondrial

TFB1M	transcription factor B1, mitochondrial
TFB2M	transcription factor B2, mitochondrial
TIRF	total internal reflection fluorescence
TNFα	tumor necrosis factor alpha
TSC2	tuberous sclerosis complex 2
UCP-1	uncoupling protein-1
UTR	untranslated region
WAT	white adipose tissue
WDFY2	WD40 and FYVE domain containing protein 2
Zfp423	zinc finger protein 423

CHAPTER I

INTRODUCTION

With the plentiful food supply of modern society, over eating and/or lack of exercise have emerged as major causes for developing metabolic diseases including obesity and type 2 diabetes. In 2007-2008, a study conducted by the Centers for Disease Control and Prevention (CDC) estimated that 68% of the adults in the US are overweight based on the criterion of body mass index (BMI) ≥25, and 33.8% are obese with the BMI ≥ 30 [BMI, the value of one's body weight (kg) divided by the square of his/her height (m)] (1). Nearly 24 million Americans or 8% of the US population are diabetic, among which 90%-95% have type 2 diabetes, often associated with obesity. The cost of diagnosed diabetes in the United States reached approximately $174 billion in 2007 as estimated by the CDC (2).

The occurrence of obesity is largely attributed to the imbalance of high energy intake (food consumption) and low energy expenditure (energy required for life functions). As a response to this imbalance, fat tissue expands in cell size and number to store excessive energy as triglycerides, resulting in adiposity. There is a high correlation between excessive adiposity and insulin resistance, type 2 diabetes, and cardiovascular disease (3). To better understand the pathology of obesity and its associated diseases, more research is being conducted on the biology of adipose tissue.

Mitochondrial Dysfunction: Thinking inside the WAT

Adipose Tissue

Adipose tissue, consisting of white adipose tissue (WAT) and brown adipose tissue (BAT) in mammals, has been recognized as not only an energy-storage and expenditure buffer system but also an endocrine organ that secretes adipokines that regulate whole body energy homeostasis (4). WAT stores excess energy in the form of triglycerides during a fed state and serves as a source of energy in the form of fatty acids during starvation. BAT is highly packed with mitochondria and is specialized to produce heat by burning fat without creating ATP, thereby dissipating energy through a process known as non-shivering thermogenesis (5). Until recently, it was believed that BAT was nonexistent in adult humans (6). However, new technology using fluorodeoxyglucose positron-emission tomography (FDG-PET) revealed that BAT actually exists in several different areas in the human body such as the supraclavicular and the neck regions (7-8). As a result of these studies, the biology of BAT is now being more interested.

On the other hand, considerable effort has been put into the study of adipogenesis and the endocrine function of WAT in the past two decades. The transcriptional components of adipogenesis have been intensely investigated, with the peroxisome proliferator-activated receptor γ (PPARγ) and CCAAT enhancer binding proteins (C/EBP) in the center of its regulatory circuit (9). More recently, the discovery of the zinc finger protein 423 (Zfp423) (10) and PRD1-BF1-RIZ1 homologous domain containing 16 (PRDM16) (11) has revealed even more details of the shared and divergent aspects of the transcriptional control of BAT and WAT. The discovery of the BAT in human adults also

raises the interests in the origins of BAT and WAT *in vivo*, as well as the potential conversion of WAT into BAT. Morphologically, WAT has unilocular fat droplets and white-like color while BAT has multilocular fat droplets and a more brown-like color, a result of numerous densely-packed mitochondria. BAT is also characterized by the expression of uncoupling protein-1 (UCP-1), which is not found in WAT. Studies showed that it is possible to confer a BAT-like phenotype to WAT by increasing the expression of UCP-1 or by stimulating mitochondrial biogenesis through PPARγ co-activator 1α (PGC-1α) (12-13). Additionally, it was reported that the BAT can arise from WAT by cold exposure (14). Some have proposed the concept that these two tissues are intermingled together and can convert to each other (15). If the transdifferentiation from white to brown adipocytes naturally occurs *in vivo* under certain conditions such as cold exposure, warm exposure and dietary change, the manipulation of the conversion of WAT to BAT would be applicably feasible and therapeutically beneficial. However, the mechanism of transdifferentiation between WAT and BAT needs to be carefully determined.

Mitochondria

Mitochondria are intracellular membrane-enclosed organelles found in most eukaryotic cells. They are considered the “powerhouse” of a cell, providing fuel in the form of ATP through oxidative phosphorylation (OXPHOS). The number of mitochondria in a cell varies by tissue and organism, as well as by different physiological conditions, including obesity, weight loss, aging, treatment with anti-diabetic agents, and in response to genetic alterations in insulin receptor number (16-27). In general,

mitochondria are usually concentrated in energy demanding tissues like heart and muscle. Classic mitochondrial biology describes the mitochondria as dispersed, rod-shape organelles; however, mitochondria are highly dynamic and form an interconnected reticulum-like network in live cells. They undergo fission and fusion to allow communication and exchange of the internal contents, including mitochondrial DNA (mtDNA) and proteins (28). The proper dynamics of mitochondria are physiologically important for cell function; abnormal mitochondrial dynamics are associated with a wide range of diseases such as type 2 diabetes, vascular proliferative disorder and neurodegenerative diseases (29).

Mitochondria maintain their own genome, a 16.5 Kb circular mitochondrial DNA molecule which encodes only thirteen proteins. More than a thousand proteins needed for mitochondrial functions in energy metabolism and other pathways are encoded by the nucleus. The thirteen mtDNA-encoded proteins are subunits for the electron transport chain (ETC) complex I, III, VI and ATP synthase embedded in the mitochondrial inner membrane, highlighting the importance of mtDNA in OXPHOS function. The transcription of mtDNA and the nuclear genome is highly regulated to support normal mitochondrial functions (30). While the transcription of mtDNA occurs in the mitochondrial reticulum, all the proteins needed for the transcription machinery are encoded by the nucleus. These proteins are translated in the cytoplasm and are transported to the mitochondria to fulfill their function. The most characterized transcription factor involved in mtDNA transcription is transcription factor A, mitochondrial (Tfam). This nuclear encoded, mitochondrial specific factor is not only

crucial for the transcription of mtDNA, but also necessary for the maintenance of mtDNA integrity (31). Other components like transcription factor B1, mitochondrial (TFB1M) and transcription factor B2, mitochondrial (TFB2M) work together with Tfam and mitochondrial RNA polymerase to transcribe mtDNA. Perturbation of Tfam causes both impaired mtDNA replication and transcription, resulting in a net decrease in mtDNA-encoded transcripts for respiratory complexes (32). The abnormality of Tfam has been reported to be associated with some diseases such as infantile mitochondrial myopathy (33), age-related type 2 diabetes (34), Down's syndrome (35), Alzheimer's disease and Parkinson's disease (36).

Besides generating ATP, mitochondria are involved in other cellular functions including the generation of reactive oxygen species (ROS), calcium signaling, and apoptosis. Mitochondrial dysfunction has been linked to a spectrum of human diseases in multiple tissues like heart, brain, muscle and pancreas (37). In fat tissue, it is a well established notion that the high density of mitochondria in BAT supports its energy expenditure function. However the importance of mitochondrial function in WAT remains largely undetermined, partly due to the historic neglect of their abundance in this seemingly inactive tissue. With the recent discoveries that mitochondrial biogenesis is inherent during *in vitro* 3T3-L1 adipogenesis and in WAT from *ob/ob* mice or diabetic patients treated with insulin sensitizer (22, 25-26), the pathological relevance of mitochondria dysfunction in WAT has become more interesting.

The following section of the introduction focuses on two aspects of white adipose tissue activity: 1) fat as an energy buffering system; and 2) fat as an endocrine organ. I

will discuss the role of mitochondrial function in these two adipose tissue functionalities and try to establish the hypothesis that mitochondria in white adipose tissue play a central role in regulating WAT function.

Mitochondria in WAT Function

WAT as an Energy Buffering System

Depending on whole body energy balance, WAT can either store fatty acids as triglycerides or release them from triglycerides to supply energy for other tissues as needed. Specifically, under fed conditions, fatty acids are esterified to form triglycerides by a process known as lipogenesis while under starved conditions, fatty acids are released from triglycerides during a process known as lipolysis. These two opposite processes constitute an important role of WAT as an energy buffering system. Obesity is the consequence of an imbalance of energy homeostasis, with triglycerides storage in WAT exceeding their dissipation.

It is now known that white adipocytes are enriched with mitochondria, as observed during ***in vitro*** adipogenesis and in animals treated with Rosiglitazone (25-26), a PPARγ agonist, which is a master regulator of adipogenesis. Although the mitochondrial density in WAT is still relatively low compared to BAT, it is much higher than in preadipocytes. We found that differentiated 3T3-L1 adipocytes and WAT have 2-5-fold more mtDNA compared to preadipocytes (Figure 2-1, ***B*** and data not shown). Since WAT is not an energetically demanding tissue compared to muscle and brain, the high density of mitochondria might function in the regulation of whole body lipid metabolism rather than in the generation of ATP. In comparison, mitochondria in BAT

are more specialized for energy dissipation in the form of heat from the futile electron transport chain in the presence of uncoupling protein UCP-1. The idea that mitochondria in WAT have a function distinct from the mitochondria in BAT is supported by the discovery that the proteomic compositions of the mitochondria from these two tissues are substantially different (38). Specifically, WAT mitochondria preferentially express proteins supporting anabolic functions such as glycerolipid and fatty acid biosynthesis, while BAT mitochondria are characterized by proteins involved in oxidative phosphorylation, fatty acid metabolism and citrate cycle, which is more similar to muscle (38).

Although lipogenesis is traditionally thought to occur exclusively in the cytoplasm, there is a definite requirement for mitochondria during lipogenesis (39). In fact, a strong association between mitochondrial DNA copy number and lipogenesis in human white adipocytes exists (17). One of the mitochondrial functions in lipogenesis is to provide the triglyceride building block glycerol 3-phosphate through a pathway defined as glyceroneogenesis (40). In rat adipose tissue glyceroneogenesis accounts for approximately 90% of the total triglyceride backbone. This holds true even when the rats are starved for 48 hours (41). The tricarboxylic acid cycle (TCA cycle) occurs in the mitochondrial intermembrane space, where the metabolic intermediate oxaloacetate is produced. In the process of glyceroneogenesis, the cytosolic phosphoenolpyruvate carboxykinase (PEPCK-C) catalyzes the conversion of oxaloacetate to phosphoenolpyruvate (PEP), which is a critical step for both gluconeogenesis and glyceroneogenesis. PEP is then converted to glycerol 3-phosphate through several

reversible reactions in the glycolysis pathway. Mitochondria contain a different version of PEPCK, PEPCK-M. Although the function of PEPCK-M is less defined, it is reasonable to speculate that it may have a similar metabolic role as PEPCK-C does in gluconeogenesis and glyceroneogenesis.

Supporting the idea that mitochondria are involved in lipogenesis, the enzymes that directly catalyze the formation of triglycerides were found to be localized or associated with the mitochondrial outer membrane. These include glycerol-3-phosphate acyltransferase 1 and 2 (GPAT1, GPAT2) and diacylglycerol O-acyltransferase 2 (DGAT2) (42-43). Interestingly, GPAT1, 1-acylglycerol-3-phosphate O-acyltransferase 2 and 3 (AGPAT2 and AGPAT3), diacylglycerol O-acyltransferase 1 (DGAT1), acylglycerol kinase (Agk), and acid phosphatase 6 (Acp6) are specifically enriched in the mitochondria from WAT but not BAT (38). This underscores the importance of mitochondrial function in WAT lipogenesis. On the other hand, mitochondria may participate in the process of *de novo* synthesis of fatty acids, the other building block of triglycerides. It has been reported that the impaired mitochondrial function due to oxidative phosphorylation uncoupling decreases the *de novo* fatty acid synthesis (44). Taken together, these studies suggest a strong relationship between mitochondria function and lipogenesis in WAT.

The reverse process of lipogenesis is lipolysis, which breaks down the triglycerides into fatty acids and glycerol. The mitochondrial role in WAT lipolysis remains largely unknown, but released free fatty acids from lipolysis are known to be oxidized in mitochondria through the β-oxidation pathway. This could be an important

source of ATP when the energy demand increases and glucose is scarce, for instance, under the conditions of fasting or extended exercise. Maintaining a stable ATP supply in WAT may be critical for adipocytes to undergo active lipolysis and provide fatty acids for other tissues. A drop in intracellular ATP levels by mitochondrial ETC uncouplers or inhibitors can decrease lipolysis induced by the adrenal hormone catecholamines (45). When activated, the AMP-activated protein kinase (AMPK) that senses the energy state determined by mitochondrial ATP production can decrease lipolysis (46). Taken together, these data support a mitochondrial function in WAT lipolysis.

WAT as an Endocrine Organ

Aside from its ability to store and mobilize energy, WAT has been recognized as an important endocrine organ in recent years. It has been found to secrete an array of hormones and cytokines called adipokines, which participate in a variety of signaling pathways regulating whole body energy homeostasis (4, 47). The list of adipokines has grown rapidly and includes leptin, adiponectin, resistin, serpin, lipocalin-2, PAI-1, RBP4, Zn α-2 glycoprotein, vaspin, visfatin, omentin, apelin, chemerin, TNFα, IL-6 and MCP-1 (48). Mitochondrial function may play a role in at least three aspects of the regulation of adipokine production in WAT: 1) the expression level; 2) the post-translational modification and folding; and 3) secretion. For example, it has been reported that adiponectin synthesis is induced by rosiglitazone treatment through mitochondrial biogenesis (49). Adiponectin exists in plasma as a multimer and requires extensive folding using ATP supplied by the mitochondria (50). High glucose increases adiponectin production and secretion in 3T3-L1 adipocytes while it decreases resistin production and

secretion through the overproduction of reactive oxygen species in mitochondria (51). Interestingly, adipokines have also been shown to target mitochondria in skeletal muscle. For example, apelin can induce skeletal muscle mitochondrial content (52) and adiponectin regulates mitochondrial bioenergetics (53).

Mitochondrial Dysfunction in WAT and Diseases

Defects in mitochondrial oxidative phosphorylation have been studied in many animal models. These include defects of nuclear-encoded components of the OXPHOS complexes, and factors involved in mtDNA integrity and transcription (54-55). Due to the embryonic lethality of such defects, most mitochondrial dysfunction transgenic models are tissue-specific; and the heart and skeletal muscle are the most targeted and studied tissues because of their high demand for energy from oxidative phosphorylation (54-55). However, due to the lack of WAT-specific knockout models, it is difficult to assess the pathological contribution of WAT mitochondrial dysfunction in diseases. Meanwhile, evidence shows that the adipose mitochondrial dysfunction is associated with obesity and diabetes (19-20, 25), but the underlying mechanisms are not yet understood. To directly test the cause and effect relationship between adipose mitochondrial dysfunction and diseases, perturbation of mitochondrial function in WAT needs to be established.

At the *in vitro* level, mitochondrial dysfunction has been studied in 3T3-L1 white adipocytes by depleting Tfam, a crucial factor for mtDNA integrity and transcription (Chapter II). The depletion of Tfam causes decreased mtDNA copy number as well as decreased mtDNA-encoded transcripts, resulting in blunted OXPHOS function in adipocytes. The consequence of this manipulation is decreased insulin-stimulated glucose

uptake, a hallmark of insulin resistance in adipose tissue (56). The mechanism of Tfam-depletion induced glucose uptake impairment is not fully understood; and it appears that insulin activation of the Akt pathway is not inhibited by Tfam-depletion (56). It should be noted that the Tfam knockdown is performed during adipogenesis; therefore it might cause a general phenotypic change in those 3T3-L1 adipocytes. However, several functional assays and whole genome expression profile analysis do not support such a hypothesis. For example, fat accumulation and adiponectin secretion are not affected in Tfam-depleted adipocytes (Figure 2-7). Less than 0.2% of total gene expression is up or down-regulated more than 50% and almost all the genes involved in mitochondrial OXPHOS and TCA cycle are not affected by Tfam-depletion (Table 4-1). Taken together, mitochondrial dysfunction induced by Tfam-depletion has a causative effect on insulin resistance in 3T3-L1 adipocytes without changing general adipogenesis.

Although a direct WAT-specific *in vivo* mitochondrial dysfunction model is not available, many studies have shown a clear correlation between WAT mitochondrial dysfunction and obesity or type 2 diabetes (19-20, 25). In fact, the mitochondrial abundance from epididymal fat of *ob/ob* mice, which are genetically predisposed for obesity and insulin resistance, is only half of that from control mice; and rosiglitazone treatment, which improves the insulin sensitivity in these *ob/ob* mice, also triggers mitochondrial biogenesis in white adipocytes (25), suggesting a positive mitochondrial role in insulin sensitivity. A systematic gene expression comparison between control and two mouse models of obesity and type 2 diabetes: *db/db* mice and high-fat diet (HFD) fed mice, shows that mitochondrial biogenesis from these mice is compromised, as revealed

by the down-regulation of genes encoding for mitochondrial ATP production, ETC uncoupling, as well as those for mitochondrial ribosome proteins, membrane translocases and heat-shock proteins (57). Pioglitazone, another insulin sensitizer, induces mitochondrial biogenesis through the activation of PGC-1α and β-oxidation in subcutaneous fat from diabetic individuals (22). The expression of PGC-1α, a master inducer of mitochondrial biogenesis, is down-regulated in adipose tissue from morbidly obese patients (58). Taken together, the abnormal mitochondrial function in WAT is highly associated with the pathophysiology of obesity and type 2 diabetes. Studies with WAT-specific mitochondrial dysfunction model will help to clarify the *in vivo* cause and effect relationship.

Insulin Signaling and Akt Regulation in Glucose Uptake

Insulin Signaling Overview

Insulin plays a central role in energy homeostasis and glucose metabolism. The general effect of insulin is to control blood glucose homeostasis. Specifically, insulin stimulates glucose uptake in muscle and adipose tissue, and stimulates anabolic processes to store glucose as glycogen in liver and muscle, and as triglycerides in adipose tissue. In addition, insulin prevents the utilization of fatty acids, inhibits lipolysis in adipose tissue and liver gluconeogenesis, a process that maintains blood glucose supply during fasting. The effects of insulin are regulated at multiple levels, from its biosynthesis, secretion from the pancreas, stimulation of target cells, to as well as downstream intracellular signal cascades. Insufficient insulin production or activity results in diabetes mellitus:

type 1 diabetes results from the failure of the pancreatic insulin production; and type 2 diabetes is characterized by the inability of normal or even higher level of insulin to stimulate target cells.

Intracellular insulin signaling is mediated by the insulin receptor (IR) located on the cell surface. The insulin receptor is a transmembrane tyrosine kinase that undergoes autophosphorylation/activation upon insulin binding. The secondary messengers, insulin receptor substrates (IRS), are then phosphorylated at specific tyrosine residues, providing docking sites for further downstream Src Homology 2 (SH2)-domain containing proteins. One such SH2-domain containing protein is phosphatidylinositol 3-kinase (PI-3K), which binds to the phosphorylated tyrosine residues of IRS and is activated near the cell surface. PI-3K catalyses the formation of phosphatidylinositol (3,4,5)-trisphosphate ($PI(3,4,5)P_3$ or PIP_3) and the later activates 3-phosphoinositide-dependent protein kinase 1(PDK1) and PDK2 (also known as mammalian target of rapamycin complex 2, mTORC2), which phosphorylate protein kinase B (or Akt) on residue Thr^{308} and Ser^{473}, respectively. In muscle and adipocytes, phosphorylated Akt facilitates glucose uptake by mobilizing glucose transporter 4 (GLUT4)-containing vesicles towards the cell membrane. The mechanism of PI-3K dependent GLUT4 translocation in adipocytes is believed to involve the activation of Akt. The establishment of a direct link between Akt kinases and GLUT4 vesicle trafficking is largely attributed to the identification of Akt substrates AS160 and TBC1D1(59).

The signaling transduction from the insulin receptor to downstream effectors is a complex network. Many intermediates lead to branched or parallel pathways, giving the

entire network more flexibility and greater complexity. For example, there are four closely related insulin receptor substrates (IRS-1, 2, 3, 4) in mice; each variant has a distinct spatial expression and substrate specificity (60). Akt not only regulates glucose uptake, but also participates in other cellular functions such as cell survival, glycogen synthesis and apoptosis (61). In addition, Akt also has multiple isoforms Akt1, Akt2 and Akt3, which have different physiological roles in development and disease (62).

Insulin Signaling in Adipocyte Glucose Uptake

In adipocytes, the most studied metabolic regulatory function of insulin is its potent stimulation of glucose uptake. Glucose uptake is mediated through a solute carrier family of proteins, the facilitated glucose transporters (GLUT). There are currently more than a dozen GLUTs identified, among which GLUT1-GLUT4 are the most characterized. GLUT1 is expressed widely in fetal tissues and enriched in adult erythrocytes and endothelial cells of the blood-brain barrier. GLUT2 is expressed in renal tubular cells and small intestinal epithelial cells, as well as in liver and pancreatic β cells. GLUT3 is mostly expressed in neurons and placenta. GLUT4 is expressed in adipose tissue and muscle, and is the transporter that is responsive to insulin stimulation (63).

The study of the mechanism of insulin-stimulated glucose uptake has mainly focused on the activation of insulin signaling transduction and the trafficking of GLUT4-containing vesicles. The PI-3K pathway plays an important role in insulin signaling and glucose uptake. The activation of PI-3K results in the accumulation of PIP_3, which recruits pleckstrin homology (PH)-domain containing proteins to the plasma membrane including the serine/threonine protein kinase Akt. Akt is activated through

phosphorylation by PDK1 and PDK2 (mTORC2) on Thr^{308} and Ser^{473} respectively and is proposed to play a vital role in insulin-stimulated glucose uptake. A variety of studies support the Akt role in glucose uptake. The dominant negative form of Akt and siRNA-directed knockdown of Akt both inhibit insulin-stimulated glucose uptake and GLUT4 translocation (64-66). Conversely, expression of a constitutively active form of Akt can mimic the insulin effect on GLUT4 translocation and glucose uptake (67-72). Finally, Akt2 knockout mice demonstrate traits of insulin resistance and type 2 diabetes (73-74).

Some studies suggest that the FYVE finger containing phosphatidylinositol 3P-5 kinase (PIKfyve) may be involved in insulin-stimulated GLUT4 translocation. PIKfyve binds to phosphatidylinositol (3)-phosphate (PI3P) and catalyses the conversion of PI3P to PI (3, 5) P_2. However the function of PIKfyve in insulin-stimulated glucose uptake is controversial. Over-expression of inactive PIKfyve or RNAi depletion of PIKfyve reduces insulin-stimulated GLUT4 translocation in 3T3-L1 adipocytes (75); but PIKfyve has also been shown to have a negative effect on GLUT4 translocation, as over-expression of a $PIKfyve^{S318A}$ mutant in 3T3-L1 adipocytes enhances insulin-stimulated GLUT4 vesicle translocation to the plasma membrane (76). It is possible that PIKfyve changes the equilibrium of phospholipids PIP_2 and PIP_3, thus influencing insulin signaling and GLUT4 translocation, but further studies are needed.

Another pathway may participate in insulin-stimulated glucose uptake is PI-3K independent, and involves the adaptor protein containing a pleckstrin homology and SH2 domain (APS), the oncoprotein c-Cbl and CAP (c-Cbl associating protein). APS facilitates the tyrosine phosphorylation of c-Cbl by the insulin receptor, and GLUT4

translocation in 3T3-L1 adipocytes (77). However, this CAP/APS/c-Cb1 pathway in insulin-stimulated glucose uptake is elusive. In 3T3-L1 adipocytes, siRNA knockdown of TC10α, a GTPase thought to mediate CAP/APS/c-Cbl pathway, causes partial inhibition of insulin-stimulated glucose uptake and GLUT4 translocation (78); however knockdown of CAP, c-Cbl, have no effect on insulin-stimulated glucose uptake (79). APS knockout mice exhibit increased insulin sensitivity and hypoinsulinaemia (80); while knockout of c-Cbl has no effect on insulin sensitivity (81).

The Role of Akt Substrates in Glucose Uptake

Akt constitutes a node downstream of PI-3K for many signaling cascades, regulating metabolism, protein synthesis, cell growth and survival, and plays an important role in insulin-stimulated glucose uptake in muscle and adipose tissue. The missing gap between insulin stimulation of Akt and GLUT4 translocation is partially filled by the identification of the Akt substrates, AS160 and TBC1D1. Kane et al. discovered AS160 in an effort to screen insulin-stimulated phospho-proteins using an antibody that recognizes phosphorylated Akt substrates in 3T3-L1 adipocytes (82). AS160, also known as TBC1D4, contains two phosphotyrosine binding domains (PTB) and a Rab GTPase-activating protein (GAP) domain. Akt phosphorylates AS160 at six of its seven potential phosphorylation sites *in vivo* (82-83), suggesting a phosphorylation regulatory mechanism. The phosphorylation defective mutant $AS160_{4P}$, when over-expressed in 3T3-L1 adipocytes, inhibits the insulin-stimulated membrane translocation of a tagged GLUT4 transporter (83). AS160 is believed to regulate GLUT4 translocation through its GAP activity on related Rab proteins, a class of small GTPases. One model

suggests that the GAP domain of AS160 facilitates the GTP hydrolysis of active GTP-bound Rabs and thereby inhibits their function in vesicle trafficking, thus retains GLUT4 in the intracellular compartment, while AS160 phosphorylation by Akt serves as a suppressor of its GAP activity. This model is supported by the various Rab components of GLUT4-containing vesicles which are critical for GLUT4 translocation. Rabs are a large family of evolutionarily conserved small GTPases that coordinate vesicle trafficking (84). In humans, more than 60 Rab members have been identified (84). Rab10 is found to be in GLUT4-containing vesicles and is a target of AS160 GAP activity; and the knockdown of Rab10 in adipocytes results in decreased GLUT4 translocation (85-86). Rab8A and Rab14 (*in vitro* targets of AS160) are found to be able to rescue the inhibition of GLUT4 translocation caused by $AS160_{4P}$ in L6 muscle cells (87). A systematic RNAi screening of the Rab family proteins in 3T3-L1 adipocytes shows that many are involved in insulin-stimulated glucose uptake, and have either a positive or negative effect. Interestingly, RNAi knockdown of many 3T3-L1 Rabs alters Akt phosphorylation by insulin stimulation (data not shown and Figure 4-1, *A*), further complicating this pathway. It is therefore important to distinguish both the direct and indirect involvement of Rabs in GLUT4 translocation.

TBC1 domain family member 1 (TBC1D1), a GAP-containing protein related to AS160, is also found to be involved in insulin-stimulated GLUT4 translocation in adipocytes (88), but its exact role is unknown. Although TBC1D1 over-expression inhibits GLUT4 translocation in adipocytes (88), the knockdown of TBC1D1 has no effect (89), suggesting that the endogenous TBC1D1 in adipocytes has no function in

insulin-stimulated GLUT4 translocation. This could result from the very low expression levels of TBC1D1 in adipocytes. A coding variant R125W in TBC1D1 is associated with the predisposition of severe obesity (90-91), suggesting a role of TBC1D1 in energy metabolism. Subsequent work showed that TBC1D1 is a substrate that can be phosphorylated by AMP-activated protein kinase (AMPK) on Ser^{237} (89, 92).This finding together with the fact that TBC1D1 is expressed highly in muscle (89, 93) underscores a pathway through which contraction-activated AMPK signaling stimulates glucose uptake in skeletal muscle (94). More recently, the different mechanism of TBC1D1 in insulin-stimulated and contraction-induced GLUT4 translocation is being revealed in more details (95-98). Studies suggest that insulin-stimulated phosphorylation of TBC1D1 is PI-3K/Akt dependent; while the contraction-induced phosphorylation of TBC1D1 is AMPK dependent (98). Insulin regulation of TBC1D1 is similar to that of AS160, where TBC1D1 phosphorylation by Akt increases GLUT4 translocation (97). While insulin only stimulates the phosphorylation of Thr^{596} on TBC1D1, contraction induces the phosphorylation of both Ser^{237} and Thr^{596} (96). Disruption of AMPK signaling abolishes both insulin and contraction-induced TBC1D1 phosphorylation (96).

Akt Isoform Specificity

By interacting with an array of different substrates, Akt fulfills various distinct functions in cells. Adding to its already versatile signaling pathways, Akt has three isoforms Akt1, Akt2 and Akt3. They all contain an N-terminal PH-domain that binds to phospholipids PIP_3 or PIP_2 and a C-terminal serine/threonine kinase domain. From Akt isoform-specific knockout mouse models, it has become clear that Akt isoforms exhibit

distinct but overlapping functions. $Akt1^{-/-}$ mice are smaller, indicating a critical role for Akt1 in cell growth (99-100); $Akt2^{-/-}$ mice exhibit a type 2 diabetes phenotype, with decreased insulin sensitivity, suggesting a role for Akt2 in the glucose homeostasis (73); and $Akt3^{-/-}$ mice have impaired brain development, suggesting a major defect in neurons (101). Interestingly, $Akt1^{-/-}Akt3^{-/-}$ or $Akt1^{-/-}Akt2^{-/-}$ double knockout mice are embryonic lethal or die after birth (102) (103), while $Akt2^{-/-}$ $Akt3^{-/-}$ double knockout mice are viable (104). This shows that despite the distinct function of the three isoforms, there is overlapping function.

Isoform-specific studies have provided more information about the diversity of Akt signaling pathways, but the mechanism of isoform specificity remains poorly understood. There could be several different models to explain or contribute to the isoform specificity. First, each isoform may have distinct intrinsic kinase activity on specific substrates; second, each isoform may have differential temporal and spatial distribution, such as tissue specific expression and intracellular compartmentalization; and third, each isoform may respond to different stimuli such as different extracellular environmental conditions, different ligands, or different membrane receptors.

One prominent example of Akt isoform specificity is Akt2 in insulin-stimulated GLUT4 translocation and glucose uptake in adipose and muscle. In these tissues, both Akt1 and Akt2 are expressed, but only Akt2 appears to be crucial for insulin-stimulated glucose uptake. The over-expression of Akt1 fails to rescue the impaired insulin-stimulated glucose uptake in Akt2-deficient adipocytes (105-106), arguing against Akt1 and Akt2 having the identical function in the same tissue. This failure of rescue could

result from Akt1 not being properly activated. However, the extent to which the Akt isoforms are activated depends on what readout is used. For example, the phosphorylation of Thr^{308} and Ser^{473} on Akt is usually considered a prerequisite for Akt activation. Based on this criterion, both Akt1 and Akt2 are activated by insulin in 3T3-L1 or primary adipocytes (106-107).

Insulin activation of Akt is facilitated by Akt translocation to the cell membrane. Preferential translocation to the cell membrane may contribute to isoform specificity in Akt function. In adipocytes, it has been observed that Akt2 is recruited to the cell membrane to a greater extent than Akt1; and the decrease in Akt2 membrane accumulation, but not activation, causes impaired GLUT4 translocation (106). Increasing the Akt1 membrane accumulation by expressing a mutant version of Akt1, $Akt1^{E17K}$ (106), or a myristoylated Akt1 (67) can confer Akt2-like signaling to Akt1, resulting in GLUT4 translocation and glucose uptake. These data suggest that the subcellular distribution, rather than the kinase activation, is important for isoform specificity in insulin-stimulated glucose uptake. Akt kinase binds to phospholipids PIP_3 or PIP_2, generated by PI-3K on the cell membrane, through its PH-domain. In fact, the PH-domain only protein PHLDA3 can compete with Akt for PIP_3 binding, therefore suppressing Akt activation and activity (108). The differences in membrane accumulation of Akt1 and Akt2 could be due to different affinities for PIP_3 or PIP_2 by their PH-domains. However, replacing the PH-domain of Akt1 with that of Akt2 failed to mimic the Akt2-like insulin-stimulated membrane accumulation (106), suggesting that the PH-domain is not the sole determinant that confers isoform specificity to Akt1 and Akt2.

In the case of GLUT4 translocation, Akt isoform specificity might also rely on preferential association with its intracellular target. Biochemical separation of cellular fractionation in adipocytes shows that Akt2, but not Akt1, is associated with GLUT4-containing vesicles after insulin stimulation (109-110). The preferential association could also occur between Akt kinase and its substrates. The most characterized Akt substrate mediating insulin signaling and GLUT4 translocation is AS160. RNAi depletion of Akt2 but not Akt1, has a strong effect on insulin-stimulated AS160 phosphorylation in adipocytes (106) and muscle (111). It appears that only Akt2 co-localizes with AS160 at the cell membrane with insulin stimulation (106). Two other proteins Myosin 5a and syntaxin interacting protein (Synip) were also reported to be important for insulin-stimulated glucose uptake, modulating GLUT4 vesicle translocation, and membrane docking and fusion, respectively. Both Myosin 5a and Synip appear to be Akt2-specific substrates (112-113). The mechanism of Akt specificity on substrate is poorly understood. One possibility is that Akt isoforms have distinct intrinsic kinase activity on specific substrates. This is supported by our own observation that HA-Akt1 has a stronger phosphorylation activity than HA-Akt2 on a GSK-3α/β peptide in an *in vitro* kinase assay (Figure A-2, *B*). However, the kinase and substrate interaction *in vivo* is subjected to additional spatial and accessibility limitation, therefore may exhibit extra levels of regulation.

Several studies provide evidence showing that the endosomes are involved in the Akt isoform and substrate specificity. Adaptor protein containing PH-domain, PTB domain, and leucine zipper motif 1 (APPL1), an endosomal protein, was reported to

physically associate with Akt2 in a complex and can be reciprocally co-immunoprecipitated (114-115). In zebrafish, Akt was found to specifically co-localize with its substrate GSK-3β but not TSC2 in APPL1-containing endosomes (116). We recently showed that Akt2, but not Akt1, co-localizes with WDFY2 (WD40 and FYVE domain containing protein 2)-containing endosomes and that RNAi depletion of WDFY2 decreases the protein level of Akt2 but not Akt1 (Chapter III). Since endosomes are highly dynamic organelles, the involvement of endosomes in the regulation of Akt isoforms brings about a new level of flexibility and complexity.

Recent studies imply that the two phosphorylation sites of Akt, Thr^{308} and Ser^{473} (numbered as for Akt1), may actually determine substrate specificity. mTORC2 was identified as the kinase that phosphorylates Akt at Ser^{473} (117). Disruption of mTORC2 ablates the phosphorylation of Ser^{473} but not Thr^{308}, and Akt phosphorylation of FOXO1/3α, but not GSK-3 or TSC2 (118-119). These data suggest that phosphorylation of Akt Ser^{473} is only required for Akt to phosphorylate certain substrates. Additionally, the levels of PTEN (phosphatase and tensin homolog**)** protein modulate Akt phosphorylation on Ser^{473}, but not on Thr^{308} (120). Functionally, the level of AKT phosphorylation on Thr^{308}, but not on Ser^{473} is associated with high-risk cytogenetics and predicts poor overall survival in acute myeloid leukaemia (121). Although it is not fully understood when or how Akt1 and Akt2 are differentially phosphorylated at Thr^{308} and/or Ser^{473}, the hypothesis that Akt1 and Akt2 acquire substrate and functional specificity through their own differential phosphorylation status of Thr^{308} and/or Ser^{473} is tempting.

Akt^{T308A} and Akt^{S473A} phospho-defective transgenic animal models will help to elucidate the distinct Akt functions determined by site-specific phosphorylation.

Protein Synthesis Regulation by Insulin

This section of introduction is to provide some background related to protein synthesis and its regulation by insulin. It helps to understand the work described in the Appendix, which does not constitute a complete result chapter.

Protein Synthesis

Protein biosynthesis begins with the transcription of DNA into an mRNA template, followed by translation of the mRNA into a protein, which can then be post-translationally modified and delivered to its appropriate intracellular locations. Translation of mRNA into protein consists of three steps: initiation, elongation and termination, all of which are subjected to regulation. In the initiation stage, the 40S small subunit of the ribosome binds to the 5' end of the mRNA with the help of other protein factors called initiation factors (IFs). The 60S large subunit of the ribosome then binds to the initiation complex. Once translation is initiated, the transfer RNA (tRNA) carries the appropriate amino acid to the site of polypeptide elongation. Another set of proteins called elongation factors (EFs) participate in this process to ensure the continuation of the amino acid addition to the nascent polypeptide chain. Once the translational machinery reaches the stop codon, the translation is stopped through a termination process, during which release factors (RFs) recognize the stop codon and facilitate the termination of translation and release of the protein from the last tRNA.

Insulin Regulation of Protein Synthesis

Insulin stimulates protein translation in cells and tissues with either a rapid or long-term effect. The rapid effect involves fast activation of existing translational

machinery while the long-term effect functions through increased protein synthesis capacity, including an increase in the number of ribosome. This insulin regulation of protein synthesis is mediated through a series of phosphorylation events downstream of PI-3K/Akt.

mTOR and Its Regulation in Protein Synthesis by Insulin

The kinase mammalian target of rapamycin (mTOR) plays an important role in insulin-stimulated protein synthesis. mTOR forms two functionally distinct complexes, mTORC1 and mTORC2, with distinct partners. mTORC1, containing Raptor, is the major complex involved in insulin-stimulated protein synthesis. mTORC2, containing Rictor, is rapamycin-insensitive and is the kinase that phosphorylates Akt on Ser^{473}. mTORC1 regulates insulin-stimulated protein synthesis through two parallel pathways. One pathway is through p70 S6K and the other is through eIF4E binding protein 1 (4E-BP1); both S6K and 4E-BP1 are direct targets of mTORC1. Phosphorylation of S6K by mTORC1 activates S6K kinase activity. The first S6K substrate to be discovered is the ribosomal protein S6 (rpS6). However the effect of rpS6 phosphorylation on protein synthesis and cell size control seems elusive (122). Mice with a phospho-defective version of rpS6 show increased protein synthesis in mouse embryonic fibroblasts (MEF) despite the fact that those MEFs are smaller (122). Since rpS6 is not the only S6K substrate involved in protein synthesis, the net effect of S6K activation by mTORC1 is not solely determined by rpS6. Among the nine known S6K substrates (123), eIF4B and eEF2K play a positive role in protein synthesis when phosphorylated by S6K. 4E-BP1 interacts with and blocks eukaryotic initiation factor 4E (eIF4E) association with eIF4G

to form initiation complexes. mTORC1, upon activation by insulin, phosphorylates 4E-BP1 and leads to its release from eIF4E, thus enhancing the formation of initiation complex and protein synthesis. It is worth noting that mTOR signaling is also activated by amino acids largely independent of PI-3K (124). Thus mTOR integrates different stimuli including growth factors, such as insulin and IGF-1, and nutrients, such as amino acids and energy to regulate protein synthesis.

The mechanism of insulin activation of mTORC1 signaling is believed to be mediated by Akt phosphorylation of the tuberous sclerosis complex (TSC) (125). The TSC is a tumor suppressor and consists of TSC1 and TSC2, which work together as a functional complex. TSC2 contains a GAP domain that acts on the small GTPase, Rheb (126). The activation of mTORC1 activity by Rheb is GTP-dependent; and the TSC2 GAP activity promotes the hydrolysis of Rheb-GTP, thus inhibiting Rheb activation of mTORC1 (127). TSC2 is a direct Akt substrate and its phosphorylation by Akt disrupts the functional TSC2/TSC1 complex, leading to the de-repression of Rheb and mTORC1 signaling (128). Thus, insulin regulates protein synthesis through modulating mTORC1 activity, linked by Akt, TSC2/TSC1 and Rheb.

Eukaryotic Initiation Factor Regulation by Insulin

Protein synthesis initiation starts with the $tRNA^{met}$ joining the ribosome at the start codon facilitated by eukaryotic initiation factor 2 (eIF2). eIF2 forms a ternary complex with GTP and $tRNA^{met}$ before joining the 40S ribosome to form a 43S preinitiation complex. During initiation, the eIF2 GTP is hydrolyzed and the GDP-bound eIF2 is then release and renewed by a GDP/GTP exchange factor, eIF2B, which is

suppressed by GSK-3 kinase (129). Insulin activates translational initiation by inhibiting GSK-3 kinase activity, which in turn dephosphorylates and activates eIF2B (129-130). GSK-3 kinase inactivation is mediated by Akt phosphorylation, elicited by insulin/PI-3K signaling activation. eIF2 is also regulated by phosphorylation. The phosphorylation of eIF2 by any one of the four mammalian eIF2 kinases impairs the GTP-eIF2 recycling and translational initiation (131).

Eukaryotic initiation factor 4B (eIF4B) lacks catalytic activity and acts as a cofactor of eukaryotic initiation factor 4A (eIF4A), which is an RNA helicase that unwinds mRNA secondary structure (132). It has been shown that S6K kinases phosphorylate eIF4B on Ser^{422} and that an alanine substitution for Ser^{422} decreases translation activity *in vivo* (133). The phosphorylation of eIF4B Ser^{422} by S6K can be induced by insulin or mitogen in a rapamycin sensitive manner (134); and this phosphorylation is required for the assembly of the translation preinitiation complex (135).

Eukaryotic Elongation Factor Regulation by Insulin

The eukaryotic protein translation elongation requires two eukaryotic elongation factors (eEF), eEF1 and eEF2. eEF1 is a macromolecule composed of two components: eEF1A and eEF1B. eEF1A, a GTPase, carries the aminoacyl-tRNA to the A site of the ribosome when in the active GTP-bound state. Upon anti-codon recognition and GTP hydrolysis, GDP-bound eEF1A is released and regenerated to the GTP-bound active form by the guanine nucleotide exchange factor (GEF), eEF1B. There are three subunits in

eEF1B, namely eEF1Bα, eEF1Bδ and eEF1Bγ. While eEF1Bα and eEF1Bδ have GEF activity, eEF1Bγ seems to only have a structural role.

eEF1 was first reported to be phosphorylated in response to phorbol ester PMA (136), a protein kinase C (PKC) activator, or directly by PKC (137); and the phosphorylation enhances the eEF1 GDP/GTP exchange activity (138). Later, it was found that insulin-stimulated phosphorylation of eEF1 enhanced its elongation activity in 3T3-L1 adipocytes, and this stimulation appeared to be mediated primarily by the multipotential S6 kinase (139). We recently found that Akt phosphorylates eEF1A on Thr^{269} and Thr^{432} *in vitro*; and these two phosphorylation sites seem to affect the stability of eEF1A (Appendix). In all cases, insulin acts as an upstream stimulus of eEF1 phosphorylation, based on its capability to activate PKC, S6K and Akt. However, regulation of protein synthesis through insulin-stimulated eEF1 phosphorylation has not been clearly established.

eEF2 is a translocase that moves the ribosome along the mRNA by three nucleotides during each protein synthesis elongation cycle. The continuation of peptide elongation is coordinated by the alternate binding of eEF1 and eEF2 to the ribosome, with eEF1 recruiting one aminoacyl-tRNA to the ribosome to form a new peptide bond, and eEF2 moving the ribosome to the next codon. Phosphorylation of eEF2 impairs its ability to bind to the ribosome and thus decreases its elongation activity (140). eEF2 is phosphorylated by the Ca^{2+}/CaM-dependent kinase eEF2K, which itself can be inhibited by phosphorylation. Insulin causes a decrease in eEF2K activity, resulting in dephosphorylation of eEF2, and an increased eEF2 activity and accelerated elongation

(141). mTOR signaling is involved in insulin-stimulated inactivation of eEF2K. This mTOR-dependent signaling phosphorylates eEF2K on at least three sites, Ser^{366}, Ser^{359} and Ser^{78} (142-144). S6K1, a direct target of mTORC1, phosphorylates eEF2K Ser^{366}(142), but the kinase(s) responsible for phosphorylation of Ser^{359} and Ser^{78} is not yet known. It is possible that insulin-activated kinases phosphorylate eEF2K on the other sites and therefore regulate eEF2 activity and translation elongation.

Rationales and Study Aims

1. WAT Mitochondrial Dysfunction and Insulin Resistance

The strong association between impaired mitochondrial function in white adipose tissue and insulin resistance in diabetes (20, 57) raises the question of whether the WAT mitochondrial dysfunction is a contributor to or just a secondary effect of insulin resistance. To answer this cause and effect question, we decided to directly introduce mitochondrial dysfunction into white adipocytes and to investigate its effect on insulin sensitivity. The mitochondrial DNA transcription factor Tfam is critical for mtDNA transcription and replication. We hypothesized that the depletion of Tfam would specifically interfere with mtDNA and its encoded gene expressions, which are key components of the electron transport chain complexes; and this manipulation would enable us to directly investigate the effect of mitochondrial dysfunction on insulin sensitivity in adipocytes.

2. Isoform-specific Regulation of Akt Signaling

The existence of three Akt isoforms and their overlapping but distinct functions in cells raises an important question of how Akt isoform specificity is achieved. In 3T3-L1 adipocytes, two isoforms of Akt, Akt1 and Akt2 are expressed, but only Akt2 plays a central role in insulin regulated glucose metabolism. Endocytic pathways are involved in modulating signal transduction (145); and endosomal protein may regulate Akt substrate specificity (116). Previously our lab has identified an endosomal protein WDFY2 in a distinct set of endosomes (146). We investigated whether WDFY2 plays a role in

determining Akt1 and Akt2 isoform specificity in glucose uptake and the insulin signaling pathway.

3. Identification of a Akt substrate and Its Implication in Protein Synthesis and Cell Growth (Appendix)

Akt plays such a pluripotent role in signal transduction that the identification of its many substrates will help to elucidate its signaling pathways controlling certain physiological functions. The availability of PAS antibody, which recognizes a phosphorylated serine or threonine in an optimal motif R*X*R*XX*p(S/T), where R represents arginine and *X* any amino acid, enables us to identify potential Akt substrates. We identified the eukaryotic elongation factor 1a (eEF1A) as a PAS recognizable phospho-protein elicited by insulin treatment in 3T3-L1 adipocytes. Akt phosphorylation of eEF1A was confirmed *in vitro* and two phosphorylation sites were determined. The exact role of the eEF1A phosphorylation in protein synthesis and cell growth needs to be determined.

CHAPTER II

PARADOXICAL EFFECT OF MITOCHONDRIAL RESPIRATORY CHAIN IMPAIRMENT ON INSULIN SIGNALING AND GLUCOSE TRANSPORT IN ADIPOSE CELLS

This chapter is in the format that it was published in the J Biol Chem. 2008;283(45):30658-67, as written by the authors, **Shi X**, Burkart A, Nicoloro SM, Czech MP, Straubhaar J and Corvera S.

Sarah Nicoloro processed the samples for Affymetrix GeneChip analysis described in this chapter. Juerg Straubhaar analyzed the GeneChip data and generated a searchable database. Alison Burkart provided 3T3-L1 preadipocytes. The fluorescence activated cell sorting (FACS) experiments were performed with assistance from the flow cytometry core facility at University of Massachusetts Medical School. Silvia Corvera and I were responsible for designing and performing all the other experiments described in this chapter.

Abstract

Adipocyte function is crucial for the control of whole body energy homeostasis. Pathway analysis of differentiating 3T3-L1 adipocytes reveals that major metabolic pathways induced during differentiation involve mitochondrial function. However, it is not clear why differentiated white adipocytes require enhanced respiratory chain activity relative to preadipocytes. To address this question, we used small interference RNA to interfere with the induction of the transcription factor Tfam, which is highly induced between days 2 and 4 of differentiation and is crucial for replication of mitochondrial DNA. Interference with Tfam resulted in cells with decreased respiratory chain capacity, reflected by decreased basal oxygen consumption, and decreased mitochondrial ATP synthesis, but no difference in many other adipocyte functions or expression levels of adipose-specific genes. However, insulin-stimulated GLUT4 translocation to the cell surface and subsequent glucose transport are impaired in Tfam knockdown cells. Paradoxically, insulin-stimulated Akt phosphorylation is significantly enhanced in these cells. These studies reveal independent links between mitochondrial function, insulin signaling, and glucose transport, in which impaired respiratory chain activity enhances insulin signaling to Akt phosphorylation, but impairs GLUT4 translocation. These results indicate that mitochondrial respiratory chain dysfunction in adipocytes can cause impaired insulin responsiveness of GLUT4 translocation by a mechanism downstream of the Akt protein kinase.

Introduction

A large body of evidence has pointed to a close relationship between ectopic fat accumulation in tissues such as muscle and liver and the development of insulin resistance (147-149). The primary defense against such ectopic lipid accumulation is a well functioning adipose tissue, capable of sequestering excess calories in the form of stored triglycerides (150). In addition to this crucial role, adipose tissue is an endocrine organ that controls whole body energy homeostasis by secreting multiple cytokines that signal to other tissues (151-152). The central role of adipose tissue in energy homeostasis is underscored by recent findings indicating that adipose tissue is a primary locus for the alterations induced by caloric restriction that accompany longevity (153-154). Thus, the cell biological mechanism involved in optimal adipose tissue development and function are crucial for the control of whole organism energy homeostasis and the determination of life span.

Adipocyte differentiation is accompanied by an expansion of mitochondrial mass (17, 26),but the functional role of the relatively high levels of mitochondria in white adipocytes compared with those in adipose stroma and other tissues is not clear. High mitochondria levels may be required for the support of adipocyte-specific ATP-requiring processes (155), or to support metabolic functions such as glyceroneogenesis, which is required for triglyceride deposition (40, 156). White adipocyte mitochondria levels in rodents and humans change markedly under different physiological conditions, including obesity, weight loss, aging, treatment with anti-diabetic agents, and in response to genetic alterations in insulin receptor number (16-27). Mitochondrial levels correlate with insulin

sensitivity, where decreased mitochondrial content correlates with diminished insulin responsiveness, and enhanced mitochondrial mass associates with increased insulin sensitivity. However, given the complexity of whole animal models, a cause-effect relationship between mitochondrial mass and insulin sensitivity in adipocytes has not been established.

Mitochondrial biogenesis depends on a coordinated interaction between nuclear and mitochondrial genomes (157-159). The vast majority of mitochondrial proteins are produced from ~1500 different nuclear localized genes. In contrast, the mitochondrial genome produces only 13 proteins, but among these are key components of the respiratory chain. The replication and transcription of the mitochondrial genome is absolutely dependent on Tfam, a transcription factor encoded in nuclear DNA (31, 160). Tfam is critical for mitochondrial biogenesis during development and for the maintenance of mitochondrial DNA copy number in mature tissues.

To directly determine the functional role of mitochondrial biogenesis in differentiated adipocytes, we have used siRNA to silence Tfam during the differentiation process. This manipulation results in the generation of adipocytes that contain only double the mitochondrial levels of preadipocytes. Analysis of these cells reveals a specific impairment in insulin-stimulated glucose transport, which occurs distal to early insulin signal transduction events. These results point to a previously unknown interaction between the mitochondrial respiratory chain and insulin sensitivity of the glucose transport pathway and provides evidence that mitochondrial dysfunction could be a primary cause of insulin resistance in adipose cells.

Experimental Procedures

Materials

Real-time PCR primers were designed using the Primer Bank (pga.mgh.harvard.edu/primerbank/index.html). All the PCR primers were synthesized by Operon. Primer sequences are available upon request. Rabbit anti-Tfam antibody was purchased from Aviva Systems Biology; goat anti-Glut4 antibody was from Santa Cruz Biotechnology (Santa Cruz, CA); rabbit anti-Acrp30/adiponectin antibody was from Affinity Bioreagents, Inc.; mouse anti-phospho-Akt and anti-Akt antibodies, and rabbit PAS antibodies (cat # 9611 and #9614, mixed 1:1 and used with a 1:1000 dilution) were from Cell Signaling; mouse anti-phosphotyrosine antibody was from Upstate; and mouse anti-β-Actin antibody was from Sigma.

Cells Culture and Differentiation

3T3-L1 preadipocytes were maintained in Dulbecco's modified Eagle's medium supplemented with 10% fetal bovine serum, 100 units/ml penicillin, and 100 μg/ml streptomycin in an atmosphere of 10% CO_2 at 37 °C (complete medium). Three days post-confluence (day 0), cells were induced to differentiate by adding a hormone mixture (0.5 mM 3-isobutyl-1-methylxanthine, 1 μm dexamethasone, and 5 μg/ml insulin). 72 hours later, the differentiation medium was replaced by complete medium, which was replaced every 48 hours until analysis.

Transfection of siRNA

siRNA against mouse Tfam mRNA was purchased from Dharmacon in a duplex form with 3′-dTdT protective overhangs (sense sequence is 5′-GAAUGUGGAUCGUG-CUAAAdTdT-3′). At day 2 of differentiation, medium was collected and cells were

trypsinized and transfected with Tfam or scrambled siRNA by electroporation. Briefly, 5 nmol of siRNA was used for each 150-mm plate of cells in a 0.4-cm GenePulser® cuvette. After electroporation (180 V, 950 microfarads), cells were resuspended in the collected day 2 medium and re-plated to 6-, 12-, or 24-well plates according to the experiment. 24 hours later, the differentiation medium was replaced by complete medium and the medium was refreshed every 2 days afterward.

Quantitative RT-PCR

Total RNA were extracted with TRIzol® Reagent. After RNase-free DNase I digestion, RNA was purified with a Qiagen RNeasy® MinElute™ cleanup kit. The purified RNA was then used to synthesize cDNA (iScript™ cDNA Synthesis Kit). Real-time PCR was performed with iQ™ SYBR® Green Supermix on MyiQ single-color real-time PCR detection system from Bio-Rad. The $2^{-\Delta\Delta CT}$ method was used to analyze the relative mRNA level. Ferritin heavy chain mRNA was used as the internal control.

Cell Lysate Preparation and Western blot

Cells were lysed in a buffer composed of 300 mM NaCl, 20 mM NaF, 1 mM $NaPP_i$, 10 mM HEPES, pH 7.4, 1% SDS, and protease inhibitors. 20 μg of cell lysate was resolved on 10% or 15% SDS-PAGE and transferred to nitrocellulose membrane. The blots were blocked with 5% fat-free milk in TBST and incubated with primary antibodies at 4 °C over night. After three washes with TBST and incubation with secondary antibody, the blot was detected by enhanced chemiluminescence (PerkinElmer Life Sciences) and exposure to film.

2-Deoxyglucose Uptake and 3-O-Methylglucose Uptake

Glucose transport was determined by measuring 2-deoxyglucose uptake in a 24-well plate. After 2-hours serum starvation in Krebs-Ringer HEPES (KRH) buffer (130 mM NaCl, 5 mM KCl, 1.3 mM $CaCl_2$, 1.3 mM $MgSO_4$, and 25 mM HEPES, pH 7.4, supplemented with 0.5% BSA, and 2 mM sodium pyruvate), the adipocytes were stimulated by insulin for 30 minutes. Glucose uptake was initiated by addition of [1,2-^{3}H]2-Deoxy-*D*-glucose to a final assay concentration of 100 μm for 5 minutes at 37 °C. After three washes with ice-cold phosphate-buffered saline (PBS), the cells were lysed with 0.4 ml of 1% Triton X-100. The ^{3}H was then determined by scintillation counting. Nonspecific 2-deoxyglucose uptake was measured in the presence of 20 μm cytochalasin B and subtracted from each determination. 3-*O*-Methylglucose uptake was carried out in a similar way with the following differences: instead of 2-deoxyglucose, the 3-*O*-[*methyl*-^{14}C]-D-glucose was added to the cells to 35.4 μm and allowed to be incubated for 60 s. Cells were then washed three times with cold PBS plus 1 mM $HgCl_2$.

Mitochondrial Staining and Flow Cytometry

Cells were trypsinized and incubated in KRH buffer without or with 100 nM MitoTracker® Green^{FM} for 30 minutes at 37 °C. 1×10^6 cells were then resuspended in 1 ml of ice-cold phosphate-buffered saline with 0.5% BSA and analyzed on an LSR II cytometer analyzer (BD Biosciences). Data were gated using non-stained cells to represent MitoTracker® Green^{FM} staining.

Mitochondrial DNA Measurement

Total DNA was extracted by DNeasy® tissue kit. Primer pairs corresponding to Nd1 (mitochondrial) and Actb (nuclear) were used to amplify a mitochondrial and

nuclear DNA fragment, respectively. The $2^{-\Delta\Delta C_T}$ method was used to analyze the relative mtDNA level.

Oxygen Consumption Assay

The oxygen consumption was measured using live intact cells with BD™ Oxygen Biosensor System. Cells (500,000 cells/ml) were suspended in KRH buffer supplemented with 0.5% BSA and 2 mM pyruvate. 150 μl of cell suspension was added to triplicate wells in an Oxygen Biosensor System 96-well plate. Fluorescence signal was read using a TECAN Safire^2 microplate reader continuously every 2 minutes at 37 °C. Oxygen concentration was calculated from the fluorescence intensity according to the manufacturer's instructions.

Intracellular and Dynamic ATP Measurement

ATP level was measured using a CellTiter-Glo® Luminescent Cell Viability Assay (Promega, Madison, WI). Equal numbers of control or knockdown cells were trypsinized and incubated in an opaque 96-well plate in six replicates for 1 hour. 100 μl of the reaction reagent was directly added to each well, and after 10 minutes the luminescence signal was detected using a microplate reader. To measure ATP synthesis dynamically, cells were first suspended in respiration buffer (0.1% BSA, 75 mM mannitol, 25 mM sucrose 100 mM KCl, 10 mM KH_2PO_4, 5 mM $MgCl_2$, 20 mM, Tris, pH 7.5, 10^6 cells/ml), and 10 μg/ml digitonin was added for 5 minutes. Digitonin was removed by resuspending the permeabilized cell in the same volume of respiration buffer. Vehicle or 10 μg/ml oligomycin was added and mixed well by gentle inverting. 100 μl of cell suspension were then transferred to wells of a 96-well plate, which contained substrates (1 mM ADP and 10 mM succinate final concentration) for different time

periods. ATP synthesis was stopped by adding 100 μl of CellTiter-Glo® reagent and luminescence was read using a Safire^2 microplate reader. ATP synthesized from mitochondria was derived by subtracting the oligomycin-treated reading from those untreated.

Reactive Oxygen Species Measurement

Cells were seeded to a 24-well plate in medium without phenol red, and incubated without or with 50 ng/ml TNFα for 3 hours. Following two washes with PBS, cells were incubated with 10 μm 5-(and 6-)chloromethyl-2′,7′-dichlorodihydrofluoresceindiacetate, acetyl ester (CM-H_2DCFDA) (Invitrogen) in Krebs-Ringer bicarbonate buffer for 15 minutes at 37 °C. The fluorescent signal was read at excitation of 485 nm and emission of 530 nm in a microplate reader.

Triglyceride Content Measurement

Cells in 6-well multiwell dishes were scrapped into 200 μl of PBS and sonicated for 20 s on ice. The lysate was subject to total glycerol determination using a Serum Triglyceride Determination Kit (Sigma, TR0100). Briefly, 10 μl of lysate or standard was mixed with 1 ml of Triglyceride Working Reagent and incubated for 30 minutes at 37 °C. The absorbance was read at 540 nm, and glycerol concentration was then calculated from the standard curve.

Oil Red O Staining for Lipids

Cells were washed with PBS twice and fixed in 4% formaldehyde for 1 hour at room temperature. After three washes with water, the cells were incubated with 5 mg/ml Oil Red O in 60% triethyl phosphate for 30 minutes. Cells were then washed with water at least six times before imaging.

Total Internal Reflection Fluorescence Microscopy

Cells seeded on coverslips were serum-starved for 2 hours in KRH buffer supplemented with 0.5% BSA and 2 mM pyruvate and were then stimulated by 0, 0.1, or 1 μm insulin for 30 minutes. Cells were fixed in 4% paraformaldehyde for 15 minutes at room temperature, permeabilized with 0.5% Triton X-100 plus 1% fetal bovine serum in PBS, and stained with goat anti-GLUT4 (1:200) antibodies overnight at 4 °C. Alexa Fluor® 488 donkey anti-goat secondary antibodies were used to detect bound primary antibody. TIRF images were taken for 10 random fields from each coverslip. Background areas containing no cells were used to threshold the images, and the total fluorescence intensity of the whole area was then obtained.

Affymetrix GeneChip Expression Analysis

Total RNA was prepared from three 150-mm dishes of 3T3-L1 cells at each day of differentiation. Affymetrix protocols were followed for the preparation of cRNA from total RNA, which was hybridized according to Affymetrix instructions to a MOE430-2 Chips. The GeneChips were washed with a GeneChip Fluidics Station 400 and were scanned with an HP GeneArrayScanner (Affymetrix). Raw expression data were analyzed with the Bioconductor statistical environment using RMA and MAS5, a Bioconductor implementation of the MAS 5.0 algorithm (Affymetrix). The “-fold change” for each gene was determined by dividing the mean of the average difference from three independent experiments.

Results

Mitochondrial Gene Expression and Insulin Responsiveness

Previously we have found that differentiation of 3T3-L1 adipocytes is accompanied by increased mitochondrial biogenesis, assessed primarily by mass spectrometry of peptides increased during adipogenesis (26). A more in-depth analysis of Affymetrix databases obtained from 3T3-L1 cells at different days during differentiation reveals that a marked increase in expression of mitochondrial genes occurs between days 2 and 4 of differentiation. This is the period at which the most pronounced changes in gene expression occur, evidenced by the many changes in both non-mitochondrial and mitochondrial transcripts (Table 2-1). Of all transcripts changed between days 2 and 4 of differentiation, approximately half were increased and half decreased (2229 increased, 1888 decreased by >1.25-fold between days 0 and 6 of differentiation). In contrast, of the transcripts identified by the gene ontology term “mitochondrion,” many more were increased than decreased in the same interval (435 increased, 37 decreased by >1.25-fold). The overrepresentation of mitochondrial genes in the pool of genes that increased during differentiation was also seen when only high abundance (***i.e.*** signals > 1500) genes undergoing changes of >1.5-fold were counted (Table 2-1, lower half). Their high representation is also reflected when the numerical averages of all observed changes are plotted (Figure 2-1, *A*). The predominant increase in mitochondrial gene expression occurs between days 2 and 4 of differentiation and is stable thereafter (Figure 2-1, *A*). The relevance of mitochondrial gene expression during adipocyte differentiation is underscored by pathway analysis using the Kyoto Encyclopedia of Genes and Genomes

(161). The top 20 pathways that are highly enriched in genes that increase during adipocyte differentiation are shown in Table 2-2; 14 of these pathways, including the top 5, are mitochondrial metabolic pathways.

Probe signal > 50 on any day						
Interval	Probes increased > 1.25	Probes decreased > 1.25	Probes unchanged	Mito Probes increased > 1.25	Mito Probes decreased > 1.25	Mito Probes unchanged
Days 0–6	2,834	3,374	32,265	530	70	985
Days 0–2	19	20	38,967	0	2	1,711
Days 2–4	2,229	1,888	35,148	435	37	1,126
Days 4–6	342	496	36,976	37	13	1,529
Probe signal > 1500 on any day						
Interval	Probes increased > 1.5	Probes decreased > 1.5	Probes unchanged	Mito Probes increased > 1.5	Mito Probes decreased > 1.5	Mito Probes unchanged
Days 0–6	807	677	2,541	294	15	254
Days 0–2	1	0	3,549	0	0	412
Days 2–4	631	327	3,202	233	11	322
Days 4–6	35	34	3,552	7	1	564

Table 2-1 Number of probes displaying changes at specific interval during differentiation

M	KEGG pathway	*p* value
*	Oxidative phosphorylation	<2.22e−16
*	Valine, leucine, and isoleucine degradation	<2.22e−16
*	Citrate cycle (trichloroacetic acid cycle)	<2.22e−16
*	Glycolysis/gluconeogenesis	<2.22e−16
*	Pyruvate metabolism	<2.22e−16
	Carbon fixation	<2.22e−16
	Pentose phosphate pathway	<2.22e−16
*	Fatty acid metabolism	<2.22e−16
*	Butanoate metabolism	<2.22e−16
*	Fatty acid elongation in mitochondria	<2.22e−16
*	Propanoate metabolism	<2.22e−16
	Glycerophospholipid metabolism	<2.22e−16
*	ATP synthesis	<2.22e−16
*	Lysine degradation	<2.22e−16
*	Benzoate degradation via CoA ligation	<2.22e−16
	Insulin signaling pathway	<2.22e−16
*	Reductive carboxylate cycle (CO_2 fixation)	4.29E−16
*	Glyoxylate and dicarboxylate metabolism	4.80E−16
	Biosynthesis of steroids	9.69E−15
	Starch and sucrose metabolism	2.01E−14

[a] * indicates a mitochondrial metabolic pathway (*M*).

Table 2-2 Top 20 Kyoto Encyclopedia of Gene and Genome (KEGG) pathways enriched for genes that increase between days 0 and 6 of differentiation

The pronounced changes in expression of mitochondrial proteins could produce mitochondrial remodeling, without necessarily requiring mitochondrial biogenesis, understood here as a process of expansion of mitochondrial mass and mitochondrial DNA copy number. Nevertheless, a significant increase in mitochondrial DNA did occur between days 2 and 4 of differentiation (Figure 2-1, *B*). Importantly, this increase coincided with the differentiation-dependent induction of insulin responsiveness, as seen by the magnitude of the effect of insulin on the stimulation of glucose transport at different days of differentiation (Figure 2-1, *C*). Mitochondrial DNA replication requires the transcription factor Tfam, and indeed Tfam mRNA increased significantly between days 2 and 4 of differentiation (Figure 2-1, *D*). Interestingly, although the levels of mitochondrial DNA remained high after day 4 of differentiation, Tfam levels decreased, suggesting that the maintenance of mitochondrial DNA in these cells is not sensitive to Tfam levels over this short time period. These results also suggest that interference with Tfam induction prior to day 4 of differentiation could produce cells harboring a selective impairment in those mitochondrial functions dependent on mitochondrial DNA-encoded transcripts.

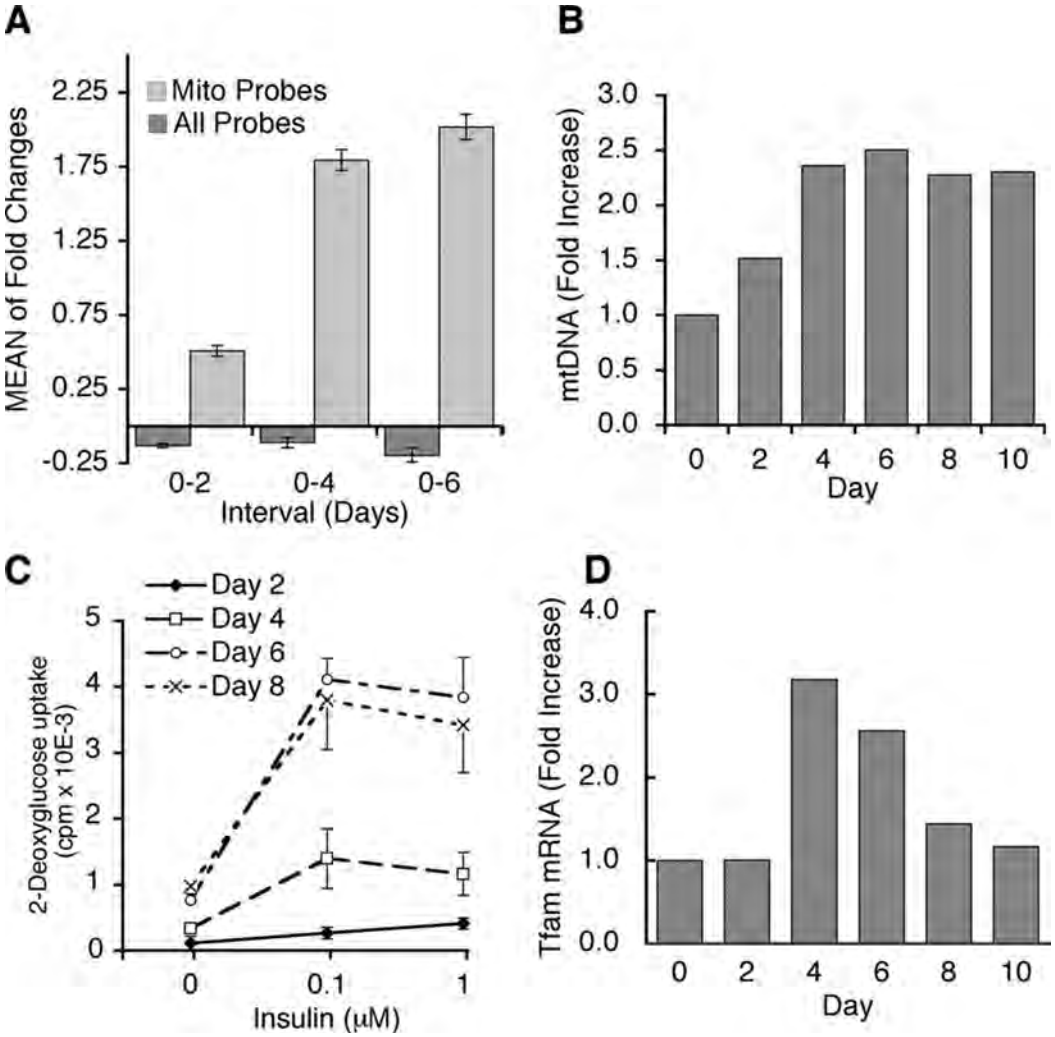

Figure 2-1 Changes in mitochondrial gene expression during 3T3-L1 adipogenesis

(*A*), "All probes" refers to those detected with the MOE430-2 Affymetrix GeneChip, with a signal > 50. "Mito Probes" refers to probes annotated with gene ontology cellular component term "mitochondrion" retrieved directly from the Affymetrix website. Plotted are the average of all -fold increases and decreases in probe signal between the days of differentiation indicated on the abscissa. (*B*), total DNA was extracted at the days indicated on the abscissa. Mitochondrial DNA (mtDNA) copy number was determined by qRT-PCR taking nuclear DNA as internal control and expressed as -fold change over day 0 of differentiation. (*C*), the uptake of 2-deoxyglucose was measured after 30 minutes of incubation with the indicated concentrations of insulin at the times of differentiation indicated. Points represent means, and lines ±S.E. of two independent experiments performed in triplicate. (*D*), Tfam mRNA expression determined by qRT-PCR, using ferritin mRNA as internal control and expressed as -fold change over day 0 of differentiation.

Tfam-depletion and Impaired Respiratory Chain Function

The effectiveness of Tfam knockdown by siRNA oligonucleotides, introduced on day 2 of differentiation, was evaluated by measuring both mRNA and protein levels at day 5 of differentiation. Compared with cells electroporated with scrambled control oligonucleotides, Tfam knockdown cells displayed an 80% reduction in Tfam mRNA (Figure 2-2, *A*). Tfam protein levels, evaluated by western blot, were concomitantly reduced by ~70% (Figure 2-2, *B*). Tfam knockdown led to a 30% decrease in mtDNA copy number compared with cells electroporated with scrambled control oligonucleotides (Figure 2-2, *C*). Thus, whereas in control cells mtDNA increased by ~2-fold from days 2 to 5, in the Tfam knockdown cell mtDNA increased by only ~33% (Figure 2-2, *D*). Consistent with our observation that Tfam does not appear to be absolutely required for maintenance of mtDNA in these cells over the period of time studied, mtDNA was not reduced when Tfam siRNA was introduced at day 6 of differentiation and mtDNA copy number measured at day 9 (data not shown)

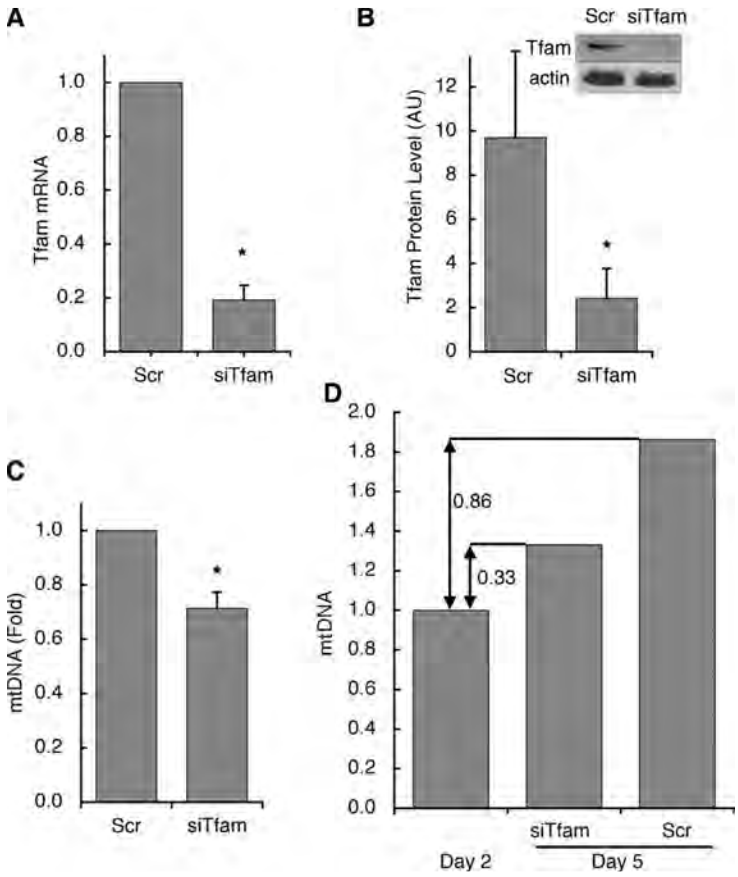

Figure 2-2 Inhibition of Tfam induction and mtDNA amplification

Cells were transfected with scrambled (*Scr*) or Tfam-directed (*siTfam*) siRNA oligonucleotides at day 2 of differentiation. 72 hours later: (*A*), Tfam mRNA levels were determined by qRT-PCR. (*B*), Tfam protein levels were analyzed by western blot and densitometry. Actin levels are included as a loading control. (*C*), mtDNA copy number was assessed relative to nuclear DNA. (*D*), comparison of mtDNA increase from the time of transfection (day 2) to day 5, in cells transfected with scrambled or Tfam-directed siRNA oligonucleotides. *, $p < 0.05$ relative to Scr, using two-tailed paired Student *t* tests with a minimum of three independent experiments.

Because transcripts from mtDNA might be expected to have different lifetimes than mtDNA itself, we tested the effect of siRNA against Tfam on genes encoded by mtDNA. Nd1, Cytb, Cox1, and Atp6 encode for polypeptides that form part of respiratory chain complexes I, III, IV, and V, respectively. The levels of all four of these transcripts were reduced by ~30% in cells transfected with siRNA against Tfam compared with scrambled control (Figure 2-3, *A*). We then investigated if the reduced mtDNA expression of these subunits had a functional effect on electron transport. Oxygen is consumed in the end step of the respiratory chain. Thus, the rate of oxygen consumption provides a global estimate of the functionality of the entire respiratory chain. Oxygen consumption can be measured in 96-well multiwell plates using the BD™ Oxygen Biosensor System, in which the quenching by ambient oxygen of a fluorophore embedded on the bottom of the well is measured continuously in a fluorescence microplate reader. Figure 2-3, *B* illustrates the typical readout from this assay, where quenching occurs in a non-linear fashion, which depends on the number of cells plated, and is responsive to changes in respiratory rate, as seen in the accelerated response in cells pre-treated with carbonyl cyanide-4-(trifluoromethoxy)-phenylhydrazone (FCCP), and the impaired response in cells pretreated with rotenone, an inhibitor of complex I. The activity of the electron transport chain was significantly impaired as estimated by the decrease in oxygen consumption seen in Tfam knockdown cells compared with controls (Figure 2-3, *C*). This impairment persisted in the presence of FCCP, which by uncoupling the proton gradient maximizes electron transport and thereby oxygen consumption. Thus,

the maximal capacity of the electron transport chain was diminished in adipocytes in which Tfam induction was impaired during differentiation.

As an alternative way to monitor the activity of the electron transport chain, the capacity of mitochondria to synthesize ATP was measured. Digitonin-permeabilized adipocytes were incubated in the presence or absence of oligomycin A, to inhibit the activity of the mitochondrial ATPase. ATP synthesis driven by ADP and succinate was then measured dynamically using a luciferase-based ATP assay. Mitochondrial ATP synthesis was obtained by subtracting the values obtained in the presence from those in the absence of oligomycin A. A significant impairment in mitochondrial ATP production was seen in Tfam knockdown cells compared with controls (Figure 2-3, *E*), whereas no difference was seen in non-mitochondrial ATP levels, which remained unchanged during the incubation (not illustrated).

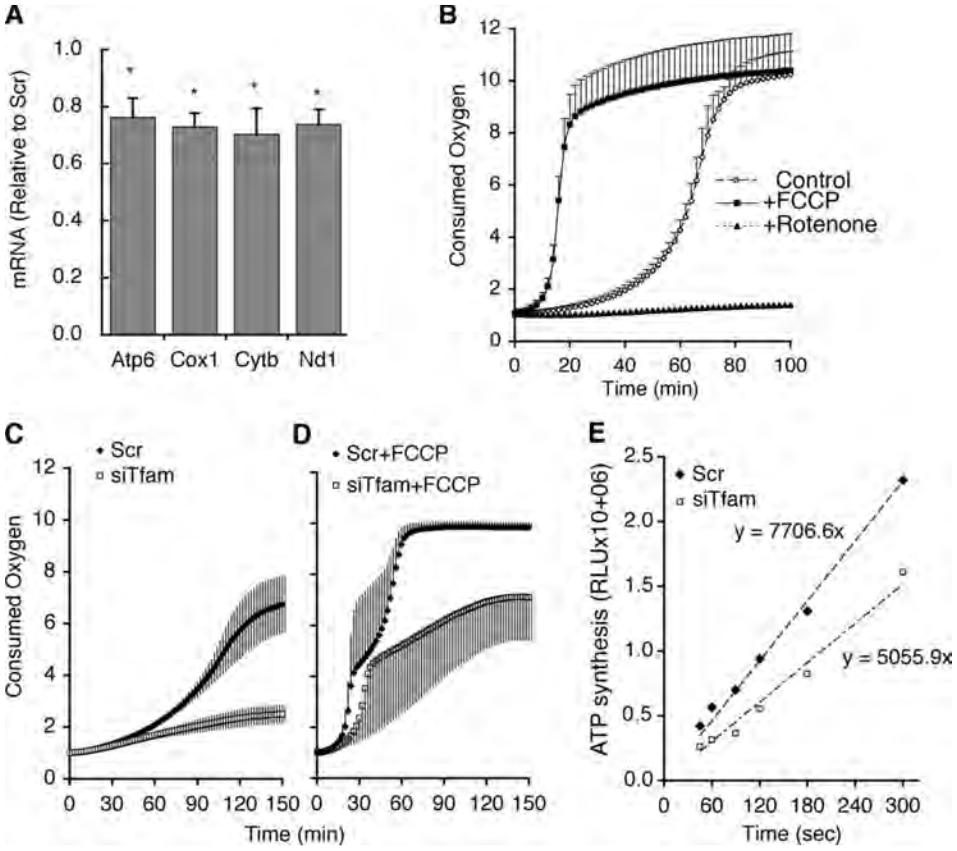

Figure 2-3 Decreased levels of mitochondrial DNA-encoded genes and respiratory chain function in Tfam knockdown cells

(*A*), mRNA levels of four mtDNA encoded genes determined at day 5 in cells transfected at day 2 with scrambled (*Scr*) or Tfam-directed (*siTfam*) siRNA oligonucleotides. *Bars* represent values in siTfam cells relative to Scr. Statistical significance was calculated using two-tailed paired Student *t* tests; *, $p < 0.05$. (*B*), adipocytes at day 6 were aliquoted into a BD Oxygen Biosensor System 96-well plate. FCCP or rotenone was added, and recording of fluorescence was immediately initiated. (*C*) and (*D*), control and Tfam knockdown cells at day 5 were aliquoted into a BD Oxygen Biosensor System 96-well plate and fluorescence was recorded in the absence (*C*) or presence (*D*) of FCCP. Fluorescence was monitored every 2 minutes at 37 °C and is expressed as fluorescence units relative to time 0 values. Plotted are the means, and *vertical lines* represent ±S.E. of three independent experiments preformed in triplicate. *p* values obtained from paired two-tailed Student *t* tests of the means were: 3.1E-17 for Scr *versus* siTfam; 5.2E-32 for Scr *versus* Scr+FCCP; 9.9E-34 for Scr+FCCP *versus* siTfam+FCCP; and 1.7E-35 for siTfam *versus* siTfam+FCCP. (*E*), mitochondrial ATP production in digitonin-permeabilized cells. Shown is a representative example of three independent experiments performed in triplicate. *p* value obtained from paired two-tailed Student *t* tests from the means of three experiments was 0.0025 for Scr *versus* siTfam.

Unchanged Nuclear Gene Expression and Mitochondrial Mass

The vast majority of mitochondrial proteins are encoded by nuclear DNA. To determine whether siRNA to Tfam might indirectly affect the expression of nuclear-encoded mitochondrial genes, we examined the levels of mRNA for enzymes involved in the tricarboxylic acid cycle, fatty acid oxidation, and oxidative phosphorylation. No significant changes in these mRNAs were seen in response to Tfam knockdown (Figure 2-4, *A*). Moreover, functional assessment of fatty acid oxidation using exogenous palmitate revealed no significant changes in response to Tfam knockdown (not illustrated). We also determined the expression of a group of nuclear encoded regulators of mitochondrial biogenesis, which were also unchanged in Tfam knockdown cells (Figure 2-4, *B*). Consistent with a lack of effect of Tfam-depletion on non-mtDNA encoded mitochondrial genes, the overall cellular abundance of mitochondria assessed by staining with specific fluorescence marker MitoTracker® Green^{FM} was found to be unchanged in Tfam knockdown cells; neither fluorescence-activated cell sorting analysis of live cells stained with MitoTracker® Green^{FM} (Figure 2-4, *C*) nor visual inspection of individual cells (Figure 2-4, *D*) revealed any detectable difference in density or mitochondrial morphology.

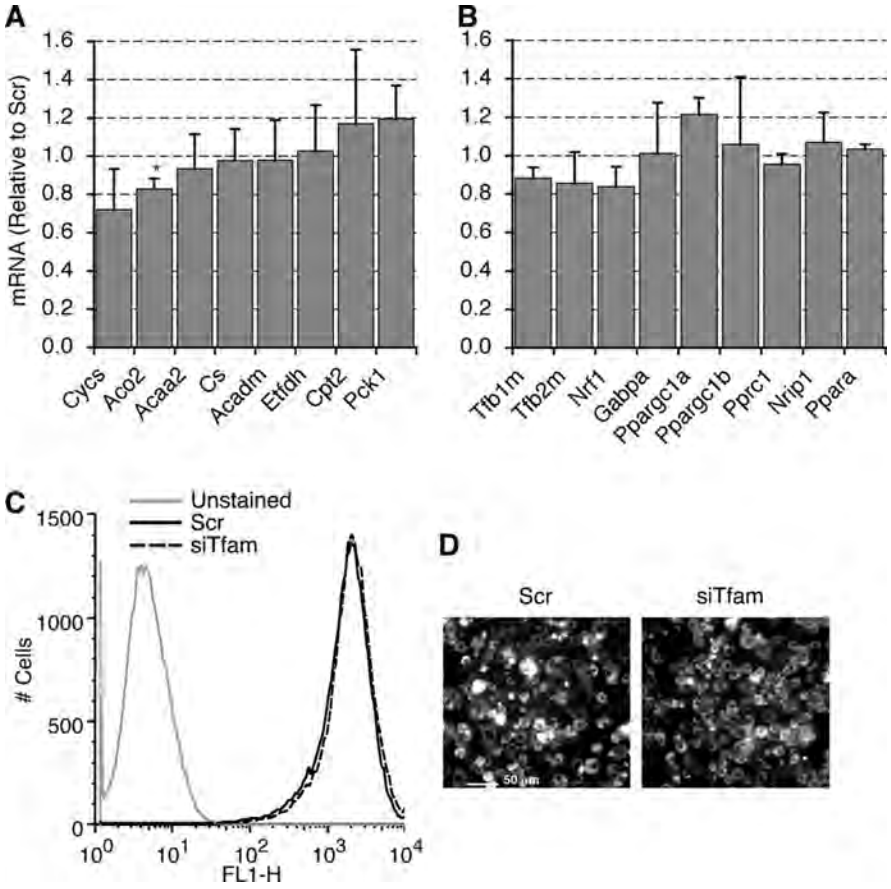

Figure 2-4 Nuclear encoded mitochondrial gene expression and mitochondrial mass in Tfam knockdown cells

The relative mRNA level of various nuclear-encoded mitochondrial genes (*A*) and nuclear encoded mitochondrial related regulators (*B*) was determined by qRT-PCR at day 5 in cells transfected at day 2 with scrambled or Tfam-directed siRNA oligonucleotides. Results are expressed relative to scrambled control values. Cells were stained with MitoTracker Green and subjected to fluorescence-activated cell sorting analysis (*C*) or visualized by fluorescence microscopy (*D*).

Insulin-stimulated Glucose Uptake is Impaired

Alterations in adipose tissue mitochondrial gene expression correlated with insulin sensitivity in animal models, but this correlation may be spurious, or perhaps even secondary to altered insulin sensitivity. 3T3-L1 adipocytes depleted of Tfam provide a straightforward model system to determine whether impairment of adipose respiratory chain function can affect insulin sensitivity. To this end, we examined the effects of insulin on glucose uptake in Tfam-depleted cells. Preadipocytes were transfected with Scr or Tfam-directed siRNA oligonucleotides at day 2 of differentiation, and glucose transport was measured at day 6. A clear response to insulin to stimulate 2-deoxyglucose uptake could be observed at day 6 (Figure 2-5, *A*). Although Tfam-depletion did not significantly affect basal 2-deoxyglucose uptake, the stimulatory effect of insulin was significantly impaired in Tfam knockdown cells (Figure 2-5, *A*). To rule out the possibility that impaired insulin responsiveness could be due to off-target effects of the silencing oligonucleotides, cells were electroporated on day 6 of differentiation, and glucose uptake was measured on day 8, a period during which Tfam-directed siRNA has no effect on mtDNA levels, as described above. No differences in basal or insulin-stimulated glucose uptake were seen between cells transfected with Scr or Tfam-directed siRNA at day 6 (4508 ± 212 *versus* 4433 ± 298 cpm Scr or Tfam-directed siRNA in response to 0.1 μM insulin). Thus, impairment of insulin-stimulated glucose uptake correlates specifically with suppression of Tfam induction.

Impaired 2-deoxyglucose uptake can result from a decreased rate of glucose transport across the plasma membrane, or from a decreased rate of phosphorylation of 2-

deoxyglucose by hexokinase. To distinguish between these possibilities, we measured the uptake of 3-*O*-methylglucose in response to insulin, which specifically reflects transport, and found that it was also impaired by Tfam-depletion (Figure 2-5, *B*). Thus impairment in respiratory chain function results in impaired insulin action to stimulate glucose transport, independently of glucose metabolism.

To determine whether decreased insulin-stimulated glucose transport was due to alterations in GLUT4 translocation to the cell surface, we analyzed GLUT4 trafficking using total internal reflection fluorescence (TIRF). This imaging technique allows the specific visualization of fluorophores residing ~100 nm from the plasma membrane (162). Because insulin stimulates translocation of GLUT4 to the TIRF zone as well as fusion with the plasma membrane (85), TIRF imaging of endogenous GLUT4 provides a direct estimation of insulin action on GLUT4 trafficking. Insulin-stimulated recruitment of endogenous GLUT4 to the TIRF zone was significantly impaired in Tfam knockdown cells (Figure 2-5, *C* and *D*). This decrease did not result from decreased protein levels of GLUT4, assessed by western blot analysis of total cell extracts (Figure 2-5, *E*). Thus, insulin stimulation of GLUT4 translocation and subsequent glucose transport are impaired in adipocytes with decreased respiratory chain function.

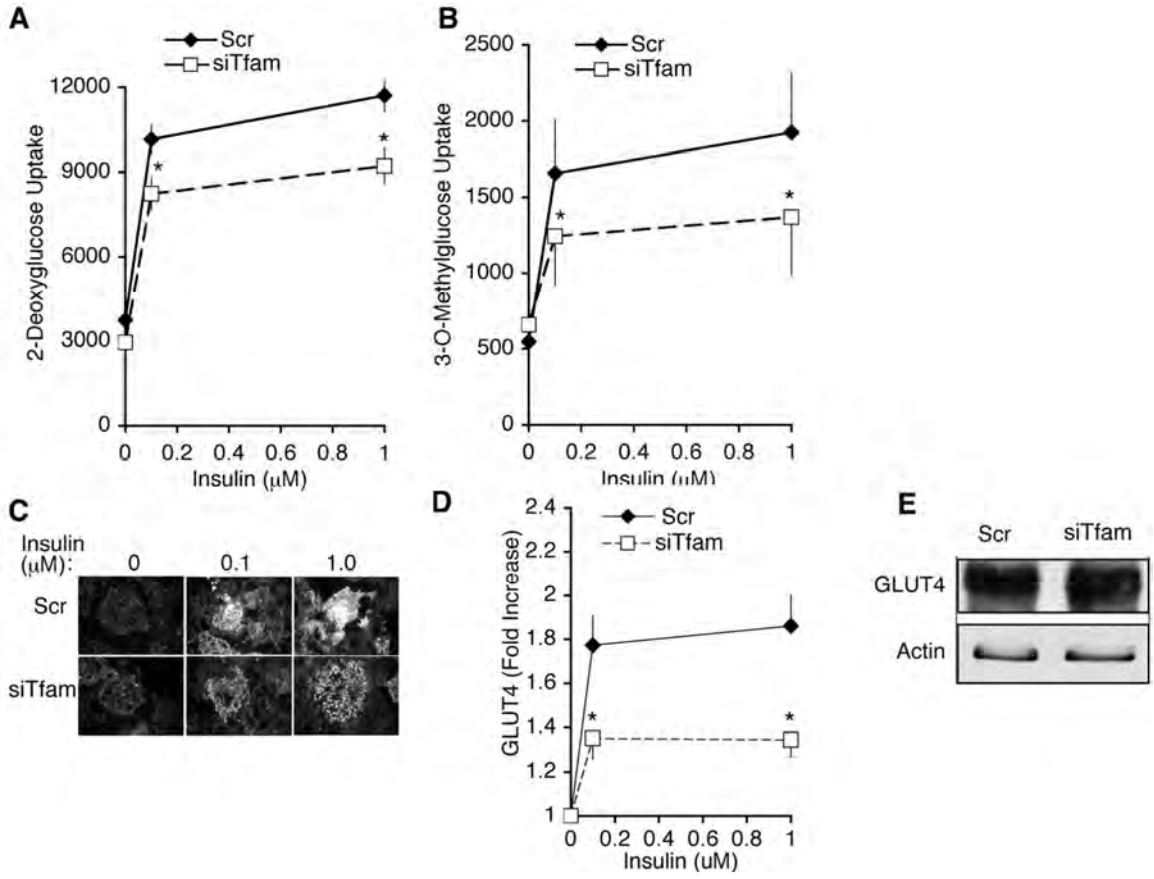

Figure 2-5 Glucose transport and GLUT4 trafficking in Tfam knockdown cells

Cells were transfected with scrambled (*Scr*) or Tfam-directed (*siTfam*) siRNA oligonucleotides at day 2 of differentiation. At day 6, cells were serum-starved for 2 hours; (*A*), the uptake of 2-deoxyglucose was measured after 30 minutes of incubation with the indicated concentrations of insulin. *Points* represent means, and *lines* are ±S.E. of three independent experiments performed in triplicate. *p* values obtained by two-tailed paired Student *t* tests were 0.0039 and 0.0057 for Scr *versus* siTfam at 0.1 and 1 μm insulin, respectively. (*B*), measurement of 3-*O*-methylglucose under the same conditions as in *A*. *p* values obtained by two-tailed paired Student *t* tests were 0.07 and 0.0025 for Scr *versus* siTfam at 0.1 and 1 μm insulin, respectively. Cells treated with the indicated concentrations of insulin were fixed and stained with antibodies to endogenous GLUT4 and imaged by TIRF. (*C*), representative images of random fields; (*D*), quantification of average intensity of random fields. *Points* represent means of four independent experiments from which 10 random fields from each coverslip were averaged. *Lines* represent ± S.E. *p* values obtained by two-tailed paired Student *t* tests were 0.008 and 0.006 for Scr *versus* siTfam at 0.1 and 1 μm insulin, respectively. (*E*), representative western blot of GLUT4 in cells transfected with scrambled (*Scr*) or Tfam-directed (*siTfam*) siRNA oligonucleotides at day 2 of differentiation and lysed at day 6. Similar results were obtained in three independent experiments.

ATP Level and Phosphorylation of Akt

One possible mechanism by which insulin-simulated glucose uptake might be impaired in Tfam knockdown cells would be through decreased ATP levels, which would in these cells lead to impairment in insulin signal transduction (155). Steady-state ATP levels in Tfam knockdown cells were indeed decreased, albeit only by a small (~10%) amount (Figure 2-6, *A*). This decrease did not result in impaired insulin signaling, as assessed by the levels of tyrosine phosphorylation and Akt phosphorylation in response to insulin (Figure 2-6, *B*). Indeed, a highly reproducible increase in Akt phosphorylation was consistently observed in Tfam knockdown cells (Figure 2-6, *C*). This effect contrasted markedly with that seen in response to rotenone, an acute inhibitor of Complex I. After 60 minutes, rotenone decreased ATP levels by an amount only slightly greater than that produced by Tfam knockdown (Figure 2-6, *A*). However, rotenone treatment markedly impaired insulin-stimulated Akt phosphorylation (Figure 2-6, *D*) and adiponectin secretion (data not shown). These results point to important differences in cellular response to acute ***versus*** progressive impairment of electron transport. A large, transient decrease in ATP levels and stimulation of glucose uptake are known to occur within minutes after rotenone exposure (163). These changes are not observed in Tfam knockdown cells, where Complex I dysfunction is probably less severe than that elicited by direct chemical inhibition, and in which compensatory changes can occur during several days of differentiation.

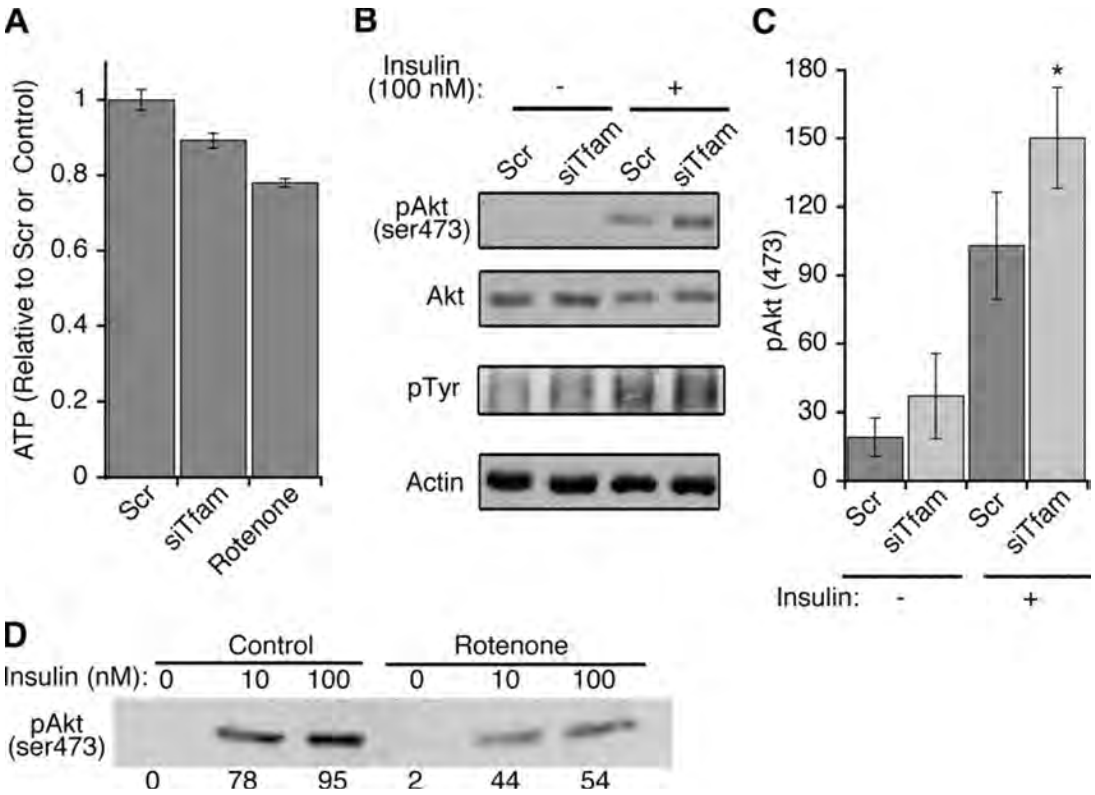

Figure 2-6 ATP levels and insulin signaling in Tfam knockdown cells

(*A*), cells were transfected with scrambled (*Scr*) or Tfam-directed (*siTfam*) siRNA oligonucleotides at day 2 of differentiation, and at day 6 ATP levels were determined by luminescence. Where indicated, rotenone (5 μm) was added to control cells for 60 minutes prior to measurement. *Bars* are means, and *lines* are ±S.E. of three experiments performed in triplicate. *p* values obtained by one-tailed paired Student *t* tests were 0.048 and 0.00018 Scr *versus* siTfam and control *versus* rotenone, respectively. (*B*), cells prepared as above were stimulated with 10 nM insulin for 15 minutes and then harvested in lysis buffer with phosphatase and protease inhibitors. Western blots were performed using antibodies to phospho-Akt (serine 473) and phosphotyrosine antibody (4G10), respectively. Shown is the area of the gel (~180 molecular weight) showing maximal stimulation in phosphotyrosine signal. Antibodies to total Akt and actin were used to control for loading. (*C*), quantification of Akt phosphorylation from four independent experiments. *, *p* value obtained by one-tailed Student *t* tests was 0.031 for Scr *versus* siTfam in the presence of insulin. (*D*), adipocytes at day 6 of differentiation were treated without (*Control*) or with 500 nM rotenone for 60 minutes, and then with the indicated concentrations of insulin for 15 minutes prior to lysis and western blot with anti-phospho Akt antibody. The values from the densitometry scan of this representative experiment are shown below each band.

Unaffected Adipocyte Functions in Tfam Knockdown Cells

The observed small decrease in ATP levels and impaired respiratory chain function in Tfam knockdown cells was also without a detectable effect on numerous parameters that reflect basic functional characteristics of differentiated adipocytes, including mRNA levels of adipogenic genes (Figure 2-7, *A*), triglyceride accumulation (Figure 2-7, *B* and *C*), and basal adiponectin secretion (Figure 2-7, *D*). This later lack of effect is also indicative of the differences between acute *versus* chronic impairment in respiratory chain function, as adiponectin secretion has been shown to decrease in response to acute inhibition of mitochondrial ATP synthesis, and is not inconsistent with prior studies where Tfam-depletion mitigates the enhancement of adiponectin secretion seen in response to enhanced mitochondrial biogenesis (49). Thus, the results shown here indicate that progressive impairment of respiratory chain function through Tfam knockdown in adipocytes leads to impaired insulin-stimulated glucose uptake, by a mechanism probably unrelated to changes in ATP levels. Moreover, insulin signaling to Akt is in fact significantly increased in cells with impaired respiratory chain function.

Other signaling pathways in adipocytes that involve mitochondrial function include those elicited by inflammatory cytokines. The effects of TNFα, for example, involve changes in mitochondrial reactive oxygen species (ROS) production (164-165). To explore whether this pathway would be affected in cells depleted of mtDNA, control and Tfam knockdown adipocytes were treated with 50 ng/ml TNFα, and ROS was then measured in live cells. Basal ROS production was indistinguishable between control and Tfam knockdown cells, as was the 40% increase in ROS production elicited by TNFα

(Figure 2-7, *E*). Thus, chronic impairment in respiratory chain function results in a specific impairment of glucose transport stimulation by insulin, without detectable effects on multiple other adipocyte-specific functions or signal transduction events.

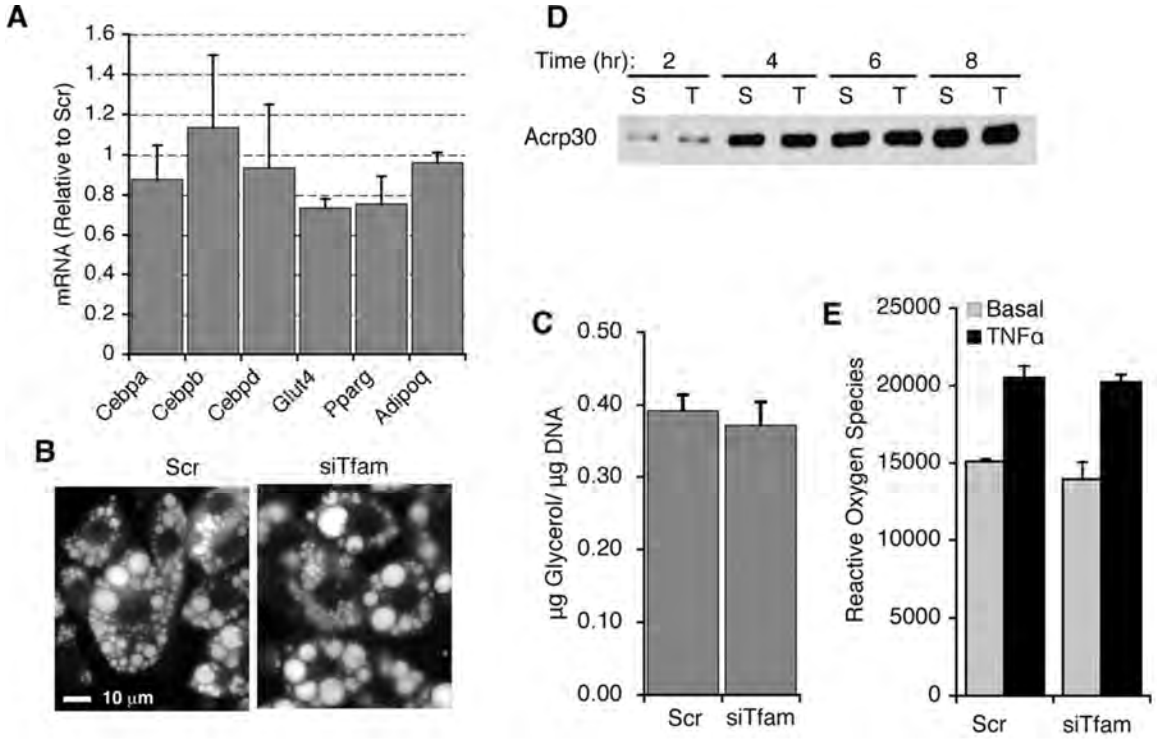

Figure 2-7 Adipocyte functions in Tfam knockdown cells

(*A*), the relative mRNA level of various transcription factors and adipocyte-specific proteins was determined by qRT-PCR at day 5 in cells transfected at day 2 with scrambled or Tfam-directed siRNA oligonucleotides. Results are expressed relative to scrambled values. (*B*) and (*C*), Oil red O staining and triglyceride content of cells at day 5. (*D*), cells were washed in PBS and placed in fresh medium. An aliquot of the medium was collected at the time points indicated and analyzed by western blot with an antibody to adiponectin (Acrp30). (*E*), cells were incubated without or with 50 ng/ml TNFα for 3 hours, and reactive oxygen species were measured by 5-(and 6-)chloromethyl-2',7'-dichlorodihydroflioresceindiacetate, acetyl ester fluorescence, detected directly in cells grown on 24-well multiwell plates using a TECAN Safire^2 microplate reader.

Tfam Knockdown Effect on Insulin Signaling Pathway

To better understand the mechanism by which insulin signaling to glucose transport might be affected by Tfam knockdown, additional pathways downstream of insulin receptor activation were analyzed. Neither the stimulation of ERK1 and -2 phosphorylation (Figure 2-8, *A*), nor the phosphorylation of the S6 protein (Figure 2-8, *B*) by insulin were significantly affected by Tfam knockdown. To analyze whether the observed enhancement of Akt phosphorylation seen in Tfam knockdown cells was accompanied by changes in the phosphorylation of Akt substrates, we utilized phospho-specific antibodies directed to Akt substrates (PAS, Figure 2-8, , *C* and *D*) (82, 166). Several insulin-stimulated phosphoproteins could be observed, including bands at ~75, 105, 160, and 250 kDa that have been previously reported in 3T3-L1 adipocytes (166). Several of these were increased in intensity in Tfam knockdown cells in response to insulin (Figure 2-8, *C*, ***arrowheads***), consistent with the increased phosphorylation of Akt (Figure 2-6,). However, one phosphoprotein, at ~49 kDa, seen at higher exposures, was significantly decreased in response to Tfam knockdown (Figure 2-8, *D*, ***arrow***). Preliminary experiments using antibodies and siRNA to a previously identified 47-kDa Akt substrate (167) suggest that the Tfam-sensitive phosphoprotein is different and has not been previously identified. These results indicate that, whereas most signal transduction events downstream of insulin receptor activation and Akt phosphorylation are not impaired by Tfam knockdown, at least one specific protein is impaired under these conditions. This impairment correlates with the observed inhibition of insulin-

stimulated glucose uptake, but more experiments, including the positive identification of this protein, will be required to establish a causal correlation between these two events.

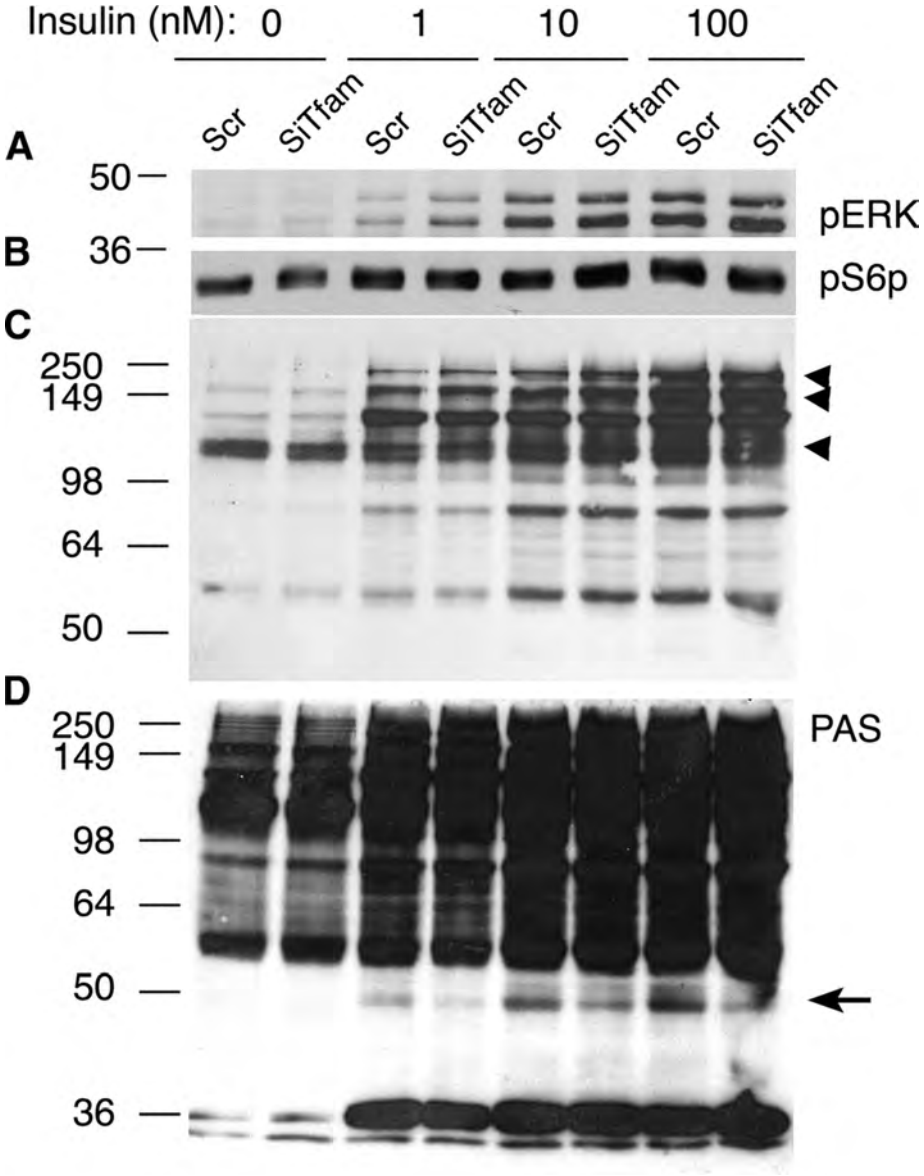

Figure 2-8 Effect of Tfam knockdown on insulin signaling pathways

Cells were transfected with scrambled (*Scr*) or Tfam-directed (*siTfam*) siRNA oligonucleotides at day 2 of differentiation, and at day 6 were stimulated with the indicated concentrations of insulin for 15 minutes prior to harvest in lysis buffer with phosphatase and protease inhibitors. Western blots were performed using antibodies to ERK1 and -2 (*A*), Phospho S6 protein (*B*), and PAS antibodies (*C* and *D*). Shown are representative blots at lower (*C*) or higher (*D*) exposures. *Arrowheads* point to substrates that were increased, and the *arrow* points to one substrate detected that was decreased by Tfam knockdown. Similar results were obtained in three independent experiments.

Discussion

A possible relationship between mitochondrial levels and adipose tissue function has been inferred from results in animals and humans indicating that alterations in mitochondrial levels correlate with changes in insulin sensitivity (16-19, 21-27). In this report we have turned to a simple model, 3T3-L1 adipocytes, to determine whether a direct relationship between mitochondrial function and insulin sensitivity might indeed exist. Our results indicate that impaired induction of Tfam during differentiation results in cells with a relative deficiency in respiratory chain function but that still display many of the phenotypic characteristics of normal adipocytes. However, these cells have a reduced responsiveness to the stimulatory action of insulin on glucose transport. These results strongly suggest a specific link between respiratory chain function and glucose transport in adipose cells.

An unexpected finding in this study is that insulin stimulation of Akt phosphorylation is significantly increased in the Tfam-depleted cells. Thus, impairment of insulin action on glucose transport in cells depleted of Tfam is not due to defects in the early steps of the insulin-signaling pathway. This finding reveals a direct link between mitochondrial function and insulin action, where the activity of the respiratory chain impacts negatively upon insulin signaling to Akt. Importantly, these results are consistent with those seen in mice lacking apoptosis-inducing factor in muscle and liver, which display a progressive decrease in mitochondrial respiratory chain function (168), but have increased insulin sensitivity assessed by Akt phosphorylation and insulin tolerance. These findings as well as ours are also consistent with the finding that muscle-specific Tfam

knockout mice have enhanced glucose tolerance (169) , possibly resulting from improved insulin signaling. Thus, in muscle, liver, and 3T3-L1 adipocytes, a progressive defect in respiratory chain function results in enhanced insulin stimulation of Akt phosphorylation.

However, in contrast to that observed *in vivo* in muscle or liver of mice, glucose transport is clearly impaired in 3T3-L1 cells with respiratory chain deficiency. One potential cause for this difference is that the levels of GLUT4 and GLUT1 transporters are increased in muscle and liver of respiratory chain-deficient mice (168), yet no increase in expression of these transporters is seen in Tfam-depleted 3T3-L1 adipocytes. Moreover, compensatory mechanisms involving other tissues and longer adaptation times may resolve an initial impairment in insulin-stimulated glucose transport in muscle of respiratory chain-deficient mice. It also remains possible that the response of muscle and adipose tissue to respiratory chain dysfunction may differ *in vivo*. Further work to determine the effect of adipose-tissue-specific impairment of mitochondrial function on glucose homeostasis in whole animals will be required to answer these questions. Nevertheless, the results presented here provide evidence that, in adipose cells, impaired respiratory chain function results in impaired insulin-stimulated glucose transport under conditions where compensatory adaptative mechanisms are minimized.

The results shown here point to independent links between mitochondrial function, insulin signaling, and glucose transporter trafficking. The mechanisms by which a relative deficiency in respiratory chain activity could lead to enhanced insulin signaling to Akt are not known but are areas of great interest. Mitochondrial products that are known to enhance Akt phosphorylation include H_2O_2 and perhaps other ROS (170-171).

However, we do not see any increase in ROS in Tfam KO cells (Figure 2-7,), and elevated ROS was not seen in tissues from apoptosis-inducing factor knockout mice (168), perhaps reflecting the requirement for integrity of the electron transport chain for ROS production (172-174). Elucidating the mechanisms that link mitochondrial respiratory chain deficiency to enhanced insulin signaling will require identification of the potential compensatory pathways elicited by Tfam-depletion in adipose cells.

With respect to the mechanisms by which Tfam knockdown might lead to impaired glucose transport despite enhanced insulin signaling to Akt, the results shown here using antibodies directed to phospho-Akt substrates suggest the possibility that mitochondrial dysfunction might affect specific substrates potentially involved in GLUT4 translocation. A clear defect in the insulin-stimulated phosphorylation of a substrate of ~49 kDa is seen in Tfam knockdown cells, which correlates with the impairment in insulin-stimulated glucose transport. Although Akt substrates such as AS160 have been shown to be important in insulin-stimulated GLUT4 translocation (83, 175-176), additional factors are clearly necessary to mediate the full effect of insulin, and Tfam-sensitive ~49 kDa protein may be one of them. Further efforts to identify this substrate are ongoing.

In summary, two distinct functional relationships are revealed in these studies; first, a link between mitochondrial function and insulin signaling, in which impaired respiratory chain activity enhances insulin signaling to Akt phosphorylation, and second, a link between mitochondrial function and glucose transporter trafficking, where impairment of respiratory chain function leads to impaired GLUT4 translocation, perhaps

through specific defects in phosphorylation of one or more Akt downstream substrates. The net result of these effects is impairment in insulin-stimulated glucose transport in adipocytes. Although further work is necessary to assess the effects of impaired adipocyte mitochondrial function on whole body glucose homeostasis, our results indicate that such impairment can be a primary cause of insulin-resistant glucose transport at a cellular level.

CHAPTER III

ISOFORM-SPECIFIC REGULATION OF AKT SIGNALING BY THE ENDOSOMAL PROTEIN WDFY2

This chapter is in the format that it was published in the J Biol Chem. 2010;285(19):14101-8, as written by the authors, Walz HA[*], **Shi X[*]**, Chouinard M, Bue CA, Navaroli DM, Hayakawa A, Zhou QL, Nadler J, Leonard DM, and Corvera S. (*, These authors contributed equally)

Akira Hayakawa initiated the project. Qionglin Zhou performed the glucose uptake assay. My Chouinard performed most of the siRNA knockdowns, and all the qRT-PCR experiments in Figure 3-6. Catherine Bue performed the yeast two-hybrid interaction assays. I was responsible for the analysis of Akt signaling pathway using the PAS antibody and helped to make some constructs for yeast two-hybrid assays. Helena Walz performed all the imaging work and data processing. She also did some knockdown and immunoblotting experiments.

Abstract

Recent work has led to the identification of novel endocytic compartments with functional roles in both protein trafficking and growth factor signal transduction. The phosphatidylinositol 3-phosphate binding, FYVE domain-containing protein WDFY2 is localized to a distinct subset of early endosomes, which are localized close to the plasma membrane. Here, we find that the serine/threonine kinase Akt interacts with these endosomes in an isoform-specific manner. Using quantitative fluorescence microscopy we demonstrate specific co-localization of WDFY2 with endogenous Akt2, but not Akt1. Moreover, depletion of WDFY2 leads to impaired phosphorylation of Akt in response to insulin due to isoform specific reduction of Akt2, but not Akt1, protein levels, and to a marked reduction in the insulin-stimulated phosphorylation of numerous Akt substrates. This is accompanied by an impairment in insulin-stimulated glucose transport and, after prolonged silencing, a reduction in the level of expression of adipogenic genes. We propose that WDFY2-enriched endosomes serve as a scaffold that enables specificity of insulin signaling through Akt2.

Introduction

The early endocytic pathway is increasingly being recognized as a complex and heterogeneous membrane population in which distinct endosomal populations are specialized for the trafficking of different receptor types (177-178). Complexity and specialization in the endosomal pathway are achieved by the action of small GTPases and by the generation of specific phosphoinositides on the endosomal surface. One of the best studied examples of this mechanism is the specific and temporal targeting of proteins containing FYVE domains to phosphatidylinositol 3-phosphate (179-182), which is present almost exclusively in endosomal membranes. The human genome encodes for >30 proteins that contain FYVE domains, several of which are highly conserved and which may contribute in different ways toward establishing the complexity and functionality of the endocytic pathway. We recently characterized one of these proteins, WDFY2, named for its content of WD40 motifs and a FYVE domain (146). In *Caenorhabditis elegans*, WDFY2 depletion impairs endocytosis in coelomocytes, and in mammalian cells it defines a distinct set of endosomes that lack the canonical markers EEA1 and Rab5 and are further distinguished by their close proximity to the plasma membrane (146, 183).

In addition to internalization, the endosomal pathway plays a critical role in modulating signal transduction. Growth factor receptors are internalized immediately following activation, and both their fate and their signaling functions are affected by their transit through the endocytic pathway (184-188). Different receptors traffic through distinct early endosomal compartments (177-178), and their signaling functions are

modulated by the specific nature of the endosomes through which they traffic. For example, signaling by transforming growth factor β is influenced by the endosomal localization of the SMAD-interacting protein SARA, which is found in endosomes containing the canonical marker EEA1 (189-190).

In another example, the endosomal proteins APPL (adaptor protein containing PH domain, PTB domain, and leucine zipper motif) 1 and APPL2, which reside in an endosomal population devoid of EEA1 (191), regulate signaling by interacting with downstream effectors, such as the protein kinase Akt (114-116, 191-193). It has been proposed that the interaction of Akt with APPL facilitates the phosphorylation of specific substrates (116). Interestingly, WDFY2 has been identified in a yeast two-hybrid screen as an interacting partner with protein kinases Akt and protein kinase Cζ (194-195). In addition, recent studies indicate that endosomes that contain APPLs bind WDFY2 as they lose APPL (183). These studies suggest that WDFY2 may have a specific role in modulating signaling through Akt downstream of the interaction of this kinase with APPL.

Akt constitutes a node for many signaling cascades downstream of phosphatidylinositol (3,4,5)-trisphosphate, regulating metabolism, protein synthesis, cell growth, and survival (62, 196). This diversity in Akt signaling is orchestrated by three mammalian isoforms, Akt1, Akt2, and Akt3, that share a conserved structure with three functional domains: an N-terminal PH domain, a kinase domain, and a C-terminal regulatory domain containing a phosphorylation site (F*XX*F(S/T)Y) (197). These isoforms share ~80% sequence homology and phosphorylate substrates containing the

minimal consensus sequence R*X*R*XX*p(S/T), where S/T is the phosphorylation site and *X* any amino acid. Studies in isoform-specific Akt knock-out mice indicate that the three isoforms have overlapping but distinct physiological functions (196). For example, $Akt2^{-/-}$ mice display a strong metabolic phenotype, with diabetes type 2-like symptoms (73-74), not seen in $Akt1^{-/-}$ or $Akt3^{-/-}$ mice (142, 198). Similarly, on a cellular level, siRNA knockdown studies of Akt1 and Akt2 in 3T3-L1 adipocytes revealed Akt2 as the primary isoform involved in insulin signaling despite the presence of both Akt1 and Akt2 in these cells (199). The mechanisms that fine tune the activities of the three Akt isoforms for them to achieve their specific physiological functions are not clear.

Here, we investigate the role of WDFY2-enriched endosomes in Akt signaling in mature 3T3-L1 adipocytes. Using quantitative image analysis, we find an isoform-specific selective interaction between WDFY2 and Akt2, as opposed to the Akt1 isoform. We observe that WDFY2 depletion leads to decreased levels of Akt2 protein levels and attenuated insulin-stimulated phosphorylation of Akt. The functional importance of the isoform-specific interaction between WDFY2 and Akt2 was demonstrated by decreased insulin-stimulated glucose uptake and a global attenuation of phospho-Akt substrate phosphorylation in WDFY2-depleted cells. Together, these results indicate that WDFY2 serves as a molecular scaffold that enables signaling specificity, demonstrating a mode of regulation that distinguishes between Akt1 and Akt2.

Experimental Procedures

Tissue Culture and Gene Silencing

3T3-L1 cells were obtained from American Type Culture Collection and were grown under 5% CO_2 in Dulbecco's modified Eagle's medium supplemented with 10% fetal bovine serum, 50 units of penicillin/ml, and 50 μg of streptomycin/ml, which was replaced every 48 hours unless otherwise stated. Three days after confluence, the medium was replaced with Dulbecco's modified Eagle's medium containing a differentiation mixture consisting of 0.5 mm 3-isobutyl-1-methylxanthine (Sigma), 0.25 μm dexamethasone (Sigma), and 1 μm insulin (Sigma). 72 hours later, the medium was replaced with Dulbecco's modified Eagle's medium. Gene silencing was conducted 4 days after differentiation through electroporation (10 nmol of siRNA/15-cm plate). Scrambled (Scr) siRNA or siRNA oligonucleotides against mouse WDFY2 were obtained from Dharmacon. Electroporation was performed using a Bio-Rad Gene Pulser II (0.18 kV and 960 microfarads).

Antibodies and Fluorescent Probes

Rabbit antibodies to the full-length WDFY2 protein were affinity-purified against full-length bacterially expressed WDFY2. Mouse antibodies to the N terminus of EEA1, rabbit PAS antibody (R*X*R*XX*p(S/T)) (catalog no. 9614, 1:1000 dilution), phospho-Akt (Ser^{473}) antibody (catalog no. 9271), Akt2 (5B5) rabbit monoclonal antibody (catalog no. 2964), and Akt1 (2H10) mouse monoclonal antibody (catalog no. 2967) were from Cell Signaling. Mouse anti-β-actin antibody was from Sigma. Secondary detection was with

Alexa Fluor-coupled species-specific antibodies obtained from Molecular Probes (Eugene, OR).

2-Deoxyglucose Uptake

3T3-L1 adipocytes were plated in a 24-well multiwell tissue culture plate and differentiated. The cells were serum-starved for 2 hours in Krebs-Ringer HEPES buffer (130 mm NaCl, 5 mm KCl, 1.3 mm $CaCl_2$, 1.3 mm $MgSO_4$, and 25 mm HEPES, pH 7.4, supplemented with 0.5% bovine serum albumin, and 2 mm sodium pyruvate) and then stimulated with 1 or 100 nM insulin for 30 minutes. Glucose uptake was initiated by addition of [1,2-^{3}H]2-deoxy-D-glucose at a final assay concentration of 100 μm, for 5 minutes, at 37 °C. The cells were washed in ice-cold phosphate-buffered saline and lysed with 0.4 ml of 1% Triton X-100. ^{3}H content was determined by scintillation counting. Nonspecific deoxyglucose uptake was measured in the presence of 20 μm cytochalasin B and subtracted from each determination to obtain specific uptake.

Quantitative Real-time PCR (qRT-PCR)

mRNA isolation was performed using the TRIzol reagent protocol (Invitrogen). Prior to mRNA collection, the cells were washed twice with ice-cold phosphate-buffered saline. The concentration and purity of mRNA were determined by absorbance measurement at 260/280 nm. 2 μg of mRNA was used for cDNA synthesis (20-μl reaction) using an iScript cDNA synthesis kit (Bio-Rad). For RT-PCR, 1 μl of cDNA was used for detection of specific gene targets. Primers used were designed using PrimerBank and were synthesized by Operon. Ferritin was used as an internal control. Quantitative RT-PCR was run using the MyIQ Real-time PCR system (Bio-Rad).

Immunoblotting

The cells were washed twice with ice-cold phosphate-buffered saline and scraped into lysis buffer (1% SDS, 120 mm NaCl, 1.6 mm HEPES, pH 7.4, 800 mm NaF, 4 μm $NaPP_i$, and protease inhibitors) and homogenized by seven passages through a 27-gauge needle. The samples were centrifuged for 5 minutes at 500 × *g*, and protein concentration was determined by BCA (Pierce). 10 μg of proteins was separated on SDS-PAGE and transferred to nitrocellulose. The membranes were blocked with 5% nonfat milk in Tris-buffered saline with 0.1% Tween 20 and incubated with primary antibodies overnight. Anti-rabbit or anti-mouse IgG horseradish peroxidase-conjugated antibodies (Promega) were used in combination with enhanced chemiluminescence (PerkinElmer Life Sciences) for detection.

Optical System and Image Analysis

Epifluorescence images were taken using a Zeiss Axiovert 200 inverted microscope with a Zeiss 100 × 1.40 NA oil-immersion objective equipped with a Zeiss AxioCam HR CCD camera with 1300 × 1030 pixel resolution. To visualize WDFY2-enriched endosomes, images were smoothed by convolving with a small, two-dimensional Gaussian spot that preserved the mean intensity. The local background around the endosomes was estimated by convolving with a larger, two-dimensional Gaussian and subtracting this from the smoothed images. From this we generated a binary masking image by setting the intensity of all positive-valued pixels to 1 and all other pixels to 0. We then multiplied the mask by the original images (200).

Yeast Two-hybrid Assays

Strains were made by co-transforming two vectors (pGAD-T7 and pGBK-T7) into AH109 (mat a) yeast (Clontech) using standard yeast transformation procedures (lithium acetate transformation). AH109 contains *MEL1*, *ADE2*, *HIS3*, and *LACZ*, reporter genes, such that interaction of the bait and prey constructs will allow transcription of these four gene products. Vectors used were: pGAD-T7 (empty vector), pGBK-T7 (empty vector), pGBK-T7-WDFY2, pGAD-T7-Akt1, and pGAD-T7-Akt2. Co-transformed strains were maintained on Synthetic defined-Trp-Leu agar plates. Strains were grown overnight (~16 hours) on a 30 °C wheel in Synthetic defined-Trp-Leu + kanamycin. Cultures were back-diluted to A = 0.1 in Synthetic defined-Trp-Leu-Ade-His + kanamycin medium, and after 18–20 hours at 30 °C a quantitative X-α-gal assay was performed as described(201). Cultures were combined with X-α-gal buffer, and 145 μl was added to a row or column on a 96-well plate. One row/column contained medium and X-α-gal buffer only as a blank. Once cell cultures with X-α-gal buffer were added to 96-well plates, plates were placed on a shaker at room temperature, and readings were done at different time points in a Tecan SAFIRE II at 410 and 600 nm, to monitor α-galactosidase activity and growth, respectively. Averages of 8 wells from each strain were calculated, and the average blank reading was subtracted.

Results

To elucidate the function of WDFY2-enriched endosomes in a specific functional context, we utilized 3T3-L1 adipocytes, where both trafficking of GLUT4 and signaling through the insulin receptor can be evaluated. Depletion of WDFY2 led to a significant inhibition of insulin-stimulated glucose uptake in 3T3-L1 adipocytes (Figure 3-1, *A*). This effect was due to the combination of decreased insulin sensitivity and reduced basal uptake of glucose compared with cells exposed to Scr siRNA and was comparable with that seen upon depletion of Akt2, a known required signaling component in insulin-stimulated glucose uptake. The effectiveness of WDFY2 and Akt2 knockdown by siRNA oligonucleotides was evaluated by measuring both mRNA and protein levels of each. Compared with Scr, WDFY2 and Akt2 knockdown cells showed a highly significant ~85–90% decrease in their respective mRNA (Figure 3-1, *B*). The levels of WDFY2 protein, evaluated by immunoblotting, were found to be reduced by ~60% (Figure 3-1, *C*, *top panel*), and Akt2 protein was reduced to undetectable levels (Figure 3-1, *C*, *middle panel*, *right lane*). Analysis of GLUT4 by immunofluorescence did not reveal significant alterations in the levels of the transporter (not illustrated). However, an unexpected marked reduction of Akt2 protein levels was observed in WDFY2-depleted cells (Figure 3-1, *C*, *middle panel*), suggesting that the impairment in insulin-stimulated glucose transport seen in response to WDFY2 depletion is due to impaired signaling through the Akt pathway.

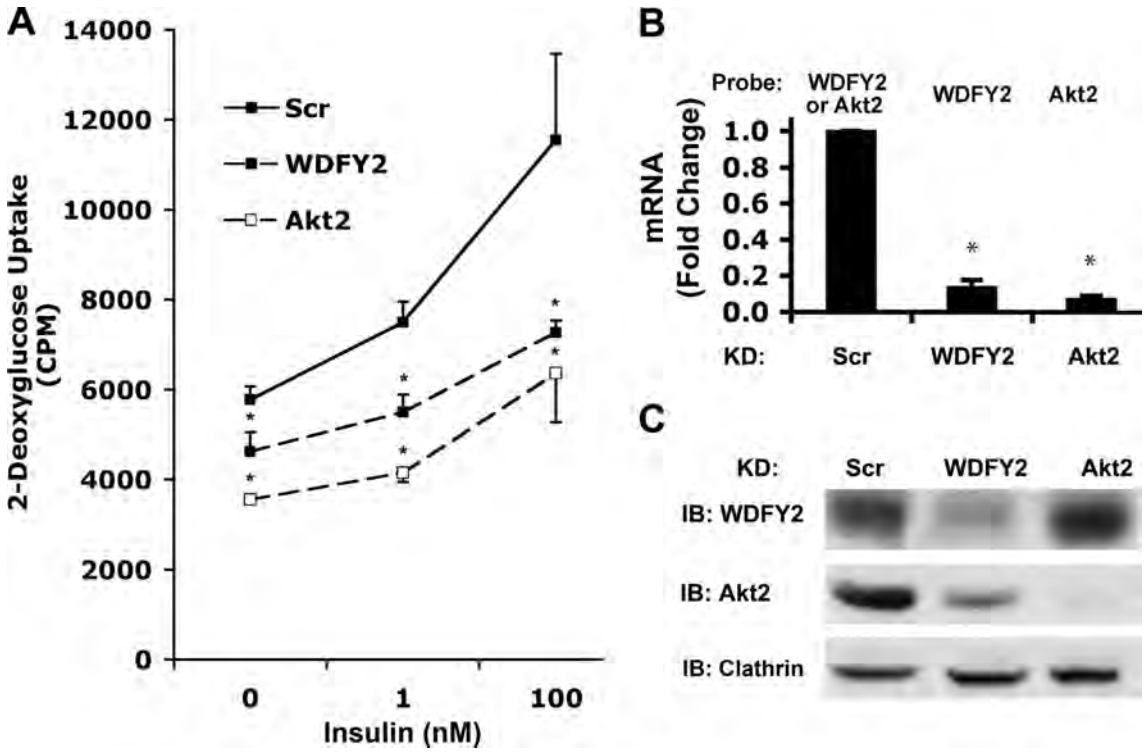

Figure 3-1 Effect of WDFY2 depletion on insulin-stimulated glucose uptake

(*A*), 3T3-L1 adipocytes, day 5 of differentiation, were transfected with Scr, WDFY2, or Akt2 siRNA. 48 hours after transfection, the cells were serum-starved (3 hours), and 2-deoxyglucose uptake was measured after 30 minutes of insulin stimulation (1 or 100 nM) (n = 3, mean cpm ± S.E. (*error bars*), $p < 0.01$, Student's t test). (*B*), WDFY2 and Akt2 mRNA levels were determined by qRT-PCR (n = 3, $p < 0.01$, Student's t test). (*C*), lysates from (*A*) were subjected to SDS-PAGE, and WDFY2 and Akt2 protein levels were analyzed by immunoblotting (*IB*). Clathrin was used as a loading control.

Effects of WDFY2 Depletion on Akt

To determine whether WDFY2 depletion impaired Akt activation, we used a phospho-specific antibody to Akt serine 473. Insulin stimulation resulted in a pronounced increase in staining intensity in all regions of the cell, predominating in the cell periphery and in the nucleus (Figure 3-2, *A, lower left panel*). Staining in cells depleted of Akt2 was much dimmer and probably corresponded to the remaining phosphorylated Akt1 (Figure 3-2, *A*, compare *upper left* and *upper* and *lower center panels*). Consistent with a negative effect of WDFY2 depletion on Akt signaling, pAkt(473) immunofluorescence in insulin-stimulated WDFY2 knockdown cells was significantly reduced compared with insulin-stimulated controls (Figure 3-2, *A*, compare *lower left* with *lower right panels*). Quantification of the average intensity/cell from several independent experiments revealed an average decrease of 50–60% in pAkt(473) staining intensity in response to either Akt2 or WDFY2 knockdown in insulin-stimulated cells (Figure 3-2, *B*).

To corroborate the immunofluorescence results, we analyzed whole cell extracts by western blot. Depletion of WDFY2 caused a significant decrease in the levels of pAkt in response to insulin, in particular at submaximal insulin concentration (Figure 3-2, *C, top panel*). Surprisingly, analysis of total Akt proteins levels revealed that WDFY2 depletion caused a selective decrease in the levels of the Akt2 isoform (Figure 3-2, *C, second panel* from *top*), leaving Akt1 and control proteins such as actin unaffected (Figure 3-2, *C, bottom two panels*). This result is noteworthy because Akt2 and Akt1 are highly homologous, and the mechanisms by which insulin action is dependent specifically on Akt2 are unknown. To evaluate the specificity of the observed effects of

WDFY2 depletion on Akt2, several different oligonucleotides directed to WDFY2 (Oligo 1, 2 and 3) and knockdown of another FYVE-domain protein, EEA1, were analyzed (Figure 3-2, *D*). The decrease in Akt2 protein levels correlated with the effectiveness of the WDFY2 knockdown and was unaltered in response to EEA1 knockdown, revealing specificity for WDFY2 and Akt2 interactions.

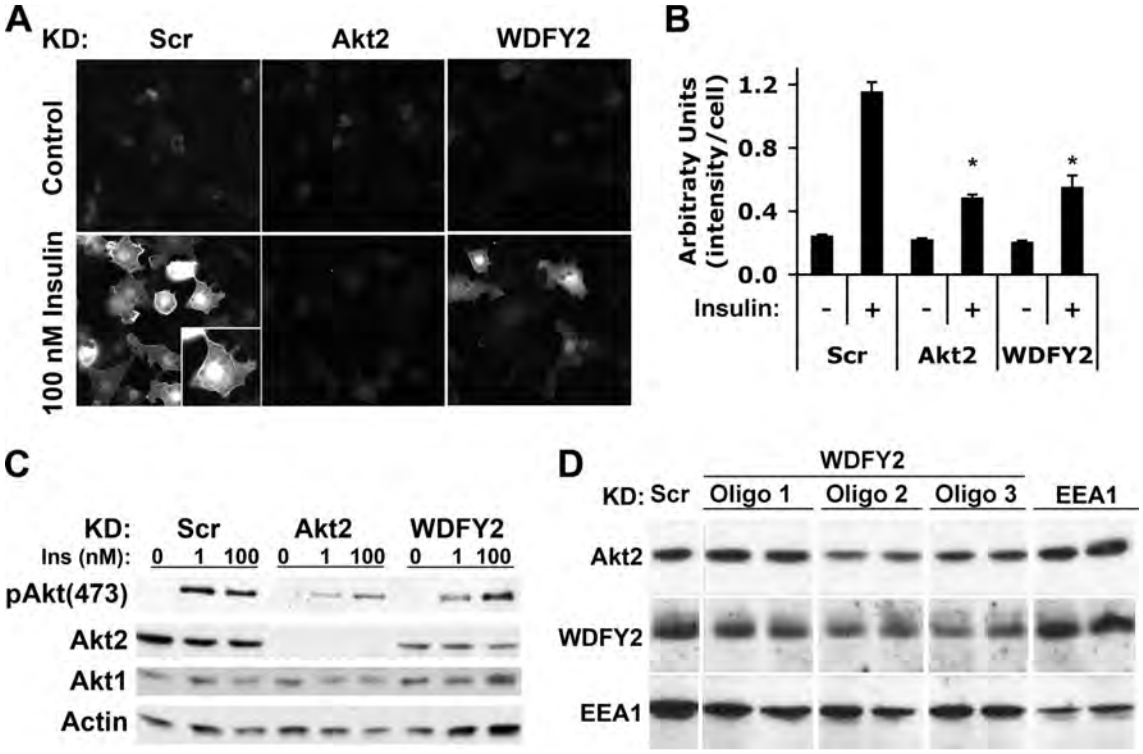

Figure 3-2 Effect of WDFY2 depletion on Akt phosphorylation

(*A*), 3T3-L1 adipocytes transfected with Scr, WDFY2, or Akt2 siRNA 48 hours prior to the experiment were serum-starved and insulin-stimulated for 15 minutes (100 nM). The cells were briefly washed and fixed in 4% formaldehyde (15 minutes) and 95% methanol (5 minutes) prior to immunofluorescence analysis of pAkt(473). (*B*), average intensity of immunofluorescence staining in control and insulin-stimulated cells from *A* is shown. 20 frames representing a total of ~375 cells per group were analyzed and are presented as mean intensity/cell ± S.E. (*error bars*), $p < 0.01$, Student's *t* test. (*C*), 3T3-L1 adipocytes transfected with Scr, WDFY2, or Akt2 siRNA 48 hours prior to the experiment were serum-starved and insulin (*Ins*)-stimulated for 15 minutes (1 or 100 nM). Lysates were subjected to SDS-PAGE and immunoblotting using pAkt(473), Akt2, Akt1, and actin antibodies. (*D*), 3T3-L1 adipocytes were transfected with Scr, WDFY2, or EEA1 siRNA 48 hours prior to lysis. Three different WDFY2 oligonucleotides (*Oligos*) 1–3 were used. Lysates were subjected to SDS-PAGE and immunoblotting using antibodies to Akt2, WDFY2, and EEA1.

To determine whether the decreased levels of Akt2 protein observed in response to WDFY2 knockdown were due to transcriptional or post-transcriptional responses, Akt2 mRNA and protein levels were analyzed after 24, 48, and 72 hours of WDFY2 knockdown. Akt2 protein levels were diminished at 24 hours and continued to decrease significantly with time (Figure 3-3, *A*). Interestingly, the initial drop in Akt2 levels, after 24 hours, was not coupled to a reduction in Akt2 mRNA (Figure 3-3, *B*). However, at 48 and 72 hours of WDFY2 knockdown Akt2 mRNA start to fall to significantly lower levels (Figure 3-3, *B*). These results suggest that the initial event following WDFY2 knockdown is a decrease in Akt2 protein levels.

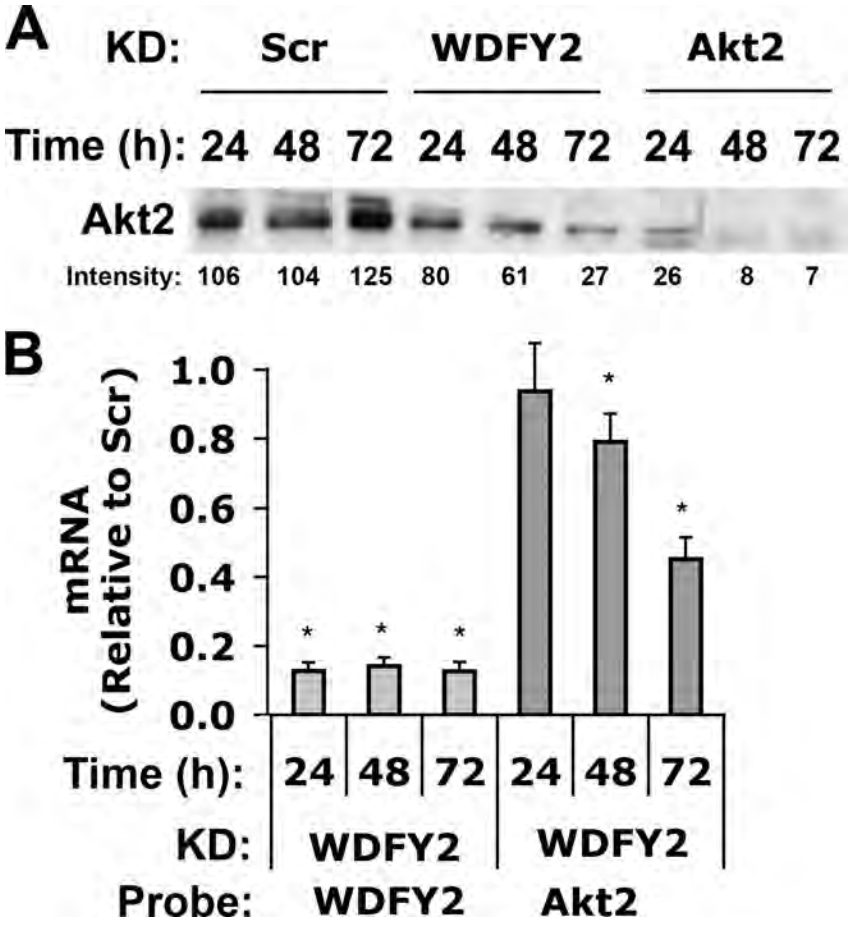

Figure 3-3 Time course of the effect of WDFY2 depletion on Akt2 mRNA and protein levels

(*A*), 3T3-L1 adipocytes transfected with Scr, WDFY2, or Akt2 siRNA were analyzed for the expression of Akt2 by western blot 24, 48, and 72 hours after transfection (n = 3, representative blot). (*B*), WDFY2 and Akt2 mRNA levels were determined 24, 48, and 72 hours after knockdown of WDFY2 using qRT-PCR (n = 3, mean ± S.E. (*error bars*), $p < 0.01$, Student's *t* test).

Localization of Endogenous Akt1 and Akt2 Relative to WDFY2

WDFY2 is localized on a population of early endosomes that lack canonical early endosome markers and reside close to the plasma membrane (146). The mechanism by which WDFY2 exerts a selective effect on Akt2 levels, but not the highly homologous kinase Akt1, could involve a preferential interaction of WDFY2 with Akt2 in response to normal cellular compartmentalization of these two kinases. To explore this possibility, the localization of endogenous WDFY2 relative to endogenous Akt1 and Akt2 was analyzed. 3T3-L1 adipocytes were stimulated with insulin, fixed, and stained with antibodies to endogenous WDFY2, and either Akt1 or Akt2. Both Akt1 and Akt2 were seen in the nuclear region as well as diffusely distributed in the cytoplasm (Figure 3-4, *A* and *B, lower panels*). In addition, punctate staining was consistently seen in both starved and insulin-stimulated cells stained for Akt2, being more predominant in cells stimulated with insulin (Figure 3-4, *A, lower panels*). WDFY2 staining was much more punctate, corresponding to its localization to endosomes (Figure 3-4, *A* and *B, upper panels*).

Because of the broad distribution of Akt1 and Akt2, image overlaps alone would be inadequate to evaluate whether meaningful co-localization of either of these kinases with WDFY2 exists. To address this issue, we generated binary masks of the images of WDFY2 to delineate the regions corresponding to WDFY2-enriched endosomes. When superimposed on each image, these masks reveal the signal specifically present in the regions occupied by WDFY2-enriched endosomes (Figure 3-4, *A* and *B, center panels*). To measure the fluorescence intensity outside WDFY2-containing endosomes, the masks were displaced by 10 pixels in the x and y axes. As expected, when the masks were

superimposed on images of WDFY2, the fluorescence intensity in the mask was much higher than that in the displaced mask (Figure 3-4, ***A*** and ***B***, compare ***upper center*** and ***right panels***). When the corresponding Akt2 image was analyzed, significantly higher fluorescence intensity was detected within the mask corresponding to WDFY2 endosomes than in the displaced mask (Figure 3-4, ***A***, compare ***lower center*** and ***right panels***). In contrast, when Akt1 staining was analyzed, similar fluorescence intensity was detected within the mask corresponding to WDFY2 endosomes than within the displaced mask (Figure 3-4, ***B***, compare ***lower center*** and ***right panels***). These results are quantified in Figure 3-4, ***C*** and ***D***, in which the fluorescence intensity in the displaced mask is expressed relative to that inside the mask from 5–10 cells from independent experiments. These results indicate that, at steady state, endogenous Akt2 associates with WDFY2-enriched endosomes to a much greater extent than endogenous Akt1.

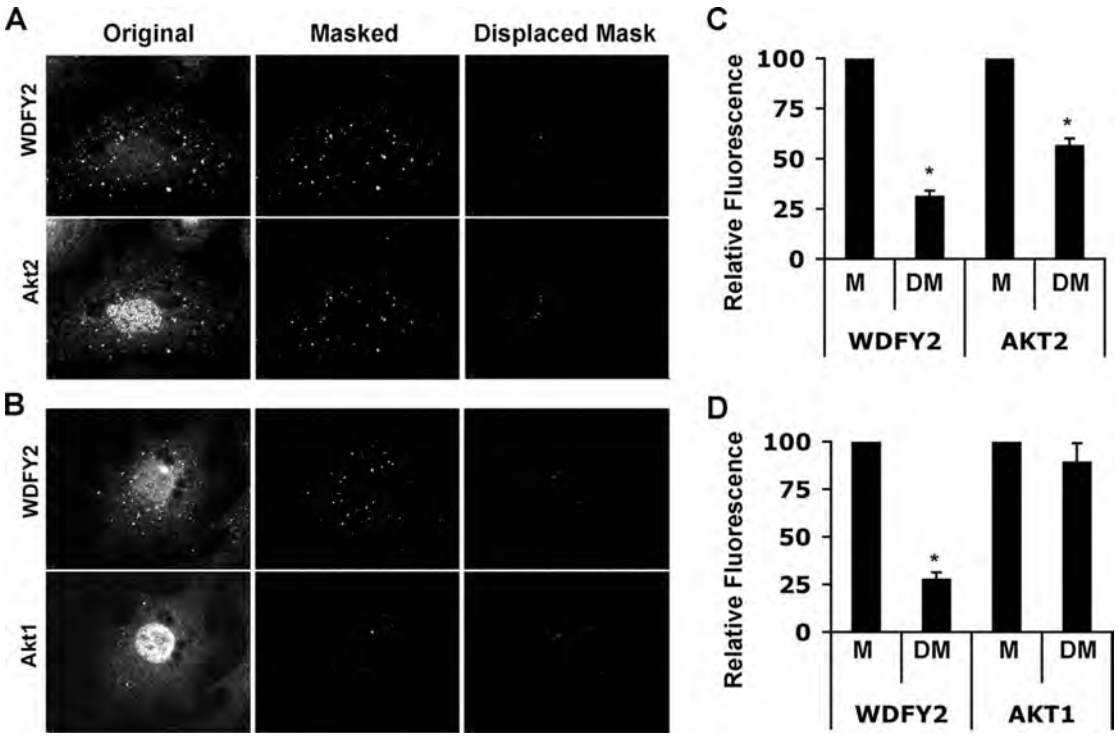

Figure 3-4 Co-localization of endogenous Akt isoforms with WDFY2

3T3-L1 adipocytes at day 7 of differentiation were serum-starved and stimulated with 100 nM insulin for 30 minutes. Endogenous WDFY2 and Akt2 or Akt1 was detected by fluorescent immunostaining. (*A*) and (*B*), the *left panels* display raw images of WDFY2, Akt2, or Akt1. Digital binary masks revealing the regions encompassed by WDFY2 endosomes exclusively were generated. The product of the raw images and the binary mask were labeled as *Masked* and are displayed in the *center panels*. As a control for nonspecificity the generated mask was shifted 10 pixels in the *x* and *y* planes and referred to as *Displaced Mask*. The product of the raw image and the Displaced Mask is displayed in the *right panels.* (*C)* and (*D*), quantification of fluorescence intensity in the Masked (*M*) or Displaced Masked (*DM*) WDFY2 and Akt2 or Akt1 images (average of 5–10 cells, mean ± S.E. (*error bars*), $p < 0.01$, Student's *t* test).

Effects of Akt2 Depletion on Akt Substrate Phosphorylation

The decrease in Akt2 levels may underlie the decrease in insulin-stimulated glucose transport seen in cells depleted of WDFY2. For this to be the case, the decrease in Akt2 levels would have to be of a magnitude sufficient to impair its signaling functions. To determine first the relationship between Akt2 levels and Akt substrate phosphorylation, we analyzed cell extracts by western blot with anti-pAkt (473) and with an antibody (PAS) to the phospho-Akt substrate motif R*X*R*XX*p(S/T). Cells transfected with Scr or Akt2-directed siRNAs were treated with 10 nM insulin for 5, 15, 30, 45, and 75 minutes (Figure 3-5, *A*). In Scr siRNA-transfected cells (Figure 3-5, *A* and *B*, *left*), maximal pAkt(473) levels were reached within 5 minutes of insulin addition. In Akt2 knockdown cells (Figure 3-5, *A*, *right*), pAkt(473) levels were diminished at every time point after insulin addition, and Akt2 protein levels were reduced to undetectable levels. Immunoblotting with PAS antibody revealed numerous substrates phosphorylated in response to insulin (Figure 3-5, *A* and *B*, *left*). Although some of these (*band I*) displayed a time course of phosphorylation that closely paralleled that of pAkt(473) (compare Figure 3-5, *C* and *D*), others (*band II*) showed maximal phosphorylation at significantly later time points (compare Figure 3-5, *C* and *E*), or a continuous increase over the time period studied (*band III*, Figure 3-5, *F*).

This result suggests that the phosphorylation of some of the proteins detected by the PAS antibody is under complex regulation, possibly reflecting variations in Akt substrate affinity, spatial constraints, phosphatase activities, or phosphorylation by kinases other than Akt2. This latter possibility is suggested by the finding that

phosphorylation of some of the proteins detected by the PAS antibody in response to insulin was in fact increased in Akt2-depleted cells (Figure 3-5, *A, bands IV* and *V*, and Figure 3-5, *G* and *H*). This finding suggests the presence of at least one kinase that can phosphorylate the R*X*R*XX*p(S/T) motif and is negatively regulated by Akt2. In addition, Akt2 depletion resulted in pronounced changes in the kinetics of phosphorylation of some substrates more than in their maximal phosphorylation level (Figure 3-5, *A, band III*, and Figure 3-5, *F*).

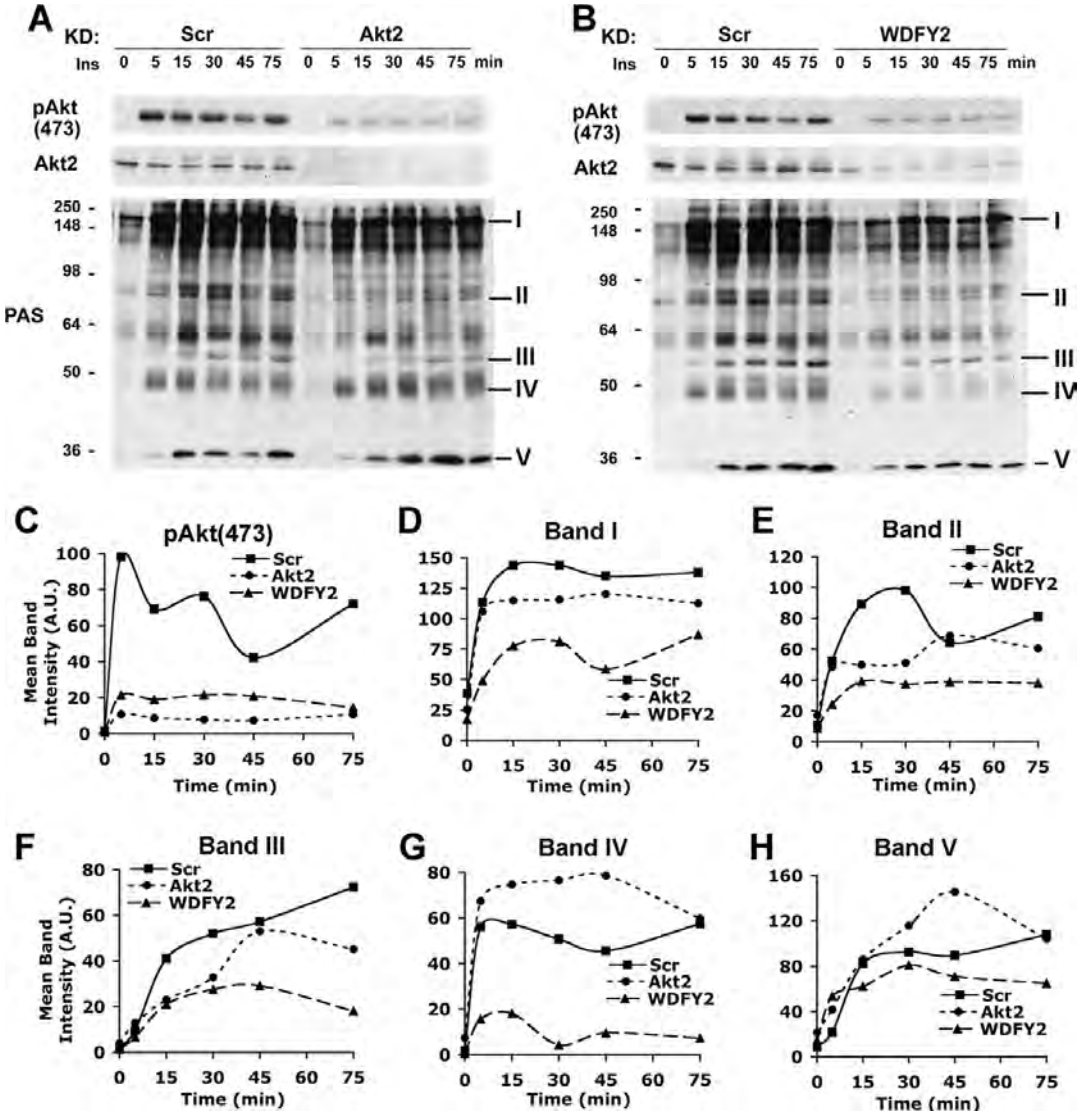

Figure 3-5 Effect of WDFY2 depletion on the dynamics of Akt substrate phosphorylation

(*A*) and (*B*), 3T3-L1 adipocytes transfected with Scr, Akt2 (*A*), or WDFY2 (*B*) siRNA on day 5 of differentiation were serum-starved and stimulated on day 7 with 10 nM insulin (*Ins*) for 0, 5, 15, 30, 45, or 75 minutes prior to lysis (n = 3, representative blot). Immunoblots were probed with pAkt(473), Akt2, or PAS antibodies. *C–H*, densitometric quantification of pAkt(473) (*C*) and *bands I–V* (*D–H*) in Scr *versus* Akt2 or WDFY2 immunoblots.

Effects of WDFY2 Depletion on Akt Substrate Phosphorylation

In cells depleted of WDFY2 (Figure 3-5, *B*, *right*), phosphorylation of Akt and of virtually all substrates detected with the PAS antibody was significantly reduced at all time points measured. This decrease in substrate phosphorylation was consistently more pronounced in WDFY2-depleted than in Akt2-depleted cells (compare *lower right panels* in Figure 3-5, *A* and *B*). Moreover, the phosphorylation of substrates such as bands IV and V, which was increased by Akt2 depletion, was also impaired by WDFY2 depletion (Figure 3-5, *A*, *B*, *G*, and *H*). The broader cellular requirements for WDFY2 than for Akt2 are also reflected by changes in gene expression patterns following knockdown of these two proteins (Figure 3-6). Indeed, we found that expression levels of numerous adipogenic and metabolic genes, including Glut-4, Glut-1, Cycs, Aco2, and nFAS, were more significantly decreased after WDFY2 knockdown than after individual Akt2 or Akt1 knockdowns, consistent with the finding that WDFY2 depletion impairs adipocyte differentiation (202). The finding that WDFY2 depletion has a broader effect on insulin-stimulated R*X*R*XX*p(S/T) substrate phosphorylation than depletion of Akt2 could reflect the need for WDFY2 for the activity of other insulin-sensitive kinases that can phosphorylate this motif. Also, it is possible that Akt1 may phosphorylate these substrates in Akt2-depleted cells, and WDFY2 may be necessary for this compensatory function of Akt1, even though under normal conditions it interacts preferentially with Akt2.

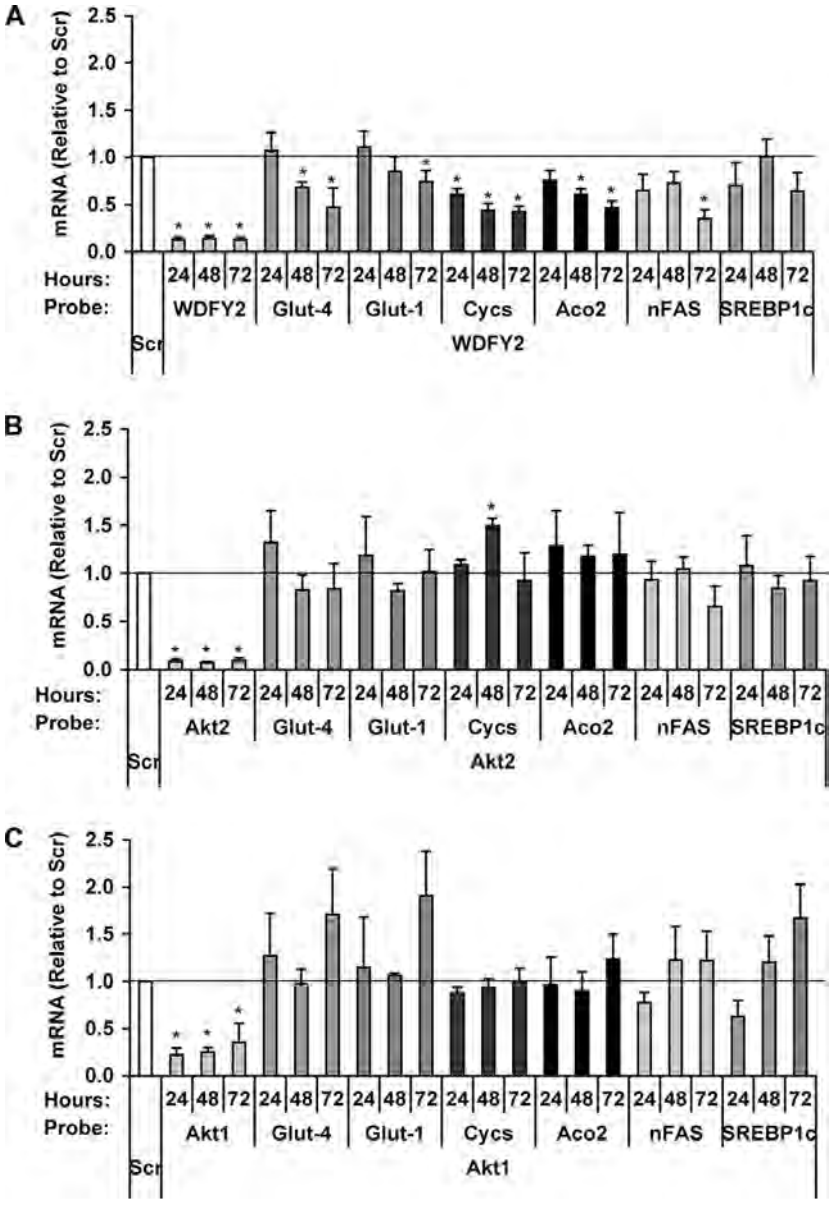

Figure 3-6 Differential effects of WDFY2 and Akt2 knockdown on mRNA of proteins key to adipocyte function

3T3-L1 adipocytes were transfected with Scr, WDFY2 (*A*), Akt2 (*B*), or Akt1 (*C*) siRNA on day 4 of differentiation. Samples collected 24, 48, or 72 hours after transfection were assayed for mRNA levels of WDFY2, Akt2, and Akt1, respectively, in addition to Glut-4, Glut-1, Cycs, Aco2, nFAS, and SREBP1c using qRT-PCR (n = 4, mean ± S.E. (*error bars*), $p < 0.01$, Student's *t* test).

Preferential Interaction of WDFY2 with Akt2 Compared with Akt1

The preferential co-localization of Akt2 in endosomes containing WDFY2 and the finding that knockdown of WDFY2 preferentially affects the levels and activity of Akt2 suggest a preferential interaction between WDFY2 and Akt2 *in vivo*. All Akt isoforms share 80% homology at the amino acid level throughout the functional domains common to all Akt isoforms. The isoform specificity of WDFY2 binding may result from a higher affinity in the interaction between the WD domains of WDFY2 with Akt2 compared with Akt1. These differences, however, are lost in over-expression studies, where WDFY2 can interact with Akt1 when both proteins are co-expressed (194) (data not shown). The difficulty in recapitulating isoform-specific behaviors of Akt isoforms upon over-expression has also been noted in studies describing a differential interaction of Akt isoforms with PH domain leucine-rich repeat protein phosphatases (203). To determine whether a significant difference exists in the ability of WDFY2 to interact with Akt1 or Akt2, we analyzed the interactions between full-length WDFY2 and full-length, hemagglutinin-tagged constructs of Akt2 and Akt1 in a quantitative yeast two-hybrid assay (Figure 3-7, *A*). A significant albeit weak interaction between WDFY2 and full-length Akt1 and Akt2 was detected by both growth and α-galactosidase in this assay, and the interaction of WDFY2 with Akt2 was significantly greater than that with Akt1 (Figure 3-7, *B* and *C*). These results indicate that subtle structural differences between these isoforms affect the affinity for WDFY2. These differences may be functionally relevant in mammalian cells, accounting for the differential localization of Akt2 and its sensitivity to WDFY2 levels.

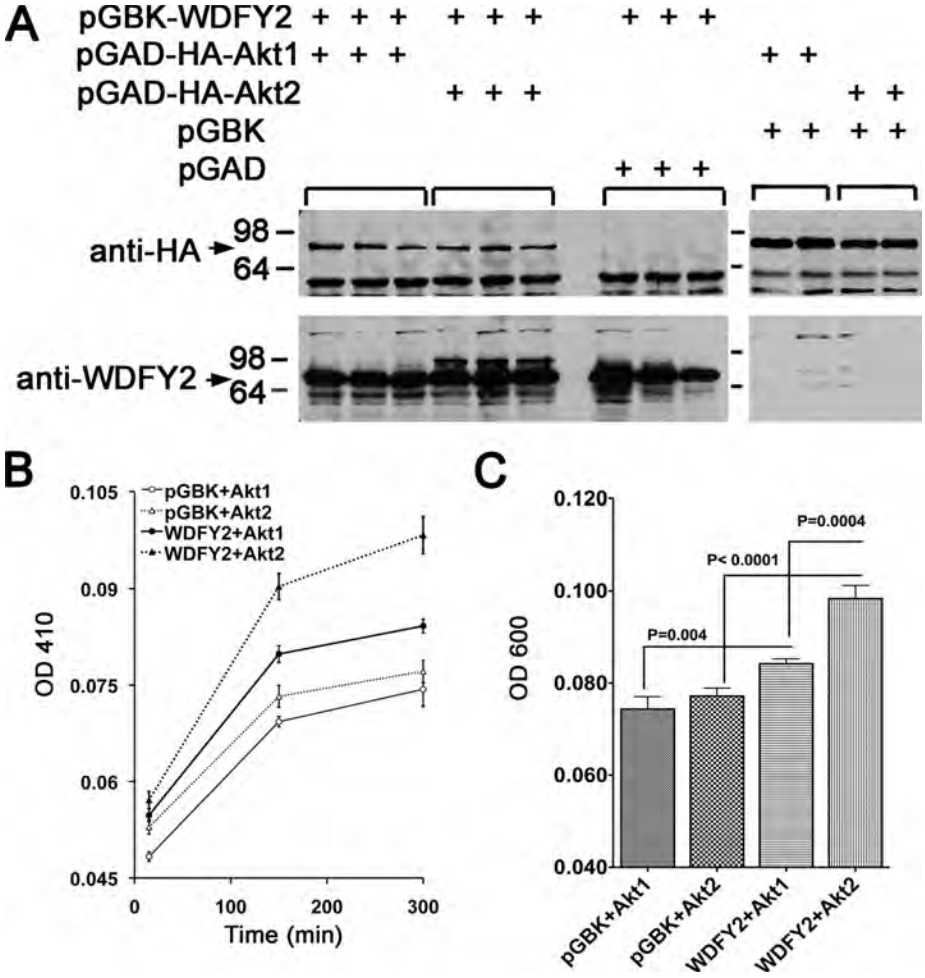

Figure 3-7 Interactions between WDFY2 and Akt1 or Akt2 in a yeast two-hybrid assay

Yeast were co-transformed with the indicated vectors and grown as described under "Experimental Procedures." (*A*), cells were lysed and analyzed by immunoblotting with anti-HA or anti-WDFY2 antibodies to confirm similar levels of expression of both Akts and expression of WDFY2 proteins. (*B*), cells were added to 96-well multiwell dishes, and α-galactosidase expression was measured over time. Similar results were obtained when measuring growth. (*C)*, quantification of growth after 300 minutes, where the statistical significance of the differences was calculated by two-tailed Student's *t* tests, is indicated in the figure.

Discussion

The mechanisms by which the different isoforms of Akt control specific aspects of cell function are not fully understood. Here, we find that the endosomal protein WDFY2 interacts preferentially with endogenous Akt2 and promotes the maintenance of Akt2 protein levels. This interaction is critical, as depletion of WDFY2 leads to generalized impairment in downstream substrate phosphorylation and in downstream effects of Akt2, such as insulin-stimulated glucose transport. Together with recent work demonstrating an important role for the endosomal protein APPL1 in the stimulation by Akt2 of glucose transporter translocation, our results underscore the critical role of the endocytic pathway in insulin signaling through Akt, and in fine tuning the specific roles of Akt isoforms in cell physiology. Thus, further experiments *in vitro* with purified proteins will be necessary to determine the structural basis and the detailed kinetics of the interactions between WDFY2 and each Akt isoform, to determine whether this mechanism could account for our observations in live cells.

Indirect mechanisms could also underlie the isoform-specific interaction between endogenous Akt2 and WDFY2. Immunofluorescence analysis of endogenous Akt1 and Akt2 shown here indicates a substantial amount of these kinases sequestered in the nucleus. Thus, subtle changes in the extent of nuclear translocation may lead indirectly to a preferential interaction of Akt2 with endosomal components. Further experiments to analyze the general determinants of Akt subcellular localization are necessary to test this hypothesis.

A salient effect of WDFY2 depletion is a decrease in total protein levels of Akt2, raising the question of how steady-state levels of Akt isoforms are controlled. The decrease in Akt2 protein levels seen in WDFY2-depleted cells occurs prior to a decrease in Akt2 mRNA levels, suggesting that posttranscriptional mechanisms such as increased degradation may be involved. Ubiquitination and degradation of Akt have been demonstrated to occur and be important during the establishment of neuronal polarity (204). Ubiquitination and degradation of Akt have also been implicated in the induction of insulin resistance by tumor necrosis factor and in tumorigenesis (205-206). However, it is not known whether the turnover of Akt1 and Akt2 proceeds at different rates or is controlled by distinct mechanisms. The association of Akt2 with WDFY2 on early endosomes may protect the kinase from ubiquitination and proteosomal degradation, whereas the sequestration of Akt1 in the nucleus may fulfill a similar protective role.

The findings that Akt interacts with two proteins that are localized to endosomes raises the possibility that these interactions may be functionally related. APPL1 has been shown to interact in adipocytes with Akt2, and its depletion leads to impairments in insulin-stimulated Akt phosphorylation and glucose uptake (115). Paradoxically, over-expression of full-length APPL1 also suppresses insulin action (115). These results, together with recent studies suggesting that APPL-enriched endosomes become enriched in WDFY2 as they lose APPL (183), suggest a model in which Akt2 may be transferred from APPL to WDFY2 to allow sustained substrate phosphorylation by this kinase (Figure 3-8). Knockout of APPL may impair insulin action by preventing the initial localization of Akt2 to the endocytic pathway, but over-expression may then impair the

transfer of Akt2 to WDFY2. A role for WDFY2 in sustaining Akt2 signaling is suggested by immunofluorescence data where cells over-expressing WDFY2 display enhanced phospho-Akt staining in response to insulin (data not shown). Further experiments imaging Akt dynamics relative to APPL and WDFY2 in live cells will be required to test this hypothesis.

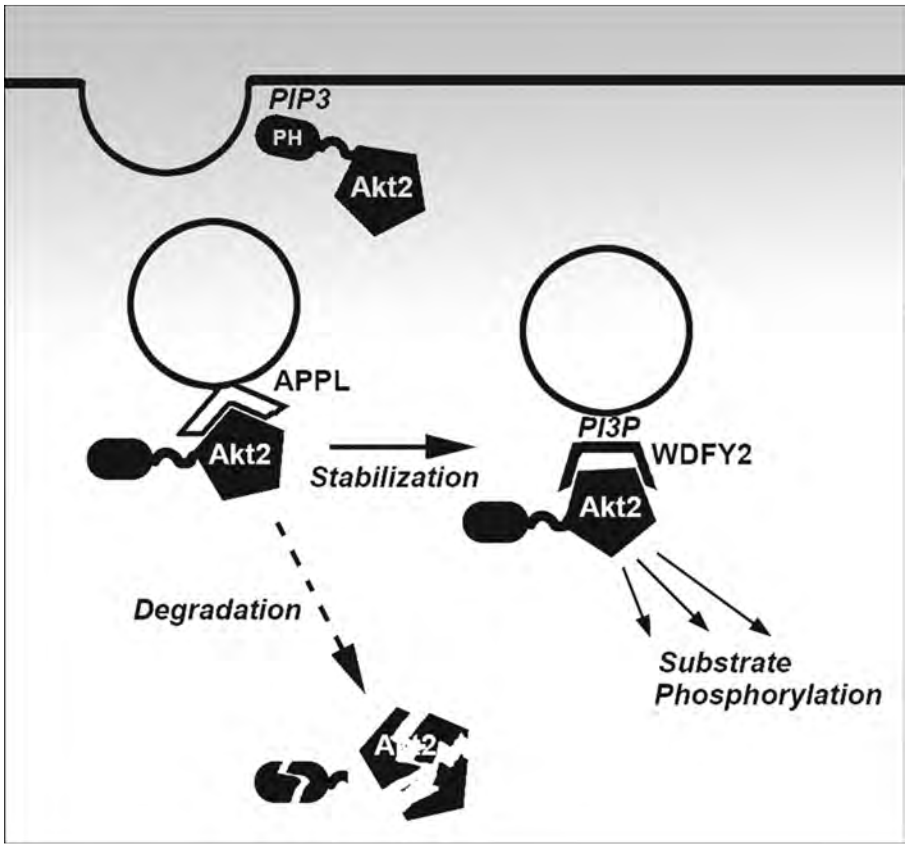

Figure 3-8 Model for role of WDFY2 in endosomal control of Akt2 signaling

In this model the initial event in Akt2 activation is the interaction of its PH domain with phosphatidylinositol (3,4,5)-trisphosphate (PIP_3) generated at the plasma membrane. Subsequently, the kinase interacts with APPL in the initial phase of endocytosis, when the levels of phosphatidylinositol (3,4,5)-trisphosphate decrease. Phosphatidylinositol 3-phosphate (PI3P) is then generated, and WDFY2 replaces APPL on endosomes. Akt2 binds to WDFY2 and becomes stabilized and protected from degradation. Substrate phosphorylation can proceed from WDFY2-enriched endosomes.

CHAPTER IV

SUMMARY AND DISCUSSION

This thesis work has investigated the effect of mitochondrial dysfunction on insulin signaling and glucose transport in 3T3-L1 adipocytes, showing that mitochondrial dysfunction can be a primary cause for insulin resistance in adipocytes. As one of the key events in insulin-stimulated glucose uptake in adipocytes, the regulation and activation of Akt is of importance. We also examined the role of another intracellular organelle, the endosome, in the regulation of signal transduction in 3T3-L1 adipocytes. Particularly we studied the endosomal protein WDFY2 and its involvement in Akt signaling transduction, revealing a mechanism through which Akt isoform specificity is regulated, at least partially, through the preferential interaction with WDFY2 (Figure 4-1).

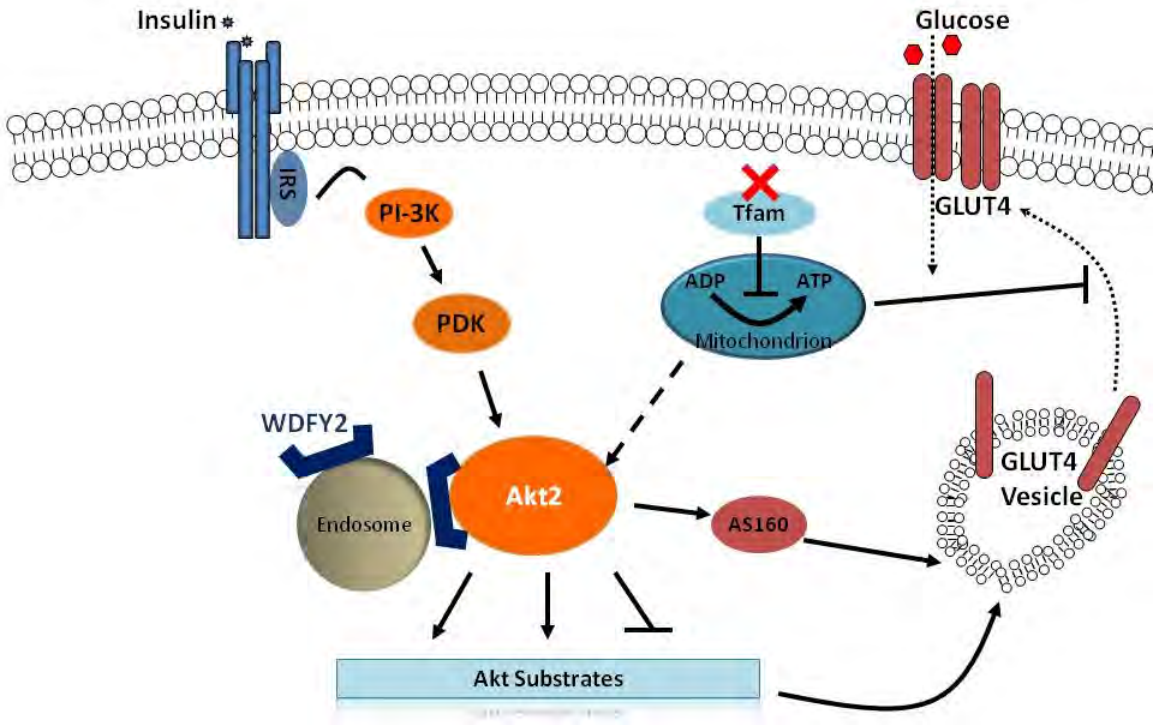

Figure 4-1 Model for insulin regulated glucose uptake in 3T3-L1 adipocytes involving the mitochondria and endosomes.

The depletion of Tfam results in reduced respiratory chain function and ATP synthesis in mitochondria, which in turn inhibits GLUT4 translocation to the cell membrane and glucose uptake, while increasing total phosphorylation of Akt at Ser^{473}. Endosomal protein WDFY2 has a higher affinity for Akt2 than for Akt1, thus specifically regulating Akt2 protein stability and its signaling transduction.

Mitochondrial Dysfunction and Insulin Resistance in WAT

In type 2 diabetes, the insulin-responsive organs including liver, skeletal muscle and adipose tissue fail to effectively respond to insulin, resulting in elevated blood glucose levels. It has been proposed that skeletal muscle accounts for the majority of the glucose uptake after a meal, based upon the fact that muscle comprises approximately 40% of the total body mass (207). However, a systematic failure of blood glucose control could be caused by a subtle imbalance between glucose production and clearance among several tissues, including adipose tissue. Therefore, even though adipose tissue does not constitute a significant portion of the whole body mass in an average person, its failure to take up blood glucose in response to insulin could still be a cause for type 2 diabetes. This leads to the idea that a healthy and functional adipose tissue is necessary for whole body energy homeostasis. In addition, compromised adipose tissue function is found to be associated with severe obesity and type 2 diabetes, further supporting such a hypothesis that healthy well-functioning adipose tissue is crucial for whole body energy homeostasis.

Adipocyte differentiation is accompanied by mitochondrial biogenesis (26), suggesting a requirement for increased mitochondrial function in adipocytes compared to preadipocytes. Although the exact role of mitochondrial biogenesis in adipocytes is not known, a growing body of evidence points to a close relationship between adipose mitochondrial dysfunction and type 2 diabetes (19-20). It appears that adipocyte mitochondrial biogenesis is an adaptive response to support its fat-specific function. Therefore we tested the hypothesis that inhibition of adipocyte mitochondrial biogenesis

could lead to impaired insulin action, particularly, impaired insulin-stimulated glucose uptake. Our approach was to create adipocytes with less mitochondrial biogenesis and then evaluate the effect on adipocyte functions.

There are many types of tissue-specific mitochondrial dysfunction animal models available; however none of them are WAT-specific (54-55). One possible reason is that adipose tissue has been conventionally considered as non-active tissue that requires limited mitochondrial activity. Another reason could be the lack of a WAT-specific promoter. To circumvent the disadvantages with *in vivo* animal models, we decided to employ the 3T3-L1 cell line, which is commonly used as a model for adipocytes differentiation and function.

In order to inhibit mitochondrial biogenesis or, equivalently, mitochondrial function, we started with the canonical master regulator of mitochondrial biogenesis PGC-1α. However, the activity of PGC-1α is so versatile that interfering with PGC-1α could lead to a very broad effect on cell functions and adipocyte differentiation, which would further complicate our interpretation of mitochondrial function in adipocytes. We then directly focused on the mitochondrial DNA, which is encapsulated in the mitochondrial membrane and encodes thirteen proteins specifically for mitochondrial ETC complexes and ATP synthase. The replication and transcription of mtDNA largely depend on Tfam. In fact, both mtDNA copy number and the expression of Tfam are markedly induced during adipocyte differentiation, suggesting a requirement for mtDNA amplification and transcription during adipogenesis. By introducing Tfam siRNA during the 3T3-L1 adipocyte differentiation, we were able to inhibit the increase in mtDNA copy

number and transcription. Further analysis revealed that general adipogenesis programming was not affected, evidenced by analysis of adipocyte functions and morphology. This was later supported by whole genome expression profiling with an Affymetrix GeneChip assay, in which less than 0.2% of total nuclear gene expressions changed by >1.5-fold (Table 4-1).

The specific inhibition of Tfam resulted in morphologically normal adipocytes with the exception that these adipocytes now showed reduced OXPHOS activity and ATP levels. The overall reduced OXPHOS activity was evidenced by a reduction in the consumption rate of oxygen, the electron acceptor of the ETC. As a result, the coupled generation of ATP from mitochondrial ATPase was also impaired. This was demonstrated in two ways: first, the steady-state intracellular ATP level was reduced by 10-15%; and second, the dynamic ATP synthesis from ATPase was reduced by 50%. Therefore, specific inhibition of Tfam allowed us to create adipocytes with impaired mitochondrial function, characterized by lower OXPHOS activity and ATP synthesis.

The effects of mitochondrial dysfunction in these Tfam-depleted adipocytes were then evaluated in the context of insulin-stimulated glucose uptake, which is an important function of adipocytes in glucose metabolism. ^{3}H-labeled 2-deoxyglucose (2-DOG) was used to determine the insulin-stimulated glucose in these adipocytes. Data showed that these Tfam-depleted adipocytes had reduced insulin-stimulated glucose uptake (Figure 2-5, *A*). 2-DOG is taken into the cell and is phosphorylated by hexokinase, but cannot be further processed along the glycolysis pathway. The removal of 2-DOG by hexokinase phosphorylation will facilitate the equilibrium of glucose towards entering the cell. To

exclude the possibility that impaired glucose uptake in Tfam-depleted adipocytes results from impaired phosphorylation of 2-DOG, a non-phosphorylatable glucose analogue 3-*O*-methylglucose was used to determine the glucose transport, which also showed reduced glucose uptake in Tfam-depleted adipocytes (Figure 2-5, *B*). These data suggest that mitochondrial dysfunction can impair insulin-stimulated glucose uptake, therefore could be a direct cause for insulin resistance in adipocytes.

We further explored the underlying mechanism for impaired insulin-stimulated glucose uptake in Tfam-depleted adipocytes. Insulin-stimulated activation of Akt and translocation of GLUT4 towards the cell membrane have been proposed to be crucial for glucose transport in adipocytes. We investigated whether these two events could be linked to the observed impairment in glucose uptake in Tfam-depleted adipocytes. First, we examined GLUT4 translocation in response to insulin stimulation. Taking advantage of TIRF technology, we were able to directly observe and quantify the membrane localization of the fixed-and-stained endogenous GLUT4 proteins, eliminating the complications of over-expressing a GLUT4 construct. Our data showed that the insulin-stimulated GLUT4 enrichment on the cell membrane significantly decreased with Tfam depletion in adipocytes, although the total cellular GLUT4 protein level was not changed, suggesting an impairment in GLUT4 trafficking to the cell surface. We speculated that this was due to a failure of Akt activation, since Akt has been shown to play a critical role in glucose uptake. At this point, we looked at the phosphorylation of Akt at Ser^{473} with insulin stimulation. Surprisingly, insulin-stimulated phosphorylation of Ser^{473} was increased in Tfam-depleted adipocytes; and this increase was not a result of elevated total

Akt protein level. This finding contradicts our belief that Akt phosphorylation should correlate with increased glucose transport.

The paradoxical effect of Tfam-depletion on glucose transport and Akt phosphorylation indicates that mitochondrial dysfunction might act through an Akt-independent mechanism to affect insulin-stimulated glucose uptake. Since Tfam-depletion impaired mitochondrial respiratory activity and ATP synthesis, we speculated whether decreased ATP level in these adipocytes caused such a phenotype. To mimic the effect of ATP depletion, we treated the cells with the ETC complex I inhibitor rotenone, which rapidly caused an ATP level drop, similar to the drop seen in Tfam-depleted cells (Figure 2-6, *A*). However, such a chemical inhibition on ETC simultaneously impaired the insulin signaling to Akt as assessed by Ser^{473} phosphorylation (Figure 2-6, *D*). The discrepancy in Akt phosphorylation between Tfam-depletion and rotenone inhibition reflects the difference between progressive and acute respiratory chain impairment, in which Tfam-depletion may elicit compensatory changes during several days of differentiation. The increased Akt phosphorylation could be one of such compensatory changes. Furthermore, acute inhibition of ETC by rotenone exposure causes a quick adaptive change with increased glucose uptake (163), which is opposite to what we observed in the Tfam-depleted cells. Thus, acute drug treatment is not an ideal model to recapitulate the Tfam-depletion effect on insulin signaling and glucose uptake.

The increased phospho-Akt in Tfam-depleted adipocytes is not accompanied by an increased glucose uptake, suggesting that Akt phosphorylation can be delinked from glucose transport. However, there are still possible explanations to reconcile this

contradiction without breaking this linkage. For example, it should be noted that, when observing phospho-Akt, we did not distinguish between Akt1 and Akt2 isoforms. Therefore, it is possible that one of the isoforms, especially Akt2, might be hypophosphorylated even though total Akt phosphorylation is enhanced. Since only Akt2 plays an indispensible role in glucose homeostasis, such a difference in phosphorylation of Akt1 and Akt2 could lead to impaired insulin-stimulated glucose uptake while exhibiting a higher total Akt phosphorylation. However, this possibility needs to be carefully evaluated in terms of Akt1 and Akt2 isoform-specific phosphorylation. Additionally, *in vivo* studies point to a similar increased Akt signaling phenotype with mitochondrial dysfunction. For example, the muscle and liver-specific apoptosis inducing factor (AIF) knockout mice showed compromised mitochondrial respiratory function, but were accompanied by increased insulin sensitivity assessed by Akt phosphorylation (168). Muscle-specific Tfam knockout mice were not diabetic and showed increased basal glucose uptake (169). Conversely, over-expression of PGC-1α in muscle dramatically increased muscle mitochondrial density and ATP synthesis, yet decreased insulin-stimulated glucose uptake, making the mice more prone to fat-induced insulin resistance (208). Therefore, it appears that cells develop a general feedback response to compensate for impaired or enhanced mitochondrial function regardless of *in vitro* and *in vivo* differences. However, such a feedback mechanism by which cells manage to maintain overall energy homeostasis may display different metabolic features depending on tissue or cellular content. In our *in vitro* 3T3-L1 model, the mitochondrial dysfunction causes decreased glucose transport, which is opposite to what was observed in *in vivo* AIF or

Tfam muscle-specific knockout mice (169, 208). This difference may result from the fact that muscle-specific AIF or Tfam knockout mice expressed increased GLUT1 and GLUT4 protein levels (169, 208), but Tfam-depleted 3T3-L1 adipocytes did not.

To better understand the mechanism by which Akt phosphorylation and glucose transport might be affected by Tfam-depletion, we analyzed the general phosphorylation of Akt substrates using the PAS antibody. In accordance with increased phospho-Akt at Ser^{473} in Tfam-depleted adipocytes, several major insulin-stimulated phosphoproteins were also increased on western blots detected by PAS. However, an unknown ~49 kDa insulin-responsive phosphoprotein had reduced phosphorylation with Tfam-depletion. Such an observation implies that, despite a total increase in Akt activation, phosphorylation of certain Akt substrate(s) can be down-regulated in Tfam-depleted adipocytes. If this observed ~49 kDa protein is a critical component for insulin-stimulated glucose transport, then it may help to explain our seemingly paradoxical effect of Tfam-depletion on Akt phosphorylation and glucose transport.

In an attempt to isolate and purify this mysterious ~49 kDa protein that is hypophosphorylated in Tfam-depleted adipocytes, we coincidently identified a 50 kDa protein eukaryotic elongation factor 1A (eEF1A) from a mass spectrometry experiment, which can be phosphorylated by Akt upon insulin stimulation (Appendix). However, knockdown of eEF1A by siRNA in adipocytes had no effect on insulin-stimulated glucose uptake (data not shown), suggesting that eEF1A is not the putative ~49 kDa protein that mediates glucose transport.

We also tried to explore the general effect of Tfam-depletion on nuclear gene expression at the whole genome level with Affymetrix Genechip analysis. Among the approximately 45,000 transcripts, only about 50 genes were either up-regulated or down-regulated by >1.5-fold with Tfam-depletion and none of them changed >3-fold except for Tfam (Table 4-1). Such a relatively mild effect on nuclear gene expression implies that Tfam-depletion does not have a dramatic impact on general transcription. This is not surprising, since the Tfam-depletion specifically interferes with mtDNA and impairs OXPHOS and intracellular ATP level, a general effect of insufficient energy supply could have occurred at other regulatory levels such as protein synthesis and signal transduction, in which energy supply is crucial. One small GTPase, Rab21, which is involved in the early endocytic pathway (209), showed a mild decrease in its expression level (67% of control) in Tfam-depleted adipocytes. Considering the important role of GTPases in vesicle trafficking (84), we tested whether Rab21 plays a role in GLUT4 translocation and glucose uptake. RNAi mediated knockdown of Rab21 in 3T3-L1 adipocytes markedly impaired insulin-stimulated glucose uptake (Figure 4-1, *B*). This impairment was accompanied by decreased Akt phosphorylation at Ser^{473} and Thr^{308} (Figure 4-1, *A*). Although the mechanism of enhanced total Akt phosphorylation in Tfam-depleted adipocytes is unclear, the down-regulation of Rab21 could be one of the factors that contributes to impaired insulin-stimulated glucose uptake in these cells. Many other Rab GTPases are also important for endocytosis, in which they help to specify vesicle destination or function (210). The observation that knockdown of Rabs (Rab21 and many other Rabs not shown here) affects Akt phosphorylation suggests a possible role for

endosomes in the regulation of Akt signal transduction. We tested this hypothesis by examining the interaction of endosomal protein WDFY2 with Akt1 and Akt2, and evaluating the effects of such interactions on Akt isoform-specificity determination. We showed that the endosome protein WDFY2 has a higher affinity for Akt2 than for Akt1; therefore preferentially regulating Akt1 protein function (Chapter III).

Gene Symbol	Down-regulation	Gene Symbol	Up-regulation
Tfam	-3.23	BC055107	1.50
BC010981	-2.12	Pdzk1	1.51
Mreg	-2.08	Car2	1.51
BC023829 /// LOC100045774	-1.92	Atp1b1	1.51
Vldlr	-1.91	Angptl1	1.51
Hmox1	-1.79	Errfi1	1.54
Scd3	-1.70	Igf2	1.55
9130401M01Rik	-1.67	A030001D16Rik	1.56
Ublcp1	-1.67	Inhbb /// LOC100046802	1.58
Kdelr3	-1.65	Chst1	1.60
Acox2	-1.65	D0H4S114	1.61
LOC100048724 /// Scd3	-1.64	Cyb561	1.61
Slc4a4	-1.63	Ear2	1.64
LOC100045709 /// Ublcp1	-1.59	Pnpla3	1.67
Pdcd11	-1.59	Ear3	1.78
1500016O10Rik	-1.59	Ear1 /// Ear12 /// Ear2 /// Ear3	1.80
Ndrg1	-1.58	Ifi27	1.89
Elovl3	-1.58	Thbd	1.92
0610010O12Rik	-1.56	Greb1 /// LOC100045413	1.96
Ddit3	-1.55	Car3	2.16
Atf3	-1.55	Hp	2.19
Spp1	-1.54	Aqp1	2.20
2900092E17Rik	-1.53		
Npc1	-1.53		
Myd116	-1.53		
Mt2	-1.52		
Smad1	-1.52		
Csnrp2	-1.51		
Slain2	-1.51		
Pvr	-1.51		
Ermp1	-1.51		
AU019823	-1.51		
Pfkp	-1.50		

Table 4-1 GeneChip analysis of Tfam knockdown in 3T3-L1 adipocytes

3T3-L1 was electroporated with Tfam siRNA at day 2 of differentiation. Total RNA was extracted at day 6 of differentiation. Gene expressions were analyzed with Affymetrix GeneChip® Mouse Genome 430 2.0 Array. The genes that changed expression level by > 1.5-fold (up or down) are listed in the table above.

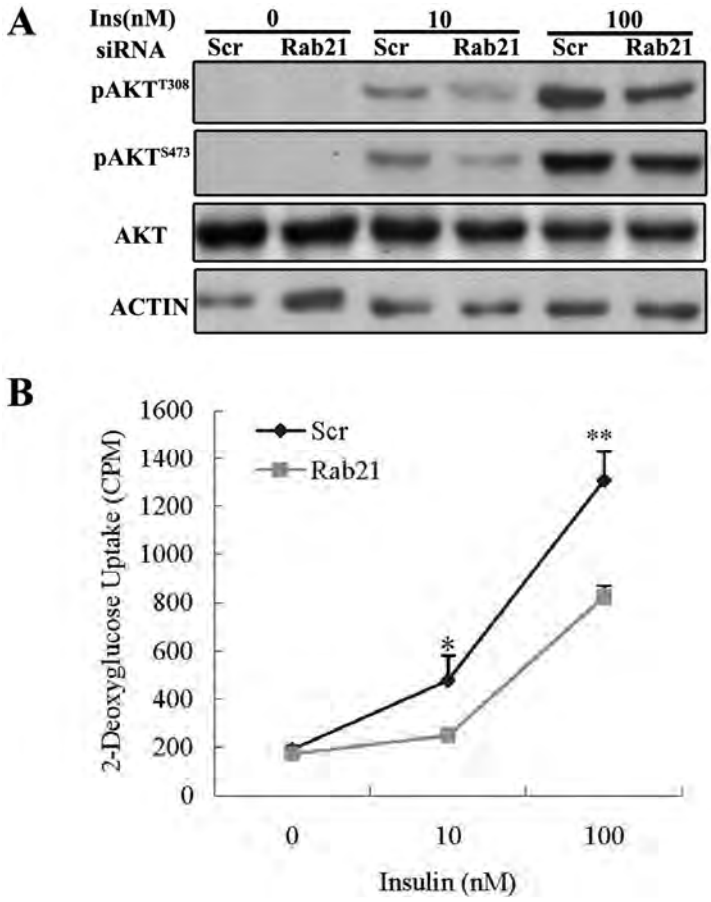

Figure 4-2 Knockdown of Rab21 impairs Akt phosphorylation and glucose transport

(*A*), siRNA were introduced by electroporation at day 4 of 3T3-L1 adipocyte differentiation. Day 7 mature adipocytes were stimulated with 0, 10 or 100 nM insulin for 15 minutes. Whole cell lysate were subjected to western detection of phospho-Akt. (*B*), Day 7 control or Rab21 knockdown adipocytes were evaluated for the insulin-stimulated glucose uptake. Experiments were repeated three times. *, p value<0.001 and **, p value<0.01 with student t-test.

One intriguing question is whether over-expression of Tfam in 3T3-L1 adipocytes increases insulin sensitivity. The actual consequences of Tfam over-expression in 3T3-L1 adipocytes is hard to predict, but remains of great interest. Although Tfam over-expression in mice generally increases mtDNA copy number (211), transient over-expression of Tfam in cultured cells does not (212). In the mice with Tfam over-expression as well as increased mtDNA, the respiratory chain capacity and mitochondrial mass is not changed (211). This suggests that the mtDNA encoded proteins are not the rate limiting factors that defines the respiratory chain capacity. Moreover, force-increased mtDNA copy number by Tfam and/or Twinkle over-expression in mice results in enlarged mtDNA nucleoids, accompanied by inhibited mtDNA transcription and increased mtDNA deletion, thus has an overall detrimental effect (213). Interestingly, Tfam over-expression in several other studies does ameliorate the mitochondrial dysfunction and symptoms under certain situations. For example, Tfam over-expression ameliorates mitochondrial deficiency and cardiac failure after myocardial infarction (214) and reverses age-dependent memory impairment and mtDNA damage (215) in mice; it also protects the cell function from the damage induced by hyperglycemia in cardiomyocytes (216) or from the oxidative damage induced by beta-amyloid in SH-SY5Y cells (217); the delayed neuronal death after transient forebrain ischemia is also reduced in Tfam over-expressing mice (218). The protective effect of Tfam over-expression is not dependent on its mtDNA transcription activity, but rather on its role in maintaining the integrity of the mtDNA nucleoid structure (217). It was recently reported that Tfam has multiple weak nuclear localization signals (NLS) (219). The Tfam nuclear

localization has also been found in a rat hepatoma where Tfam is over-expressed (220). The function of nuclear Tfam is not clear but may have cytoprotective effect on DNA damage in response to chemotherapeutic drugs (221). This might act through the Tfam binding to nuclear DNA, since Tfam has high affinity for mtDNA and help to pack mtDNA into nucleoid structure (222). Given the complexity of Tfam over-expression, it might not be a good model to evaluate the effect of enhanced mitochondrial OXPHOS function in glucose homeostasis.

In this study, the assessment of insulin action on adipocytes largely depends on the radio-labeled glucose uptake assay. Therefore, it is critical that such assays reflect as much as possible the actual glucose uptake process in the cell. In a physiological situation, the glucose molecule enters the glycolysis pathway and gets metabolized quickly after internalization, making it hard to track the uptake event. Therefore, we applied non-metabolized glucose analogue 2-deoxyglucose or 3-*O*-methylglucose in the assay. However, the non-metabolized glucose analogue continues to accumulate inside the cell and its concentration gradually reaches an equilibrium state, inhibiting the further uptake. Therefore, it is critical to measure the glucose uptake before the glucose analogue gets saturated. For 2-deoxyglucose, a 5-minute time period has been commonly used to reflect the actual speed of glucose uptake. However, the 3-*O*-methylglucose has a much shorter equilibration time. It is estimated that the half-time for achieving complete equilibration of 3-*O*-methylglucose in 3T3-L1 adipocytes is 12 and 125 seconds in insulin stimulated and basal state, respectively (223). In our study, we adopted 1-minute incubation time to accommodate the experimental setting in a multi-well plate, in which time period the

intracellular 3-*O*-methylglucose reaches ~80% of the maximal concentration (223). This prolonged incubation time might compromise the accuracy of the measurement, thus caution must be taken when interpreting the data.

Another issue arises with this study is whether Tfam depletion reflects the pathophysiological mitochondrial dysfunction in a diabetic state. In fact, in the *ob/ob* diabetic mice, a systematic mitochondrial protein down-regulation is observed (25), with about 50% of all mitochondrial protein transcripts decreased. However, the expression of Tfam transcript is not among those decreased. The direct manipulation of Tfam was used as a tool to introduce a first mitochondrial dysfunction signal to determine the cause-and-effect relationship between mitochondrial dysfunction and insulin resistance in diabetes. Although Tfam depletion caused insulin resistance in 3T3-L1 adipocytes, we did not see a general down-regulation of mitochondrial protein transcripts. Furthermore, Tfam depletion did not change the nuclear gene expression profile either. In an *in vivo* situation, however, it is possible that Tfam depletion in adipose tissue will eventually cause insulin resistance and defects in blood sugar control at the whole body level and in turn will further impair the mitochondrial protein expression and function.

In future studies, several aspects of the Akt signaling that have not been investigated in this work will be explored. The isoform-specific phosphorylation of Akt will be compared between control and Tfam-depleted adipocytes in response to insulin treatment, which will provide clues of whether Akt2 phosphorylation is decreased. Further effort will be made to identify the ~49 kDa protein, whose phosphorylation by

Akt has been impaired by Tfam-depletion. The function of this protein in glucose transport will also be determined.

Finally, I will extend my study to an *in vivo* system to test whether fat-specific mitochondrial dysfunction can cause insulin resistance in whole body animals. For example, we can cross $Tfam^{loxp}/Tfam^{loxp}$ mice with mice expressing Cre recombinase from an adipose tissue-specific promoter (e.g. adipocytes P2, aP2) to generate mice with fat-specific mitochondrial dysfunction. However, the challenge is that sometimes aP2 promoter also expresses in BAT (224) and macrophages (225). Therefore the interpretation of aP2-driven knockout mice will be complicated. An ideal WAT-specific promoter may be discovered in the future. But until then, different fat depots from aP2-driven Tfam knockout mice can be dissected and evaluated for their individual metabolic and functional changes. Such studies will provide a broader picture of fat mitochondrial dysfunction in the pathophysiology of insulin resistance and type 2 diabetes.

Our Tfam-depleted 3T3-L1 adipocytes provides a useful alternative system for studying mitochondrial dysfunction in adipose tissue, and also can be expanded to other cell lines to study mtDNA function. However, *in vivo* study is required to assess the whole body effect from a single organ mitochondrial dysfunction, especially when such an effect causes general feedback responses in the whole body animal.

As a conclusion, in this study, I have established an *in vitro* WAT-specific model to investigate the question of whether mitochondrial dysfunction causes insulin resistance in adipose tissue. The knockdown, instead of knockout, of Tfam circumvents the lethal issue accompanied with mitochondrial dysfunction, while it provides very specific and

confined effect on mitochondria. Our results show that mitochondrial dysfunction can be a primary cause for insulin resistance in adipocytes. The unexpected result is that Tfam-depletion seems to trigger a feedback response to compensate for the loss of mitochondrial function as manifested by increased insulin signaling to Akt.

Isoform-Specific Regulation of Akt Signaling by WDFY2

In insulin responsive tissues such as muscle and adipose tissue, Akt signaling plays a pivotal role mediating whole body energy homeostasis. Akt acts through a series of phosphorylation cascades to affect the functions of downstream pathways, such as glycogen synthesis, glucose uptake and fatty acid synthesis. The highly homologous Akt isoforms Akt1, Akt2 and Akt3 exhibit distinct but overlapping physiological functions during development or diseases (62). The knockout mouse model points to an indispensible role for Akt2 in glucose metabolism and insulin sensitivity (73). In adipocytes, both Akt1 and Akt2 are expressed and phosphorylated upon insulin stimulation, however only Akt2 is critical for glucose uptake. This raises the question of how the cells distinguish between these two isoforms according to different physiological requirements.

It came to our attention that Akt isoform-specific regulation may at least rely on a mechanism that involves endosomes. The endosomal pathway plays an important role in diversifying signal transduction. Different receptors traffic through distinct endosomal populations (177-178) and their fates are determined by the endocytic pathway (184-188). Recent studies have shown that the endosomal proteins APPL1 and APPL2 may help to

determine the Akt1 and Akt2 isoform specificity. For example, Akt2, but not Akt1, was found to be localized in APPL-containing endosomes (114-115); and APPL1-containing endosomes mediate Akt substrate specificity by dynamically interacting with specific Akt substrates (116). Previously, our lab has identified a new endosomal protein WDFY2, which defines a distinct endosomal population lacking the canonical markers EEA1 and Rab5 (146, 183). We investigated if WDFY2 plays a similar role as APPL1 to mediate Akt2 isoform specificity in 3T3-L1 adipocytes, which is a good model to study the insulin action and Akt signaling pathway.

We first examined if WDFY2 had any general effect on insulin signaling in mature 3T3-L1 adipocytes, in which we measured the insulin-stimulated glucose uptake. The results showed that siRNA-mediated knockdown of WDFY2 had an inhibitory effect on insulin-stimulated glucose uptake in 3T3-L1 adipocytes, comparable to Akt2 knockdown (Figure 3-1, *A*). This suggested that WDFY2 plays a role in insulin signaling and Akt regulation. Surprisingly, the WDFY2 knockdown seemed to directly affect the Akt2 protein level (Figure 3-1, *C*). Since WDFY2 is an endosomal protein, which may regulate many substrates including components for general protein synthesis and degradation, we examined whether the down regulation of Akt2 protein level is specific. In fact, the WDFY2 knockdown had no effect on protein levels of Akt1, and a house keeping protein β-actin (Figure 3-2, *C*). Additionally, the WDFY2 knockdown effect on Akt2 protein level was not due to some off-target effects. Different WDFY2 siRNA oligos showed different effectiveness on WDFY2 knockdown, which is proportional to the extent of the Akt2 protein down-regulation (Figure 3-2, *D*). Knockdown of another

endosome protein EEA1 had no effect on Akt2 protein level. These data suggest that endosomal protein WDFY2 has a preferential effect on Akt2 protein level and may distinguish the Akt1 and Akt2 functionality in 3T3-L1 adipocytes.

We were interested in the mechanism by which WDFY2 determines Akt2 specificity. By immunostaining and fluorescent microscope, we were able to visualize the subcellular distributions of endogenous WDFY2, Akt1 and Akt2. WDFY2 localized to a subpopulation of endosomes, exhibiting a punctate pattern. However, Akt1 and Akt2 displayed both nuclear and cytosolic distribution (Figure 3-4, *A* and *B*). By looking at the distribution of either Akt1 or Akt2 in WDFY2-defined regions, we saw a significant difference between these two Akt isoforms. Akt2 is more prone to localize to WDFY2-containing endosomes (Figure 3-4, *C* and *D*). These observations support a hypothesis that WDFY2 specifically regulate a portion of Akt2 by preferential co-localization. This co-localization might be through direct interaction of WDFY2 and Akt. It has been shown that WDFY2 is an Akt1 partner in a yeast two-hybrid screen (194), suggesting the existence of a direct protein-protein interaction. The stronger co-localization of Akt2 than Akt1 with WDFY2 probably reflects the stronger affinity between Akt2 and WDFY2. This was confirmed by our quantitative yeast two-hybrid interaction assay (Figure 3-7), in which the yeast strain co-expressing WDFY2 and Akt2 showed stronger reporter activity than the yeast strain co-expressing WDFY2 and Akt1.

In addition to Akt2, WDFY2 may involve in a broader range of target protein regulation. For example, protein kinase Cζ and the transcription factor FOXO1 were reported to interact with WDFY2 (195, 202). We observed that WDFY2 knockdown had

a stronger effect than Akt2 knockdown on a group of metabolic and adipogenic gene expressions (Figure 3-6), suggesting that WDFY2 may regulate a variety of different targets other than Akt2. Taken together, it appears that WDFY2 interacts with different partners to regulate different pathways.

In diseases like type 2 diabetes and cancer, Akt isoform-specific abnormalities have been described frequently in recent years (226). Therefore, understanding the mechanism of Akt isoform-specific regulation will help to develop specific therapeutic interventions. In our study, we demonstrated that endosomal proteins and the endocytic pathway could be a general mechanism by which cells can regulate Akt signal transduction in an isoform-specific manner. The molecular details of the endocytic regulatory network of Akt isoform specificity will benefit from the identification of other components in the WDFY2-containing endosomes. Additionally, investigating the differential temporospatial expression, subcellular distribution, substrate specificity, and binding partners, will reveal other regulatory mechanisms of Akt isoform specificity. Identification of new interacting partners of WDFY2 will be helpful to address the versatility of this endosomal protein.

In the future, work can be done on two aspects to deepen and expand the findings described here. First, we can further explore the Akt1 and Akt2 isoform specificity in a detailed and systematic manner to draw a bigger picture of the molecular mechanism of the specificity. For example, in a specific tissue that exhibits Akt isoform-specificity, we can utilize the quantitative proteomics to identify Akt isoform-specific binding partners. Comparisons can also be made at the whole-genome expression level with GeneChip

analysis. Since Akt mediates many phosphorylation cascades, phosphoprotein profiling may also help to identify potential Akt substrates. Second, the specific function of WDFY2 in regulating trafficking and signal transduction can be further explored. The whole body or tissue-specific WDFY2 transgenic animal can be made to evaluate its *in vivo* functions.

In summary, we provided one mechanism of how Akt2-specific function in 3T3-L1 adipocytes is regulated by the endocytic pathway, in which the endosomal protein WDFY2 preferentially interacts with and stabilizes Akt2. Our findings underscored the complexity of the regulation of Akt signaling in adipocytes and may be valuable for developing new therapeutic interventions for the treatment of obesity or type 2 diabetes.

APPENDIX

PHOSPHORYLATION OF EUKARYOTIC ELONGATION FACTOR 1A BY AKT AND ITS IMPLICATION IN PROTEIN SYNTHESIS AND CELL GROWTH

Abstract

Serine/threonine protein kinase Akt mediates signal transductions that control a variety of cellular functions including protein synthesis and cell growth. Eukaryotic elongation factor 1a (eEF1A) is a GTPase involved in protein synthesis elongation, carrying the aminoacyl-tRNA to the peptide elongation site. Here we employ the phospho-Akt substrate (PAS) antibody, which recognizes potential Akt substrates, to identify eEF1A as an insulin-stimulated phospho-protein recognized by the PAS antibody. We show that eEF1A can be phosphorylated by Akt *in vitro* and two phosphorylation sites Thr^{269} and Thr^{432} were identified. Mutation of either phosphorylation site to aspartic acid causes protein instability while mutation of either phosphorylation site to alanine did not, but decreased the protein translational activity. We hypothesize that Thr^{269} and Thr^{432} are important for eEF1A function.

Introduction

Serine/threonine kinase Akt, also known as protein kinase B (PKB), phosphorylates the hydroxyl group of a specific serine or threonine in its substrate. This phosphorylation-dependent regulation constitutes an Akt-centered signal transduction network downstream of insulin/PI-3K in the cell (227). In muscle and adipose tissue, Akt signaling plays a key regulatory role in glucose metabolism, in that Akt is required for insulin-stimulated glucose uptake. Akt also regulates protein synthesis and cell growth via mammalian target of rapamycin (mTOR) pathways.

One strategy to dissect Akt-regulated physiological processes is to identify Akt substrates, which link Akt and its regulatory targets. Since the identification of glycogen synthase kinase as the first Akt substrate (228), much effort has been taken to identify new Akt substrates. One breakthrough is that Alessi et al. described the Akt kinase minimal recognition motif R*X*R*XX*p(S/T)B (229), where R represents arginine, *X* represents any amino acid and B represents bulky hydrophobic residues. A method was then developed to identify potential Akt substrates using antibodies based on such motif recognition (230). In fact, over 100 non-redundant Akt substrates has been reported in the literature, among which approximately 75% contain this minimum motif (61). A commercially available phospho-Akt substrate antibody (PAS) has been used successfully to identify new Akt substrates in 3T3-L1 adipocytes (82, 166). Here we describe the identification of eEF1A as an Akt *in vitro* substrate using the PAS antibody in 3T3-L1 adipocytes. The phosphorylation sites of eEF1A at Thr^{269} and Thr^{432} were confirmed by an *in vitro* kinase assay. Mutation of the phosphorylation sites to alanine or

aspartic acid negatively regulated translational activity of eEF1A in HeLa cells. We hypothesized that Thr^{269} and Thr^{432} of eEF1A has regulatory functions on eEF1A activity.

Experimental Procedures

Reagents and Material

Most of the antibodies used in this study were from Cell Signaling: Rabbit Phospho-Akt Substrate (PAS) antibodies (#9611 and #9614). Rabbit eEF1A antibody (#2551), Rabbit Akt1 (#2938), Akt2 (#3063), pAkt(Thr308) (#9275), pAkt(Ser473) (#9271), pGSK-3 / (#9327). All antibodies were used at a 1:1000 dilution in TBST buffer supplemented with 4% BSA. Mouse anti-beta actin antibody was purchased from Sigma. All the active kinase proteins, Akt1 (#7535), Akt2 (#7503), PKC (#7608), S6 Kinase (#7684), GSK-3 (#7374), and GSK-3 (#7436) were from Cell Signaling.

Yeast Strain and Plasmids

The yeast strain M213 and the plasmids are kind gifts from Drs. M.G. Sandbaken and M.R. Culbertson. M213 has a following genotype: *Matα leu2-3, 112Δtef1::LEU2 tef2-Δ2 lys2-20 his4-713 met2-1 ura3-52 trp1-Δ1.* This yeast strain contains a plasmid YCpMS29 (TEF2, URA3) to support survival. YCpMS41 (TEF2, TRP1) was used to replaced YCpMS29.

Cell Culture and Treatment

3T3-L1 cells were maintained and differentiated as described before (56). For insulin stimulation, cells were serum starved for 2 hours before insulin addition. Wortmannin and rapamycin were added 30 minutes before the addition of insulin as indicated. Treated cells were then washed with PBS twice quickly and collected in lysis buffer containing 1% SDS and protease and phosphatase inhibitors.

eEF1A Recombinant Protein Preparation

Full length cDNA of mouse eEF1A was cloned into a GST-tagged prokaryotic expression vector pGEX-6P-1. eEF1A point mutation was introduced on pGEX-6P-1 backbone directly by using Quickchange II Site Directed Mutagenesis kit from Stratagene according to the manufacturer's protocol. Recombinant GST-tagged proteins were first purified from IPTG induced bacterial culture through GST affinity binding. An on-column PreScission protease cutting procedure was performed to remove the GST tag and the untagged protein was further concentrated by Amicon® Ultra centrifugal filter. The purity and identity of the recombinant proteins were confirmed by Coomassie staining and western blots.

In Vitro Kinase Assay

The *in vitro* kinase assay was performed as follows: 5 μl of recombinant protein was incubated with 100 ng of active kinase in a 50 μl reaction system (5 mM MOPS, pH 7.2, 2.5 mM -glycerophosphate, 1 mM EGTA, 0.4 mM EDTA, 5 mM $MgCI_2$, 0.05 mM DTT, 0.1mM ATP, 10 μCi ^{32}P labeled γ-ATP) at room temperature for 1 hour. The reactions were then stopped by adding 12.5 μl 5X sample buffer and separated on SDS-PAGE gel and transferred onto nitrocellulose membrane for either ^{32}P exposure or western blot detection of phosphorylated proteins. In some cases the ^{32}P labeled ATP is not required. The total protein level of eEF1A in each reaction was also detected by western blot as a loading control.

Adenoviral Delivery of eEF1A shRNA

The shRNA-expressing vector pSilencer 2.1™-U6 hygro was used to test several shRNAs' knockdown efficiency first. The shRNA sequences were designed using the

Dharmacon siDESIGN Center. The best target sequence of six tested is 5'-GGAAACAACTTGACCAAAA-3', which localizes within the 3' UTR of eEF1A mRNA. The U6-driven shRNA cassette was then transferred from pSilencer 2.1™-U6 hygro to an adenoviral shuttle vector for further cloning and packaging into adenovirus. For adenoviral infection in cell culture, the optimal multiplicity of infection (MOI) of 30,000 was used for C2C12 cells for 2 hours and a MOI of 250 for HeLa cells. Cells were treated by adenoviruses every other day to deplete the endogenous eEF1A mRNA until the end of experiments.

Yeast Plasmid Shuffle

TEF2 point mutation was introduced directly on the YCpMS41 plasmid using Quickchange® II XL site-directed mutagenesis kit per the manufacturer's instruction. The YCpMS41 was transformed into yeast strain M213. The transformed yeasts harboring two plasmids YCpMS29 (TEF2, URA3) and YCpMS41 (TEF2, TRP1) can grow on SD-Trp plates. Then the yeasts were transferred to 5-FOA containing SD-Trp plates to kick out the YCpMS29 plasmid. Before 5-FOA selection, the expression of mutant TEF2 from YCpMS41 was confirmed by sequencing the mutated region of TEF2, which was amplified by RT-PCR using total RNA extracted from SD-Trp culture.

Translational Activity Assay

For luciferase translational assay, HeLa cells were plated in a 6-well plate at day 0. At day 1, cells were infected with AdsheEF1A viruses for 2 hours at MOI of 250. At day 2, two vectors expressing eEF1A and renilla luciferase (pRL-TK, Promega) respectively, were mixed together and co-transfected into HeLa cells using FuGENE 6 transfection reagent. At day 3, cells from each well were collected and divided into two

parts for renilla luciferase activity determination (Dual-Luciferase® Reporter Assay System, Promega) and RNA extraction respectively. The raw luminescence unit (RLU) from each well was then normalized to the renilla luciferase mRNA level determined by quantitative RT-PCR from the same well. β-actin mRNA was used as an internal control for the RT-PCR. All experiments were performed in triplicate wells.

Results

Identification of eEF1A as an Insulin-stimulated Phospho-protein

Akt plays a significant role in insulin-stimulated phosphorylation cascades. To better understand the physiology and mechanism of Akt versatility, much focus has been applied to identify potential Akt substrates. With the help of phospho-Akt substrate (PAS) antibody, one that recognizes an optimal Akt substrate motif R*X*R*XX*p(S/T), where S/T is the phosphorylation site and *X* any amino acid, many Akt substrates have been identified and characterized. Among them, the Akt substrate AS160 (82) (also known as TBC1D4) and TBC1D1 (88) are best known for their activity in GLUT4 translocation. During our research on insulin-stimulated adipocytes, we constantly observed an abundance of phosphorylated protein products detected by the PAS antibody with a molecular weight around 50 kDa (denoted as PAS50 thereafter) on western blots (Figure A-1, *A*). The induction of PAS50 was insulin dose and time-dependent (Figure.A-1, *A*). One of the known Akt substrates in adipocytes around 50 kDa is AS47, which localizes in non-cytosolic subcellular fraction (166). We found the PAS50 mainly in cytosol and RNAi mediated depletion of AS47 did not reduce the PAS50 signal on western blot (data not shown), excluding the possibility of AS47 as a major product of PAS50. To identify the potential Akt substrate protein(s) in PAS50, we separated insulin-stimulated 3T3-L1 adipocytes lysate on 5%-15% gradient SDS-PAGE and excised the PAS50 band and sent it for mass spectrometry identification. The best hit was eukaryotic elongation factor 1α1 (eEF1A1), the dominant isoform of eEF1A in adipocytes. eEF1A1 has a calculated molecular weight of 50 kDa, which is consistent with its SDS-PAGE migration pattern.

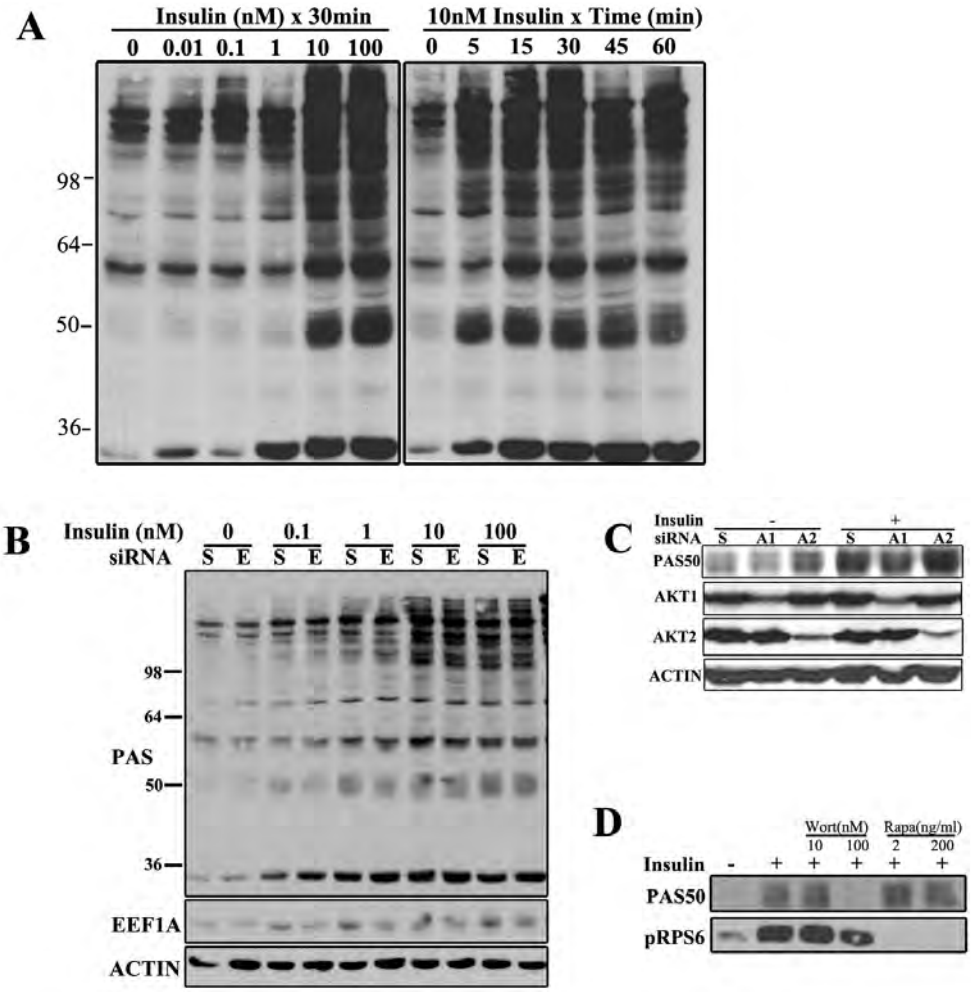

Figure A-1 eEF1A is a potential insulin-stimulated Akt substrate

(*A*), 3T3-L1 adipocytes were stimulated with insulin at different concentrations (0-100 nM) for 30 minutes or at 10 nM for different time (0-60 minutes). Whole cell lysates were separated on SDS-PAGE, transferred to nitrocellulose membrane and probed with PAS antibody. (*B*), 3T3-L1 adipocytes were transfected with scramble (S) or Eef1a (E) siRNA for 3 days and then were stimulated with insulin. Phospho-Akt substrates were detected by PAS antibody. PAS50 refers to proteins ~50 kDa recognized by PAS on western blots. (*C*), 3T3-L1 adipocytes were transfected with scramble (S) or Akt1 (A1) or Akt2 (A2) siRNA for 48 hours. Cells were treated with or without 10 nM insulin for 30 minutes. Western blots were performed to detect PAS50, Akt1 and Akt2. β-actin was used as a loading control. (*D*), 3T3-L1 adipocytes were pre-treated with or without different concentrations of PI-3K inhibitor wortmanin (Wort) or mTORC1 inhibitor rapamycin (Rapa), and then stimulated with 10 nM insulin for 30 minutes. The phosphorylation of rpS6 was detected by pRPS6 antibody.

eEF1A is an *in vitro* Akt Substrate

To confirm eEF1A is an Akt substrate, we carried out several strategies. First we used siRNA to deplete eEF1A in 3T3-L1 adipocytes. The depletion of eEF1A specifically decreased PAS50 signal but not other phospho-proteins on western blots, indicating that eEF1A could be a major protein in PAS50 bands (Figure A-1, *B*). Second, we used siRNA to knockdown the two isoforms of Akt in 3T3-L1 adipocytes. Only Akt1, but not Akt2 depletion, caused a reduction of PAS50 signal, suggesting that Akt1 is the dominant isoform that phosphorylates eEF1A in response to insulin stimulation (Figure A-1, *C*). Interestingly, Akt2 depletion slightly increased PAS50 signal (Figure A-1, *C*). However, this was not because Akt2 knockdown caused an increase in the Akt1 protein level (Figure A-1, *C*). The effect of Akt2 depletion on PAS50 might be due to: 1) Akt2 has little activity on PAS50 and 2) Akt2 might compete with Akt1 for the substrate PAS50.

To determine the location of PAS50 in the insulin/PI-3K/Akt signaling pathway, we analyzed the effect of specific inhibitors on PAS50. First, the inhibition of PI-3K, a kinase downstream of insulin and upstream of Akt, by wortmannin totally abolished PAS50 (Figure A-1, *D*), suggesting that PAS50 is phosphorylated upon insulin stimulation in a PI-3K dependent manner. Second, inhibition of mTORC1 by rapamycin totally abolished the phosphorylation of ribosomal protein S6 (rpS6), but had no effect on PAS50 phosphorylation induced by insulin (Figure A-1, *D*). These two assays indicate that PAS50 is phosphorylated by a kinase downstream of PI-3K but upstream of mTORC1. Akt is one of such kinases.

Pecorari et al. reported eEF1A as a pAkt interacting protein. eEF1A can be detected both from anti-pAkt1 and anti-pAkt2 immunoprecipitations (231). However, Pecorari et al. showed that eEF1A could not be phosphorylated by Akt in an *in vitro* kinase assay with a GST-tagged truncated recombinant eEF1A protein (1-173aa) containing a putative Akt phosphorylation site at Thr^{72}. We tested whether Akt can phosphorylate a full-length recombinant eEF1A protein *in vitro.* We first purified GST-eEF1A from bacteria and then removed the GST tag (see Experimental Procedures), producing the untagged full-length eEF1A protein. Using this full length protein as a substrate, we incubated it with a panel of recombinant protein kinases that are activated by insulin in the presence of ^{32}P labeled ATP. Despite the fact that all kinases used in this assay exhibited auto-phosphorylation activity shown by ^{32}P autoradiography, only Akt1, Akt2, S6K and PKCζ could phosphorylate eEF1A (Figure A-2, ***A***, ***^{32}P signal at 50 kDa***). However, the PAS antibody detected eEF1A only when phosphorylated by Akt1 or Akt2, with the latter to a lesser extent (Figure A-2, ***A***). The data strongly suggested that eEF1A is an Akt substrate *in vitro* and the phosphorylation site can be recognized by PAS antibody. To further confirm that Akt1 and Akt2 can phosphorylate eEF1A, we used an immobilized HA antibody to immunoprecipitated HA-Akt1 and HA-Akt2 from transfected mammalian cells. The precipitated kinases were incubated with recombinant eEF1A in a kinase assay as above except only cold ATP was used. The PAS antibody was able to detect phosphorylated eEF1A both by HA-Akt1 and HA-Akt2 (Figure A-2, ***B***). Taken together, Akt can phosphorylate eEF1A on PAS recognizable site(s) *in vitro*.

We observed that Akt1 had stronger activity than Akt2 on phosphorylation of eEF1A, even though Akt2 showed stronger auto-phosphorylation activity (Figure A-2, *A*). This was also reflected in Akt1 and Akt2 knockdown experiments, in which knockdown of Akt1 isoform showed a reduction of PAS50 signal, but Akt2 did not (Figure A-1, *C*). In a competitive phosphorylation assay, we incubated eEF1A with both Akt1 and Akt2 kinases together, while varying the amount of Akt1 and Akt2. The results showed that Akt1 had stronger phosphorylation activity on the PAS site of eEF1A (Figure A-2, *C*) and Akt2 seemed to compete for eEF1A with Akt1 (Figure A-2, *C*, ***last lane***). The differential ***in vitro*** kinase activity of Akt1 and Akt2 appeared to be intrinsic to the kinases themselves, and not eEF1A-related. This was supported by the observation of the same preferential activity on another Akt substrate GSK-3α/β (Figure A-2, *B*). Whether isoform-specific activity applies to other Akt substrates remains an open question.

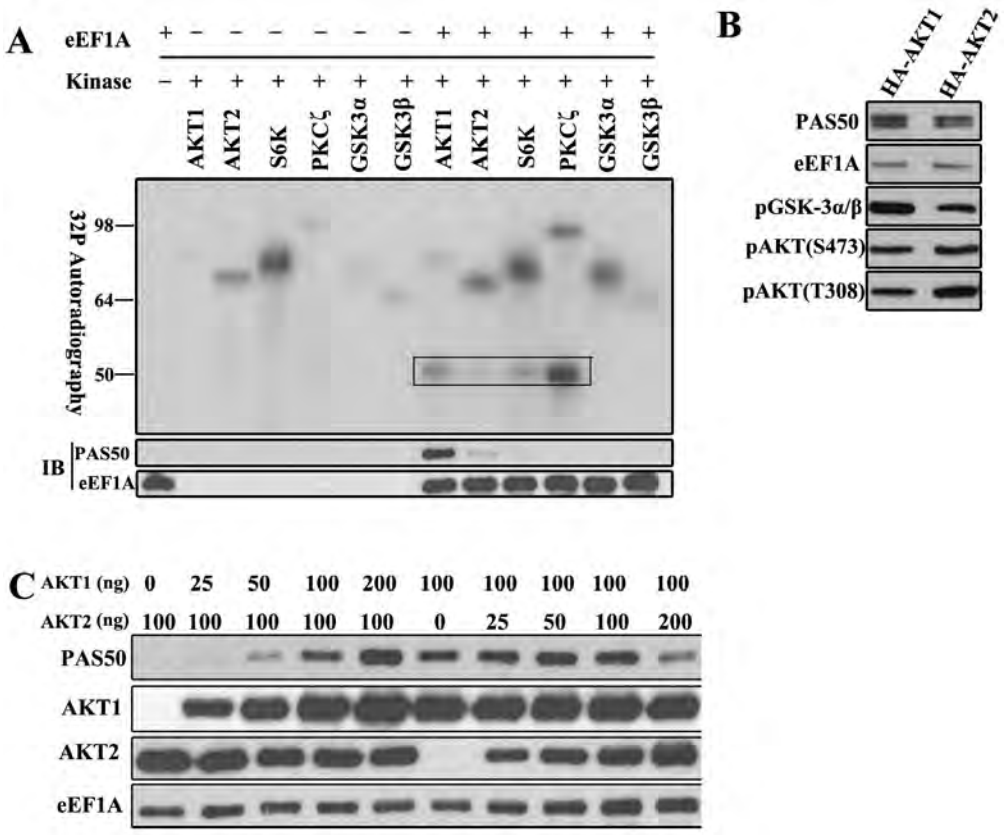

Figure A-2 eEF1A is phosphorylated by Akt *in vitro* in a PAS recognizable fashion

(*A*), Recombinant protein eEF1A was incubated with different kinases in an *in vitro* kinase assay in the presence of ^{32}P labeled ATP. The eEF1A alone or kinase without substrate was used as control. The reactions were then separated on SDS-PAGE and transferred onto nitrocellulose membrane for ^{32}P autoradiography exposure. After exposure, the same blot was subjected to western blot for detection of either phosphorylated or total eEF1A. Bands in the inset at 50 kDa are phosphorylated eEF1A; higher bands are auto-phosphorylated kinases. (*B*), HA-Akt1 or HA-Akt2 were pulled down by an immobilized HA antibody from HA-Akt1 or HA-Akt2 transfected COS-7 cell lysate. The immunoprecipitations were then incubated with recombinant eEF1A protein and GSK-3α/β polypeptide in a same *in vitro* kinase reaction. Afterwards, the reactions were separated on SDS-PAGE and probed with antibodies by western blot as indicated. The phosphorylation of Akt on Ser^{473} and Thr^{308} indicates Akt activation. (*C*), Increasing amount of Akt1 (0-200ng) and 100ng of Akt2 kinase (lane 1-6) or increasing amount of Akt2 (0-200ng) and 100ng of Akt1 kinase (lane 7-12) were combined together with fixed amount of eEF1A in an *in vitro* kinase reaction. The reactions were separated on SDS-PAGE and probed with PAS for phosphorylated eEF1A and with Akt1, Akt2, eEF1A antibodies.

eEF1A is Phosphorylated at Thr^{269} and Thr^{432}

The PAS antibody recognizes an optimal phosphorylation site within R*X*R*XX*p(S/T) motif, where S/T is the phosphorylation site and *X* any amino acid. There is only one such site in eEF1A, which is Thr^{72}. Pecorari et al. showed that this site cannot be phosphorylated by Akt *in vitro* with a truncated eEF1A (1-173aa) (231). However, we showed Akt can phosphorylate a full-length eEF1A (1-462aa) in a PAS recognizable fashion. This indicates that either the missing part (174-462aa) of eEF1A is required for the phosphorylation of Thr^{72} or there is other unknown site(s) that can be phosphorylated by Akt. To identify the potential Akt phosphorylation site on eEF1A, we first predicted several possible phosphorylation sites on eEF1A using Netphos2.0 software. Then we made point mutations of predicted serine or threonine to alanine, which cannot be phosphorylated. Wild type or mutant recombinant proteins were expressed in bacteria and purified for an *in vitro* kinase assay. Recombinant protein eEF1A^{T269A}, with an alanine substitution for Thr^{269}, failed to be recognized by PAS antibody when phosphorylated by Akt1 (Figure A-3, *A*), suggesting that Thr^{269} is the phosphorylation site on eEF1A that had been observed. Thr^{269} is located within a motif variation R*XX*p(S/T), which PAS only has minor activity on it. The T269A mutation did not totally abolish the ^{32}P signal, suggesting there may be other site(s) that can be phosphorylated by Akt1. In a further investigation into additional phosphorylation site(s), we employed another phospho-Akt substrate antibody, PAS9611, with a less stringent recognition motif (R/K)*X*(R/K)*XX*p(S/T). This led to the identification of Thr^{432} as another Akt phosphorylation site (Figure A-3, *A*). Again, Thr^{432} turned out to be within

another variant motif R*XX*R*X*p(S/T), on which PAS9611 has minor activity. In fact, Thr^{432} has been previously reported to be phosphorylated by the kinase PKCδ *in vitro* (232). We showed PKCζ, another PKC isoform, can also phosphorylate this site *in vitro* (Figure A-3, ***B***).To this point, we identified eEF1A Thr^{269} and Thr^{432} as Akt phosphorylation sites, with the Thr^{432} shared by Akt, PKCδ and PKCζ.

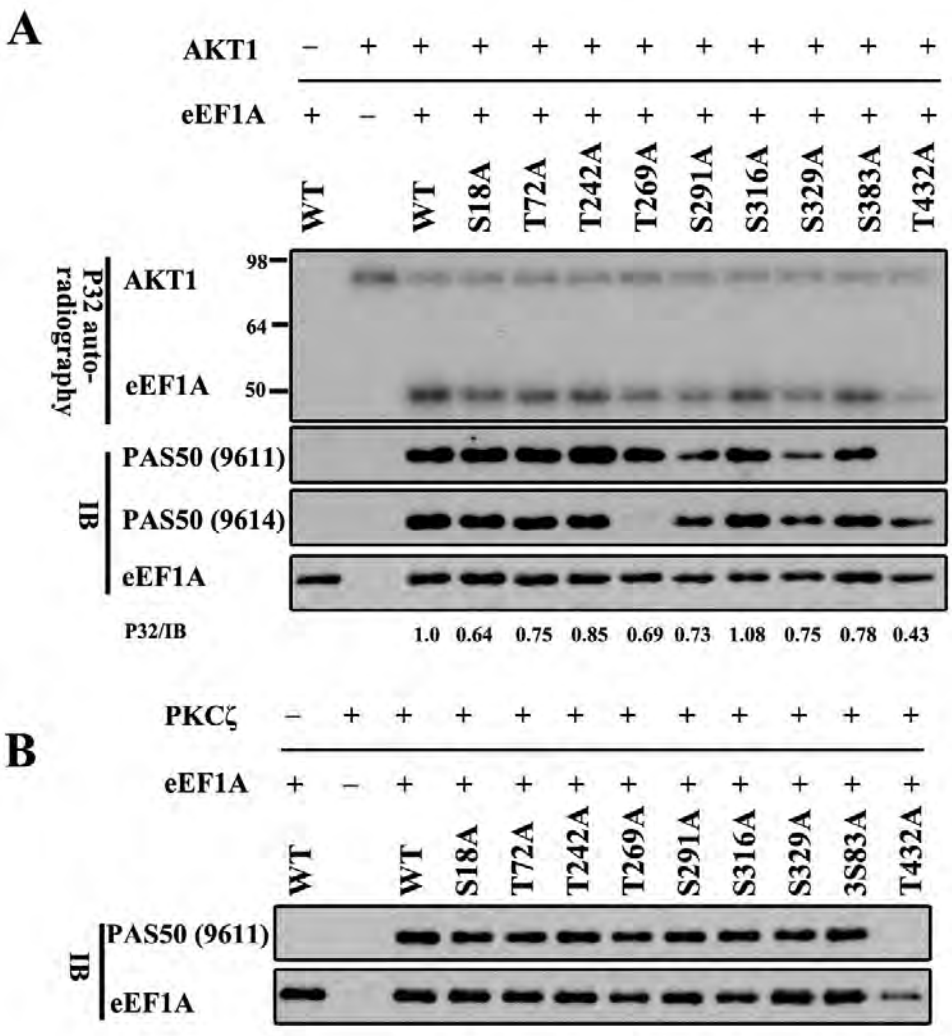

Figure A-3 Akt phosphorylates eEF1A at Thr^{269} and Thr^{432}

(*A*), Wild type and point mutant eEF1A recombinant proteins were incubated with kinase Akt1 in the presence of ^{32}P labeled γ-ATP. The reactions were then separated on SDS-PAGE and transferred to nitrocellulose membrane for ^{32}P autoradiography exposure. The bands at 50 kDa are phosphorylated eEF1A and the higher bands are Akt1 kinase by auto-phosphorylation. After exposure, the same blot was subjected to immuno-blotting for detecting either phosphorylated eEF1A by PAS or total eEF1A by its antibody. The ratios of ^{32}P/Immuno signal of eEF1A are quantified and normalized to wild type. (*B*), The same *in vitro* kinase assay was performed as in (*A*) except that kinase PKCζ was used instead of Akt1 and with cold ATP. Western blots were performed to determine phosphorylated and total proteins.

Phospho-mimic eEF1A protein fail to support cell growth in yeast

We next investigated if these phosphorylation sites of eEF1A have any biological functions. Considering eEF1A is an elongation factor that is critical for protein synthesis, we hypothesized that the phosphorylation of eEF1A regulates its function in cell growth. We took advantage of the easy genetics of yeast to test whether our eEF1A mutants (phospho-defective or phospho-mimic) are capable of supporting normal cell survival. The rationale is based on the fact that eEF1A protein is highly homologous from human, mouse to yeast, and the phosphorylation sites Thr^{269} and Thr^{432} are conserved in yeast (as Thr^{267} and Thr^{430} in yeast) (Figure A-4, *A*). Yeast eEF1A proteinis encoded by two genes, TEF1 and TEF2. A yeast strain MS213 with non-functional genomic TEF1 and TEF2 is viable by carrying a plasmid YCpMS29 (URA3, TEF2), which expresses a functional eEF1A protein from wild type TEF2. URA3 gene product converts 5-fluoroorotic acid (5-FOA) to 5-fluorouracil, which is toxic to the cell. YCpMS29 plasmid can be kicked out and replaced by YCpMS41 (TRP1, TEF2) by growing the yeast containing both plasmids on 5-FOA plates. We made phospho-defective (alanine substitution, T→A) or phospho-mimic (aspartic acid substitution, T→D) mutation of TEF2 on YCpMS41 and transformed the plasmids into strain MS213 to replace YCpMS29 via 5-FOA selection. We found that yeast harboring YCpMS29 (URA3, TEF2) and YCpMS41 (TRP1, $TEF2^{T267A}$) can successfully grow on 5-FOA plates, suggesting $TEF2^{T267A}$ can functionally replace wild type TEF2 to support cell growth. However, yeast harboring YCpMS29 (URA3, TEF2) and YCpMS41 (TRP1, $TEF2^{T267D}$) failed to grow on 5-FOA plates, suggesting $TEF2^{T267D}$ are functionally defective (Figure A-4, *B*). To exclude the

possibility that the failure of supporting cell growth was a result of untranscribed $TEF2^{T267D}$ mRNA from the construct, we extracted the total RNA from the yeast harboring both YCpMS29 (URA3, TEF2) and YCpMS41 (TRP1, $TEF2^{T267D}$). Then we performed RT-PCR to amplify TEF2 cDNA. Sequencing of the TEF2 amplicon revealed that both wild type TEF2 and $TEF2^{T267D}$ were transcribed and there were no extra mutations other than T267D (Figure A-4, *C*). This result suggests that the lost function of $TEF2^{T267D}$ occurs post-transcriptionally. Crystal structure of yeast eEF1A protein reveals that Thr^{267} and Thr^{430} localize to the surfaces of two subdomains and are in between subdomains II and III, I and III, respectively. A mutation from threonine (T) to aspartic acid (D) introduces a longer side chain and may interfere with the spatial orientation of the subdomains and thus cause protein instability (Figure A-4, *D*).

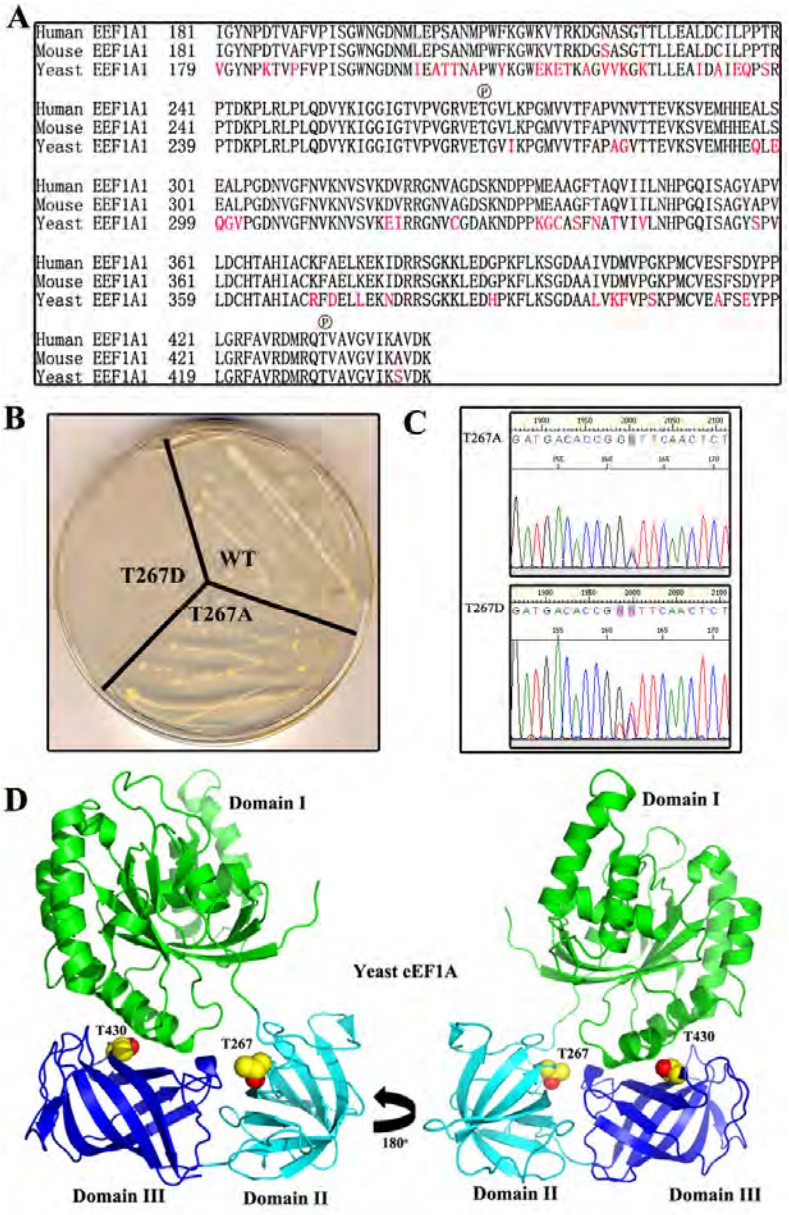

Figure A-4 Phospho-mimic eEF1A protein fail to support yeast growth

(*A*), Sequence alignment of human, mouse and yeast version of eEF1A. Shown here is only part of the protein sequence that includes Thr^{269} and Thr^{432}. Ⓟ indicates the phosphorylation site. (*B*), Yeast with $eEF1A^{T267D}$ fails to grow on a 5-FOA plate. (*C*), Sequencing confirms the coexistence of wild type and mutant transcripts. The DNA codon for the amino acid threonine (ACC), alanine (GCC) and aspartic acid (GAC) are shown in antisense as the sequencing was performed from the opposite direction. (*D*), 3-D structure of yeast eEF1A (PDB id: IF60) displayed using software Pymol. The site Thr^{267} and Thr^{430} are located in between two subdomains.

To determine the underlying mechanism that phospho-mimic eEF1A protein failed to support cell survival, we transiently transfected HA-tagged eEF1A constructs into HeLa cells. Protein levels were determined 48 hours later by anti-HA antibody on western blots. The data showed that the protein expression levels of HA-eEF1A^{T269D} and HA-eEF1A^{T432D} are significantly decreased compared to wild type or HA-eEF1A^{T269A} and HA-eEF1A^{T432A} (Figure A-5, ***A, top panel*** and ***B, left panel***). These decreased expression levels were not due to lower transfection efficiency, because the mRNA of HA-eEF1A^{T269D} and HA-eEF1A^{T432D} in these cells were similar to those of HA-eEF1A^{T269A} and HA-eEF1A^{T432A}, and were even higher than those of the wild type HA-eEF1A (Figure A-5, ***C, left panel***). Similar results were also observed in 293T cells, with the HA-eEF1A^{T269D} and HA-eEF1A^{T432D} protein levels decreased, although their mRNA levels were not significantly different compared to their phospho-defective counterparts.(Figure A-5, ***A, middle panel, B, right panel and C, right panel***). To exclude the possibility that such a decrease in phospho-mimic protein level was a transient artificial effect from transfection, we also determined the HA-protein levels from stable cell lines, which had been selected by antibiotics for at least two weeks. We observed a same result (Figure A-4, ***A, bottom panel***). Taken together, HA-eEF1A^{T269D} and HA-eEF1A^{T432D} accumulate less protein in the cell due to post-transcriptional instability.

We next sought to determine whether the translational activity of HeLa cells expressing mutant version of eEF1A were affected. By transfecting the cells with a luciferase expressing vector, we were able to determine the translation activity by measuring luciferase activity. We found that over-expression of wild type eEF1A

increased the translation activity compared to vector transfected control cells, while cells over-expressing either phospho-defective or phospho-mimic eEF1A did not increase the translational activity (Figure A-5, *D*). Since the phospho-mimic eEF1A proteins tends to accumulate very little protein level compared to wild type proteins (Figure A-5, *E*), it explains why the cells expressing phospho-mimic eEF1A did not increase translational activity. Surprisingly, the phospho-defective eEF1A expressing cells had no increase in translational activity either. This data indicates that an alanine mutation might have a negative effect on the translational activity of eEF1A.

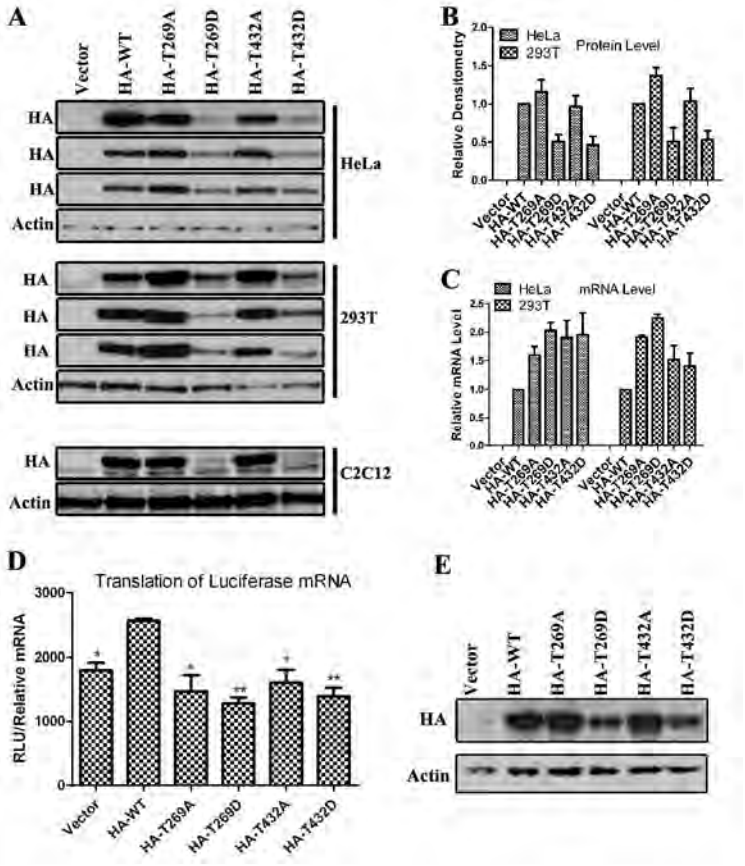

Figure A-5 Phospho-mimic eEF1A protein are not stable in mammalian cells

(*A*), HA-tagged wild type (WT) or mutant (T269A, T269D, T432A, and T432D) eEF1A were transiently transfected into HeLa or 293T cells. 48 hours later, HA-tagged eEF1A protein levels were detected with anti-HA antibody by western blot. Empty vector was used as a negative control. Three experiments in both HeLa and 293T cells are shown here. Transfected C2C12 cells were selected on G418 to screen stable cell lines. Polyclonal stable cell lysate were analyzed for the HA-tagged eEF1A protein level. Actin was used as loading control on western blots. (*B*), Quantification of HA-eEF1A protein level by the western blot densitometry from the three experiments in (*A*). (*C*), Quantification of HA-eEF1A mRNA levels by RT-PCR from the three experiments. (*D*), The translational activity of HeLa cells expressing wild-type or mutant version of eEF1A was deduced from the transfected renilla luciferase protein (measured as raw luminescence unit (RLU)) normalized to the relative luciferase mRNA level. Experiments were performed in triplicates and the data is expressed as mean ± SEM of three experimental wells. *, $P<0.05$, **, $P<0.01$ compared to HA-WT with t-test. (*E*), HA-eEF1A proteins detected by HA antibody from the cells transfected with different constructs as indicated.

REFERENCES

1. Flegal KM, Carroll MD, Ogden CL, Curtin LR. Prevalence and trends in obesity among US adults, 1999-2008. JAMA. 2010;303(3):235-41.
2. Centers for Disease Control and Prevention. National diabetes fact sheet: general information and national estimates on diabetes in the United States, 2007. Atlanta, GA: U.S. Department of Health and Human Services, Centers for Disease Control and Prevention, 2008.
3. Wild SH, Byrne CD. ABC of obesity. Risk factors for diabetes and coronary heart disease. BMJ. 2006;333(7576):1009-11.
4. Galic S, Oakhill JS, Steinberg GR. Adipose tissue as an endocrine organ. Mol Cell Endocrinol. 2010;316(2):129-39.
5. Jansky L. Non-shivering thermogenesis and its thermoregulatory significance. Biol Rev Camb Philos Soc. 1973;48(1):85-132.
6. Cannon B, Nedergaard J. Brown adipose tissue: function and physiological significance. Physiol Rev. 2004;84(1):277-359.
7. Nedergaard J, Bengtsson T, Cannon B. Unexpected evidence for active brown adipose tissue in adult humans. Am J Physiol Endocrinol Metab. 2007;293(2):E444-52.
8. Cypess AM, Lehman S, Williams G, Tal I, Rodman D, Goldfine AB, et al. Identification and importance of brown adipose tissue in adult humans. N Engl J Med. 2009;360(15):1509-17.
9. White UA, Stephens JM. Transcriptional factors that promote formation of white adipose tissue. Mol Cell Endocrinol. 2010;318(1-2):10-4.
10. Gupta RK, Arany Z, Seale P, Mepani RJ, Ye L, Conroe HM, et al. Transcriptional control of preadipocyte determination by Zfp423. Nature. 2010;464(7288):619-23.
11. Seale P, Kajimura S, Yang W, Chin S, Rohas LM, Uldry M, et al. Transcriptional control of brown fat determination by PRDM16. Cell Metab. 2007;6(1):38-54.
12. Tiraby C, Tavernier G, Lefort C, Larrouy D, Bouillaud F, Ricquier D, et al. Acquirement of brown fat cell features by human white adipocytes. J Biol Chem. 2003;278(35):33370-6.
13. Petrovic N, Walden TB, Shabalina IG, Timmons JA, Cannon B, Nedergaard J. Chronic peroxisome proliferator-activated receptor gamma (PPARgamma) activation of epididymally derived white adipocyte cultures reveals a population of thermogenically competent, UCP1-containing adipocytes molecularly distinct from classic brown adipocytes. J Biol Chem. 2010;285(10):7153-64.
14. Barbatelli G, Murano I, Madsen L, Hao Q, Jimenez M, Kristiansen K, et al. The emergence of cold-induced brown adipocytes in mouse white fat depots is determined predominantly by white to brown adipocyte transdifferentiation. Am J Physiol Endocrinol Metab. 2010;298(6):E1244-53.
15. Cinti S. Transdifferentiation properties of adipocytes in the Adipose Organ. Am J Physiol Endocrinol Metab. 2009.

16. Katic M, Kennedy AR, Leykin I, Norris A, McGettrick A, Gesta S, et al. Mitochondrial gene expression and increased oxidative metabolism: role in increased lifespan of fat-specific insulin receptor knock-out mice. Aging Cell. 2007;6(6):827-39.
17. Kaaman M, Sparks LM, van Harmelen V, Smith SR, Sjolin E, Dahlman I, et al. Strong association between mitochondrial DNA copy number and lipogenesis in human white adipose tissue. Diabetologia. 2007;50(12):2526-33.
18. Laplante M, Festuccia WT, Soucy G, Gelinas Y, Lalonde J, Berger JP, et al. Mechanisms of the depot specificity of peroxisome proliferator-activated receptor gamma action on adipose tissue metabolism. Diabetes. 2006;55(10):2771-8.
19. Dahlman I, Forsgren M, Sjogren A, Nordstrom EA, Kaaman M, Naslund E, et al. Downregulation of electron transport chain genes in visceral adipose tissue in type 2 diabetes independent of obesity and possibly involving tumor necrosis factor-alpha. Diabetes. 2006;55(6):1792-9.
20. Choo HJ, Kim JH, Kwon OB, Lee CS, Mun JY, Han SS, et al. Mitochondria are impaired in the adipocytes of type 2 diabetic mice. Diabetologia. 2006;49(4):784-91.
21. Flachs P, Horakova O, Brauner P, Rossmeisl M, Pecina P, Franssen-van Hal N, et al. Polyunsaturated fatty acids of marine origin upregulate mitochondrial biogenesis and induce beta-oxidation in white fat. Diabetologia. 2005;48(11):2365-75.
22. Bogacka I, Xie H, Bray GA, Smith SR. Pioglitazone induces mitochondrial biogenesis in human subcutaneous adipose tissue in vivo. Diabetes. 2005;54(5):1392-9.
23. Bogacka I, Ukropcova B, McNeil M, Gimble JM, Smith SR. Structural and functional consequences of mitochondrial biogenesis in human adipocytes in vitro. J Clin Endocrinol Metab. 2005;90(12):6650-6.
24. Boden G, Homko C, Mozzoli M, Showe LC, Nichols C, Cheung P. Thiazolidinediones upregulate fatty acid uptake and oxidation in adipose tissue of diabetic patients. Diabetes. 2005;54(3):880-5.
25. Wilson-Fritch L, Nicoloro S, Chouinard M, Lazar MA, Chui PC, Leszyk J, et al. Mitochondrial remodeling in adipose tissue associated with obesity and treatment with rosiglitazone. J Clin Invest. 2004;114(9):1281-9.
26. Wilson-Fritch L, Burkart A, Bell G, Mendelson K, Leszyk J, Nicoloro S, et al. Mitochondrial biogenesis and remodeling during adipogenesis and in response to the insulin sensitizer rosiglitazone. Mol Cell Biol. 2003;23(3):1085-94.
27. Sorbris R, Monti M, Nilsson-Ehle P, Wadso I. Heat production by adipocytes from obese subjects before and after weight reduction. Metabolism. 1982;31(10):973-8.
28. Chen H, Chan DC. Mitochondrial dynamics in mammals. Curr Top Dev Biol. 2004;59:119-44.
29. Liesa M, Palacin M, Zorzano A. Mitochondrial dynamics in mammalian health and disease. Physiol Rev. 2009;89(3):799-845.

30. Kelly DP, Scarpulla RC. Transcriptional regulatory circuits controlling mitochondrial biogenesis and function. Genes Dev. 2004;18(4):357-68.
31. Kang D, Kim SH, Hamasaki N. Mitochondrial transcription factor A (TFAM): roles in maintenance of mtDNA and cellular functions. Mitochondrion. 2007;7(1-2):39-44.
32. Pohjoismaki JL, Wanrooij S, Hyvarinen AK, Goffart S, Holt IJ, Spelbrink JN, et al. Alterations to the expression level of mitochondrial transcription factor A, TFAM, modify the mode of mitochondrial DNA replication in cultured human cells. Nucleic Acids Res. 2006;34(20):5815-28.
33. Poulton J, Morten K, Freeman-Emmerson C, Potter C, Sewry C, Dubowitz V, et al. Deficiency of the human mitochondrial transcription factor h-mtTFA in infantile mitochondrial myopathy is associated with mtDNA depletion. Hum Mol Genet. 1994;3(10):1763-9.
34. Choi YS, Kim S, Pak YK. Mitochondrial transcription factor A (mtTFA) and diabetes. Diabetes Res Clin Pract. 2001;54 Suppl 2:S3-9.
35. Lee SH, Lee S, Jun HS, Jeong HJ, Cha WT, Cho YS, et al. Expression of the mitochondrial ATPase6 gene and Tfam in Down syndrome. Mol Cells. 2003;15(2):181-5.
36. Belin AC, Bjork BF, Westerlund M, Galter D, Sydow O, Lind C, et al. Association study of two genetic variants in mitochondrial transcription factor A (TFAM) in Alzheimer's and Parkinson's disease. Neurosci Lett. 2007;420(3):257-62.
37. Chan DC. Mitochondria: dynamic organelles in disease, aging, and development. Cell. 2006;125(7):1241-52.
38. Forner F, Kumar C, Luber CA, Fromme T, Klingenspor M, Mann M. Proteome differences between brown and white fat mitochondria reveal specialized metabolic functions. Cell Metab. 2009;10(4):324-35.
39. Harris RA, Leland MC, Mahoney JM, Mapes JP. Regulatory function of mitochondria in lipogenesis. Lipids. 1973;8(12):711-6.
40. Reshef L, Olswang Y, Cassuto H, Blum B, Croniger CM, Kalhan SC, et al. Glyceroneogenesis and the triglyceride/fatty acid cycle. J Biol Chem. 2003;278(33):30413-6.
41. Nye CK, Hanson RW, Kalhan SC. Glyceroneogenesis is the dominant pathway for triglyceride glycerol synthesis in vivo in the rat. J Biol Chem. 2008;283(41):27565-74.
42. Gonzalez-Baro MR, Lewin TM, Coleman RA. Regulation of Triglyceride Metabolism. II. Function of mitochondrial GPAT1 in the regulation of triacylglycerol biosynthesis and insulin action. Am J Physiol Gastrointest Liver Physiol. 2007;292(5):G1195-9.
43. Stone SJ, Levin MC, Zhou P, Han J, Walther TC, Farese RV, Jr. The endoplasmic reticulum enzyme DGAT2 is found in mitochondria-associated membranes and has a mitochondrial targeting signal that promotes its association with mitochondria. J Biol Chem. 2009;284(8):5352-61.

44. Rossmeisl M, Syrovy I, Baumruk F, Flachs P, Janovska P, Kopecky J. Decreased fatty acid synthesis due to mitochondrial uncoupling in adipose tissue. FASEB J. 2000;14(12):1793-800.
45. Fassina G, Dorigo P, Gaion RM. Equilibrium between metabolic pathways producing energy: a key factor in regulating lipolysis. Pharmacol Res Commun. 1974(6):1-21.
46. Daval M, Diot-Dupuy F, Bazin R, Hainault I, Viollet B, Vaulont S, et al. Anti-lipolytic action of AMP-activated protein kinase in rodent adipocytes. J Biol Chem. 2005;280(26):25250-7.
47. Fonseca-Alaniz MH, Takada J, Alonso-Vale MI, Lima FB. Adipose tissue as an endocrine organ: from theory to practice. J Pediatr (Rio J). 2007;83(5 Suppl):S192-203.
48. Vazquez-Vela ME, Torres N, Tovar AR. White adipose tissue as endocrine organ and its role in obesity. Arch Med Res. 2008;39(8):715-28.
49. Koh EH, Park JY, Park HS, Jeon MJ, Ryu JW, Kim M, et al. Essential role of mitochondrial function in adiponectin synthesis in adipocytes. Diabetes. 2007;56(12):2973-81.
50. Braakman I, Helenius J, Helenius A. Role of ATP and disulphide bonds during protein folding in the endoplasmic reticulum. Nature. 1992;356(6366):260-2.
51. Sun J, Xu Y, Deng H, Sun S, Dai Z, Sun Y. Intermittent high glucose exacerbates the aberrant production of adiponectin and resistin through mitochondrial superoxide overproduction in adipocytes. J Mol Endocrinol. 2010;44(3):179-85.
52. Frier BC, Williams DB, Wright DC. The effects of apelin treatment on skeletal muscle mitochondrial content. Am J Physiol Regul Integr Comp Physiol. 2009;297(6):R1761-8.
53. Civitarese AE, Ukropcova B, Hulver M, Defronzo R, Mandarino L, Scherer P, et al. Adiponectin receptors mediated regulation of mitochondrial bioenergetics in skeletal-muscle. Diabetes. 2005;54:A91-A.
54. Vempati UD, Torraco A, Moraes CT. Mouse models of oxidative phosphorylation dysfunction and disease. Methods. 2008;46(4):241-7.
55. Torraco A, Diaz F, Vempati UD, Moraes CT. Mouse models of oxidative phosphorylation defects: powerful tools to study the pathobiology of mitochondrial diseases. Biochim Biophys Acta. 2009;1793(1):171-80.
56. Shi X, Burkart A, Nicoloro SM, Czech MP, Straubhaar J, Corvera S. Paradoxical effect of mitochondrial respiratory chain impairment on insulin signaling and glucose transport in adipose cells. J Biol Chem. 2008;283(45):30658-67.
57. Rong JX, Qiu Y, Hansen MK, Zhu L, Zhang V, Xie M, et al. Adipose mitochondrial biogenesis is suppressed in db/db and high-fat diet-fed mice and improved by rosiglitazone. Diabetes. 2007;56(7):1751-60.
58. Semple RK, Crowley VC, Sewter CP, Laudes M, Christodoulides C, Considine RV, et al. Expression of the thermogenic nuclear hormone receptor coactivator PGC-1alpha is reduced in the adipose tissue of morbidly obese subjects. Int J Obes Relat Metab Disord. 2004;28(1):176-9.

59. Sakamoto K, Holman GD. Emerging role for AS160/TBC1D4 and TBC1D1 in the regulation of GLUT4 traffic. Am J Physiol Endocrinol Metab. 2008;295(1):E29-37.
60. Giovannone B, Scaldaferri ML, Federici M, Porzio O, Lauro D, Fusco A, et al. Insulin receptor substrate (IRS) transduction system: distinct and overlapping signaling potential. Diabetes Metab Res Rev. 2000;16(6):434-41.
61. Manning BD, Cantley LC. AKT/PKB signaling: navigating downstream. Cell. 2007;129(7):1261-74.
62. Dummler B, Hemmings BA. Physiological roles of PKB/Akt isoforms in development and disease. Biochem Soc Trans. 2007;35(Pt 2):231-5.
63. Mueckler M. Facilitative glucose transporters. Eur J Biochem. 1994;219(3):713-25.
64. Cong LN, Chen H, Li Y, Zhou L, McGibbon MA, Taylor SI, et al. Physiological role of Akt in insulin-stimulated translocation of GLUT4 in transfected rat adipose cells. Mol Endocrinol. 1997;11(13):1881-90.
65. Wang Q, Somwar R, Bilan PJ, Liu Z, Jin J, Woodgett JR, et al. Protein kinase B/Akt participates in GLUT4 translocation by insulin in L6 myoblasts. Mol Cell Biol. 1999;19(6):4008-18.
66. Katome T, Obata T, Matsushima R, Masuyama N, Cantley LC, Gotoh Y, et al. Use of RNA interference-mediated gene silencing and adenoviral overexpression to elucidate the roles of AKT/protein kinase B isoforms in insulin actions. J Biol Chem. 2003;278(30):28312-23.
67. Kohn AD, Summers SA, Birnbaum MJ, Roth RA. Expression of a constitutively active Akt Ser/Thr kinase in 3T3-L1 adipocytes stimulates glucose uptake and glucose transporter 4 translocation. J Biol Chem. 1996;271(49):31372-8.
68. Andjelkovic M, Alessi DR, Meier R, Fernandez A, Lamb NJ, Frech M, et al. Role of translocation in the activation and function of protein kinase B. J Biol Chem. 1997;272(50):31515-24.
69. Tanti JF, Grillo S, Gremeaux T, Coffer PJ, Van Obberghen E, Le Marchand-Brustel Y. Potential role of protein kinase B in glucose transporter 4 translocation in adipocytes. Endocrinology. 1997;138(5):2005-10.
70. Ducluzeau PH, Fletcher LM, Welsh GI, Tavare JM. Functional consequence of targeting protein kinase B/Akt to GLUT4 vesicles. J Cell Sci. 2002;115(Pt 14):2857-66.
71. Chen X, Al-Hasani H, Olausson T, Wenthzel AM, Smith U, Cushman SW. Activity, phosphorylation state and subcellular distribution of GLUT4-targeted Akt2 in rat adipose cells. J Cell Sci. 2003;116(Pt 17):3511-8.
72. Ng Y, Ramm G, Lopez JA, James DE. Rapid activation of Akt2 is sufficient to stimulate GLUT4 translocation in 3T3-L1 adipocytes. Cell Metab. 2008;7(4):348-56.
73. Cho H, Mu J, Kim JK, Thorvaldsen JL, Chu Q, Crenshaw EB, 3rd, et al. Insulin resistance and a diabetes mellitus-like syndrome in mice lacking the protein kinase Akt2 (PKB beta). Science. 2001;292(5522):1728-31.

74. Garofalo RS, Orena SJ, Rafidi K, Torchia AJ, Stock JL, Hildebrandt AL, et al. Severe diabetes, age-dependent loss of adipose tissue, and mild growth deficiency in mice lacking Akt2/PKB beta. J Clin Invest. 2003;112(2):197-208.
75. Ikonomov OC, Sbrissa D, Dondapati R, Shisheva A. ArPIKfyve-PIKfyve interaction and role in insulin-regulated GLUT4 translocation and glucose transport in 3T3-L1 adipocytes. Exp Cell Res. 2007;313(11):2404-16.
76. Berwick DC, Dell GC, Welsh GI, Heesom KJ, Hers I, Fletcher LM, et al. Protein kinase B phosphorylation of PIKfyve regulates the trafficking of GLUT4 vesicles. J Cell Sci. 2004;117(Pt 25):5985-93.
77. Liu J, Kimura A, Baumann CA, Saltiel AR. APS facilitates c-Cbl tyrosine phosphorylation and GLUT4 translocation in response to insulin in 3T3-L1 adipocytes. Mol Cell Biol. 2002;22(11):3599-609.
78. Chang L, Chiang SH, Saltiel AR. TC10alpha is required for insulin-stimulated glucose uptake in adipocytes. Endocrinology. 2007;148(1):27-33.
79. Mitra P, Zheng X, Czech MP. RNAi-based analysis of CAP, Cbl, and CrkII function in the regulation of GLUT4 by insulin. J Biol Chem. 2004;279(36):37431-5.
80. Minami A, Iseki M, Kishi K, Wang M, Ogura M, Furukawa N, et al. Increased insulin sensitivity and hypoinsulinemia in APS knockout mice. Diabetes. 2003;52(11):2657-65.
81. Molero JC, Jensen TE, Withers PC, Couzens M, Herzog H, Thien CB, et al. c-Cbl-deficient mice have reduced adiposity, higher energy expenditure, and improved peripheral insulin action. J Clin Invest. 2004;114(9):1326-33.
82. Kane S, Sano H, Liu SC, Asara JM, Lane WS, Garner CC, et al. A method to identify serine kinase substrates. Akt phosphorylates a novel adipocyte protein with a Rab GTPase-activating protein (GAP) domain. J Biol Chem. 2002;277(25):22115-8.
83. Sano H, Kane S, Sano E, Miinea CP, Asara JM, Lane WS, et al. Insulin-stimulated phosphorylation of a Rab GTPase-activating protein regulates GLUT4 translocation. J Biol Chem. 2003;278(17):14599-602.
84. Stenmark H. Rab GTPases as coordinators of vesicle traffic. Nat Rev Mol Cell Biol. 2009;10(8):513-25.
85. Sano H, Eguez L, Teruel MN, Fukuda M, Chuang TD, Chavez JA, et al. Rab10, a target of the AS160 Rab GAP, is required for insulin-stimulated translocation of GLUT4 to the adipocyte plasma membrane. Cell Metab. 2007;5(4):293-303.
86. Sano H, Roach WG, Peck GR, Fukuda M, Lienhard GE. Rab10 in insulin-stimulated GLUT4 translocation. Biochem J. 2008;411(1):89-95.
87. Ishikura S, Bilan PJ, Klip A. Rabs 8A and 14 are targets of the insulin-regulated Rab-GAP AS160 regulating GLUT4 traffic in muscle cells. Biochem Biophys Res Commun. 2007;353(4):1074-9.
88. Roach WG, Chavez JA, Miinea CP, Lienhard GE. Substrate specificity and effect on GLUT4 translocation of the Rab GTPase-activating protein Tbc1d1. Biochem J. 2007;403(2):353-8.

89. Chavez JA, Roach WG, Keller SR, Lane WS, Lienhard GE. Inhibition of GLUT4 translocation by Tbc1d1, a Rab GTPase-activating protein abundant in skeletal muscle, is partially relieved by AMP-activated protein kinase activation. J Biol Chem. 2008;283(14):9187-95.
90. Stone S, Abkevich V, Russell DL, Riley R, Timms K, Tran T, et al. TBC1D1 is a candidate for a severe obesity gene and evidence for a gene/gene interaction in obesity predisposition. Hum Mol Genet. 2006;15(18):2709-20.
91. Meyre D, Farge M, Lecoeur C, Proenca C, Durand E, Allegaert F, et al. R125W coding variant in TBC1D1 confers risk for familial obesity and contributes to linkage on chromosome 4p14 in the French population. Hum Mol Genet. 2008;17(12):1798-802.
92. Chen S, Murphy J, Toth R, Campbell DG, Morrice NA, Mackintosh C. Complementary regulation of TBC1D1 and AS160 by growth factors, insulin and AMPK activators. Biochem J. 2008;409(2):449-59.
93. Taylor EB, An D, Kramer HF, Yu H, Fujii NL, Roeckl KS, et al. Discovery of TBC1D1 as an insulin-, AICAR-, and contraction-stimulated signaling nexus in mouse skeletal muscle. J Biol Chem. 2008;283(15):9787-96.
94. Bilan PJ, Schertzer JD. Brought in by force: AMPK, TBC1D1, and contraction-stimulated glucose transport in skeletal muscle. Am J Physiol Endocrinol Metab. 2009;296(5):E965-6.
95. An D, Toyoda T, Taylor EB, Yu H, Fujii N, Hirshman MF, et al. TBC1D1 regulates insulin- and contraction-induced glucose transport in mouse skeletal muscle. Diabetes. 2010;59(6):1358-65.
96. Pehmoller C, Treebak JT, Birk JB, Chen S, Mackintosh C, Hardie DG, et al. Genetic disruption of AMPK signaling abolishes both contraction- and insulin-stimulated TBC1D1 phosphorylation and 14-3-3 binding in mouse skeletal muscle. Am J Physiol Endocrinol Metab. 2009;297(3):E665-75.
97. Peck GR, Chavez JA, Roach WG, Budnik BA, Lane WS, Karlsson HK, et al. Insulin-stimulated phosphorylation of the Rab GTPase-activating protein TBC1D1 regulates GLUT4 translocation. J Biol Chem. 2009;284(44):30016-23.
98. Funai K, Cartee GD. Inhibition of contraction-stimulated AMP-activated protein kinase inhibits contraction-stimulated increases in PAS-TBC1D1 and glucose transport without altering PAS-AS160 in rat skeletal muscle. Diabetes. 2009;58(5):1096-104.
99. Chen WS, Xu PZ, Gottlob K, Chen ML, Sokol K, Shiyanova T, et al. Growth retardation and increased apoptosis in mice with homozygous disruption of the Akt1 gene. Genes Dev. 2001;15(17):2203-8.
100. Cho H, Thorvaldsen JL, Chu Q, Feng F, Birnbaum MJ. Akt1/PKBalpha is required for normal growth but dispensable for maintenance of glucose homeostasis in mice. J Biol Chem. 2001;276(42):38349-52.
101. Tschopp O, Yang ZZ, Brodbeck D, Dummler BA, Hemmings-Mieszczak M, Watanabe T, et al. Essential role of protein kinase B gamma (PKB gamma/Akt3) in postnatal brain development but not in glucose homeostasis. Development. 2005;132(13):2943-54.

102. Peng XD, Xu PZ, Chen ML, Hahn-Windgassen A, Skeen J, Jacobs J, et al. Dwarfism, impaired skin development, skeletal muscle atrophy, delayed bone development, and impeded adipogenesis in mice lacking Akt1 and Akt2. Genes Dev. 2003;17(11):1352-65.
103. Yang ZZ, Tschopp O, Di-Poi N, Bruder E, Baudry A, Dummler B, et al. Dosage-dependent effects of Akt1/protein kinase Balpha (PKBalpha) and Akt3/PKBgamma on thymus, skin, and cardiovascular and nervous system development in mice. Mol Cell Biol. 2005;25(23):10407-18.
104. Dummler B, Tschopp O, Hynx D, Yang ZZ, Dirnhofer S, Hemmings BA. Life with a single isoform of Akt: mice lacking Akt2 and Akt3 are viable but display impaired glucose homeostasis and growth deficiencies. Mol Cell Biol. 2006;26(21):8042-51.
105. Bae SS, Cho H, Mu J, Birnbaum MJ. Isoform-specific regulation of insulin-dependent glucose uptake by Akt/protein kinase B. J Biol Chem. 2003;278(49):49530-6.
106. Gonzalez E, McGraw TE. Insulin-modulated Akt subcellular localization determines Akt isoform-specific signaling. Proc Natl Acad Sci U S A. 2009;106(17):7004-9.
107. Kim YB, Peroni OD, Franke TF, Kahn BB. Divergent regulation of Akt1 and Akt2 isoforms in insulin target tissues of obese Zucker rats. Diabetes. 2000;49(5):847-56.
108. Kawase T, Ohki R, Shibata T, Tsutsumi S, Kamimura N, Inazawa J, et al. PH domain-only protein PHLDA3 is a p53-regulated repressor of Akt. Cell. 2009;136(3):535-50.
109. Calera MR, Martinez C, Liu H, Jack AK, Birnbaum MJ, Pilch PF. Insulin increases the association of Akt-2 with Glut4-containing vesicles. J Biol Chem. 1998;273(13):7201-4.
110. Hill MM, Clark SF, Tucker DF, Birnbaum MJ, James DE, Macaulay SL. A role for protein kinase Bbeta/Akt2 in insulin-stimulated GLUT4 translocation in adipocytes. Mol Cell Biol. 1999;19(11):7771-81.
111. Bouzakri K, Zachrisson A, Al-Khalili L, Zhang BB, Koistinen HA, Krook A, et al. siRNA-based gene silencing reveals specialized roles of IRS-1/Akt2 and IRS-2/Akt1 in glucose and lipid metabolism in human skeletal muscle. Cell Metab. 2006;4(1):89-96.
112. Yoshizaki T, Imamura T, Babendure JL, Lu JC, Sonoda N, Olefsky JM. Myosin 5a is an insulin-stimulated Akt2 (protein kinase Bbeta) substrate modulating GLUT4 vesicle translocation. Mol Cell Biol. 2007;27(14):5172-83.
113. Yamada E, Okada S, Saito T, Ohshima K, Sato M, Tsuchiya T, et al. Akt2 phosphorylates Synip to regulate docking and fusion of GLUT4-containing vesicles. J Cell Biol. 2005;168(6):921-8.
114. Nechamen CA, Thomas RM, Dias JA. APPL1, APPL2, Akt2 and FOXO1a interact with FSHR in a potential signaling complex. Mol Cell Endocrinol. 2007;260-262:93-9.

115. Saito T, Jones CC, Huang S, Czech MP, Pilch PF. The interaction of Akt with APPL1 is required for insulin-stimulated Glut4 translocation. J Biol Chem. 2007;282(44):32280-7.
116. Schenck A, Goto-Silva L, Collinet C, Rhinn M, Giner A, Habermann B, et al. The endosomal protein Appl1 mediates Akt substrate specificity and cell survival in vertebrate development. Cell. 2008;133(3):486-97.
117. Sarbassov DD, Guertin DA, Ali SM, Sabatini DM. Phosphorylation and regulation of Akt/PKB by the rictor-mTOR complex. Science. 2005;307(5712):1098-101.
118. Guertin DA, Stevens DM, Thoreen CC, Burds AA, Kalaany NY, Moffat J, et al. Ablation in mice of the mTORC components raptor, rictor, or mLST8 reveals that mTORC2 is required for signaling to Akt-FOXO and PKCalpha, but not S6K1. Dev Cell. 2006;11(6):859-71.
119. Jacinto E, Facchinetti V, Liu D, Soto N, Wei S, Jung SY, et al. SIN1/MIP1 maintains rictor-mTOR complex integrity and regulates Akt phosphorylation and substrate specificity. Cell. 2006;127(1):125-37.
120. Wan X, Helman LJ. Levels of PTEN protein modulate Akt phosphorylation on serine 473, but not on threonine 308, in IGF-II-overexpressing rhabdomyosarcomas cells. Oncogene. 2003;22(50):8205-11.
121. Gallay N, Dos Santos C, Cuzin L, Bousquet M, Simmonet Gouy V, Chaussade C, et al. The level of AKT phosphorylation on threonine 308 but not on serine 473 is associated with high-risk cytogenetics and predicts poor overall survival in acute myeloid leukaemia. Leukemia. 2009;23(6):1029-38.
122. Ruvinsky I, Sharon N, Lerer T, Cohen H, Stolovich-Rain M, Nir T, et al. Ribosomal protein S6 phosphorylation is a determinant of cell size and glucose homeostasis. Genes Dev. 2005;19(18):2199-211.
123. Ruvinsky I, Meyuhas O. Ribosomal protein S6 phosphorylation: from protein synthesis to cell size. Trends Biochem Sci. 2006;31(6):342-8.
124. Avruch J, Long X, Ortiz-Vega S, Rapley J, Papageorgiou A, Dai N. Amino acid regulation of TOR complex 1. Am J Physiol Endocrinol Metab. 2009;296(4):E592-602.
125. Huang J, Manning BD. The TSC1-TSC2 complex: a molecular switchboard controlling cell growth. Biochem J. 2008;412(2):179-90.
126. Inoki K, Li Y, Xu T, Guan KL. Rheb GTPase is a direct target of TSC2 GAP activity and regulates mTOR signaling. Genes Dev. 2003;17(15):1829-34.
127. Long X, Lin Y, Ortiz-Vega S, Yonezawa K, Avruch J. Rheb binds and regulates the mTOR kinase. Curr Biol. 2005;15(8):702-13.
128. Potter CJ, Pedraza LG, Xu T. Akt regulates growth by directly phosphorylating Tsc2. Nat Cell Biol. 2002;4(9):658-65.
129. Welsh GI, Miller CM, Loughlin AJ, Price NT, Proud CG. Regulation of eukaryotic initiation factor eIF2B: glycogen synthase kinase-3 phosphorylates a conserved serine which undergoes dephosphorylation in response to insulin. FEBS Lett. 1998;421(2):125-30.

130. Welsh GI, Proud CG. Regulation of protein synthesis in Swiss 3T3 fibroblasts. Rapid activation of the guanine-nucleotide-exchange factor by insulin and growth factors. Biochem J. 1992;284 (Pt 1):19-23.
131. Proud CG. eIF2 and the control of cell physiology. Semin Cell Dev Biol. 2005;16(1):3-12.
132. Rogers GW, Jr., Richter NJ, Lima WF, Merrick WC. Modulation of the helicase activity of eIF4A by eIF4B, eIF4H, and eIF4F. J Biol Chem. 2001;276(33):30914-22.
133. Raught B, Peiretti F, Gingras AC, Livingstone M, Shahbazian D, Mayeur GL, et al. Phosphorylation of eucaryotic translation initiation factor 4B Ser422 is modulated by S6 kinases. EMBO J. 2004;23(8):1761-9.
134. Shahbazian D, Roux PP, Mieulet V, Cohen MS, Raught B, Taunton J, et al. The mTOR/PI3K and MAPK pathways converge on eIF4B to control its phosphorylation and activity. EMBO J. 2006;25(12):2781-91.
135. Holz MK, Ballif BA, Gygi SP, Blenis J. mTOR and S6K1 mediate assembly of the translation preinitiation complex through dynamic protein interchange and ordered phosphorylation events. Cell. 2005;123(4):569-80.
136. Venema RC, Peters HI, Traugh JA. Phosphorylation of valyl-tRNA synthetase and elongation factor 1 in response to phorbol esters is associated with stimulation of both activities. J Biol Chem. 1991;266(18):11993-8.
137. Venema RC, Peters HI, Traugh JA. Phosphorylation of elongation factor 1 (EF-1) and valyl-tRNA synthetase by protein kinase C and stimulation of EF-1 activity. J Biol Chem. 1991;266(19):12574-80.
138. Peters HI, Chang YW, Traugh JA. Phosphorylation of elongation factor 1 (EF-1) by protein kinase C stimulates GDP/GTP-exchange activity. Eur J Biochem. 1995;234(2):550-6.
139. Chang YW, Traugh JA. Insulin stimulation of phosphorylation of elongation factor 1 (eEF-1) enhances elongation activity. Eur J Biochem. 1998;251(1-2):201-7.
140. Carlberg U, Nilsson A, Nygard O. Functional properties of phosphorylated elongation factor 2. Eur J Biochem. 1990;191(3):639-45.
141. Redpath NT, Foulstone EJ, Proud CG. Regulation of translation elongation factor-2 by insulin via a rapamycin-sensitive signalling pathway. EMBO J. 1996;15(9):2291-7.
142. Wang X, Li W, Williams M, Terada N, Alessi DR, Proud CG. Regulation of elongation factor 2 kinase by p90(RSK1) and p70 S6 kinase. EMBO J. 2001;20(16):4370-9.
143. Knebel A, Morrice N, Cohen P. A novel method to identify protein kinase substrates: eEF2 kinase is phosphorylated and inhibited by SAPK4/p38delta. EMBO J. 2001;20(16):4360-9.
144. Browne GJ, Proud CG. A novel mTOR-regulated phosphorylation site in elongation factor 2 kinase modulates the activity of the kinase and its binding to calmodulin. Mol Cell Biol. 2004;24(7):2986-97.

145. Gonzalez-Gaitan M. Signal dispersal and transduction through the endocytic pathway. Nat Rev Mol Cell Biol. 2003;4(3):213-24.
146. Hayakawa A, Leonard D, Murphy S, Hayes S, Soto M, Fogarty K, et al. The WD40 and FYVE domain containing protein 2 defines a class of early endosomes necessary for endocytosis. Proc Natl Acad Sci U S A. 2006;103(32):11928-33.
147. Unger RH. Minireview: weapons of lean body mass destruction: the role of ectopic lipids in the metabolic syndrome. Endocrinology. 2003;144(12):5159-65.
148. Rasouli N, Molavi B, Elbein SC, Kern PA. Ectopic fat accumulation and metabolic syndrome. Diabetes Obes Metab. 2007;9(1):1-10.
149. Ravussin E, Smith SR. Increased fat intake, impaired fat oxidation, and failure of fat cell proliferation result in ectopic fat storage, insulin resistance, and type 2 diabetes mellitus. Ann N Y Acad Sci. 2002;967:363-78.
150. Kim JY, van de Wall E, Laplante M, Azzara A, Trujillo ME, Hofmann SM, et al. Obesity-associated improvements in metabolic profile through expansion of adipose tissue. J Clin Invest. 2007;117(9):2621-37.
151. Rajala MW, Obici S, Scherer PE, Rossetti L. Adipose-derived resistin and gut-derived resistin-like molecule-beta selectively impair insulin action on glucose production. J Clin Invest. 2003;111(2):225-30.
152. Trujillo ME, Scherer PE. Adiponectin--journey from an adipocyte secretory protein to biomarker of the metabolic syndrome. J Intern Med. 2005;257(2):167-75.
153. Picard F, Guarente L. Molecular links between aging and adipose tissue. Int J Obes (Lond). 2005;29 Suppl 1:S36-9.
154. Linford NJ, Beyer RP, Gollahon K, Krajcik RA, Malloy VL, Demas V, et al. Transcriptional response to aging and caloric restriction in heart and adipose tissue. Aging Cell. 2007;6(5):673-88.
155. Hresko RC, Heimberg H, Chi MM, Mueckler M. Glucosamine-induced insulin resistance in 3T3-L1 adipocytes is caused by depletion of intracellular ATP. J Biol Chem. 1998;273(32):20658-68.
156. Beale EG, Antoine B, Forest C. Glyceroneogenesis in adipocytes: another textbook case. Trends Biochem Sci. 2003;28(8):402-3.
157. Falkenberg M, Larsson NG, Gustafsson CM. DNA replication and transcription in mammalian mitochondria. Annu Rev Biochem. 2007;76:679-99.
158. Asin-Cayuela J, Gustafsson CM. Mitochondrial transcription and its regulation in mammalian cells. Trends Biochem Sci. 2007;32(3):111-7.
159. Scarpulla RC. Nuclear control of respiratory gene expression in mammalian cells. J Cell Biochem. 2006;97(4):673-83.
160. Larsson NG, Wang J, Wilhelmsson H, Oldfors A, Rustin P, Lewandoski M, et al. Mitochondrial transcription factor A is necessary for mtDNA maintenance and embryogenesis in mice. Nat Genet. 1998;18(3):231-6.
161. Kanehisa M, Araki M, Goto S, Hattori M, Hirakawa M, Itoh M, et al. KEGG for linking genomes to life and the environment. Nucleic Acids Res. 2008;36(Database issue):D480-4.

162. Axelrod D. Total internal reflection fluorescence microscopy in cell biology. Traffic. 2001;2(11):764-74.
163. Bashan N, Burdett E, Guma A, Sargeant R, Tumiati L, Liu Z, et al. Mechanisms of adaptation of glucose transporters to changes in the oxidative chain of muscle and fat cells. Am J Physiol. 1993;264(2 Pt 1):C430-40.
164. Nishikawa T, Araki E. Impact of mitochondrial ROS production in the pathogenesis of diabetes mellitus and its complications. Antioxid Redox Signal. 2007;9(3):343-53.
165. Imoto K, Kukidome D, Nishikawa T, Matsuhisa T, Sonoda K, Fujisawa K, et al. Impact of mitochondrial reactive oxygen species and apoptosis signal-regulating kinase 1 on insulin signaling. Diabetes. 2006;55(5):1197-204.
166. Gridley S, Lane WS, Garner CW, Lienhard GE. Novel insulin-elicited phosphoproteins in adipocytes. Cell Signal. 2005;17(1):59-66.
167. Chavez JA, Gridley S, Sano H, Lane WS, Lienhard GE. The 47kDa Akt substrate associates with phosphodiesterase 3B and regulates its level in adipocytes. Biochem Biophys Res Commun. 2006;342(4):1218-22.
168. Pospisilik JA, Knauf C, Joza N, Benit P, Orthofer M, Cani PD, et al. Targeted deletion of AIF decreases mitochondrial oxidative phosphorylation and protects from obesity and diabetes. Cell. 2007;131(3):476-91.
169. Wredenberg A, Freyer C, Sandstrom ME, Katz A, Wibom R, Westerblad H, et al. Respiratory chain dysfunction in skeletal muscle does not cause insulin resistance. Biochem Biophys Res Commun. 2006;350(1):202-7.
170. Kwon J, Lee SR, Yang KS, Ahn Y, Kim YJ, Stadtman ER, et al. Reversible oxidation and inactivation of the tumor suppressor PTEN in cells stimulated with peptide growth factors. Proc Natl Acad Sci U S A. 2004;101(47):16419-24.
171. Martindale JL, Holbrook NJ. Cellular response to oxidative stress: signaling for suicide and survival. J Cell Physiol. 2002;192(1):1-15.
172. Brunelle JK, Bell EL, Quesada NM, Vercauteren K, Tiranti V, Zeviani M, et al. Oxygen sensing requires mitochondrial ROS but not oxidative phosphorylation. Cell Metab. 2005;1(6):409-14.
173. Guzy RD, Hoyos B, Robin E, Chen H, Liu L, Mansfield KD, et al. Mitochondrial complex III is required for hypoxia-induced ROS production and cellular oxygen sensing. Cell Metab. 2005;1(6):401-8.
174. Mansfield KD, Guzy RD, Pan Y, Young RM, Cash TP, Schumacker PT, et al. Mitochondrial dysfunction resulting from loss of cytochrome c impairs cellular oxygen sensing and hypoxic HIF-alpha activation. Cell Metab. 2005;1(6):393-9.
175. Karlsson HK, Zierath JR, Kane S, Krook A, Lienhard GE, Wallberg-Henriksson H. Insulin-stimulated phosphorylation of the Akt substrate AS160 is impaired in skeletal muscle of type 2 diabetic subjects. Diabetes. 2005;54(6):1692-7.
176. Zeigerer A, McBrayer MK, McGraw TE. Insulin stimulation of GLUT4 exocytosis, but not its inhibition of endocytosis, is dependent on RabGAP AS160. Mol Biol Cell. 2004;15(10):4406-15.

177. Lakadamyali M, Rust MJ, Zhuang X. Ligands for clathrin-mediated endocytosis are differentially sorted into distinct populations of early endosomes. Cell. 2006;124(5):997-1009.
178. Leonard D, Hayakawa A, Lawe D, Lambright D, Bellve KD, Standley C, et al. Sorting of EGF and transferrin at the plasma membrane and by cargo-specific signaling to EEA1-enriched endosomes. J Cell Sci. 2008;121(Pt 20):3445-58.
179. Corvera S, D'Arrigo A, Stenmark H. Phosphoinositides in membrane traffic. Curr Opin Cell Biol. 1999;11(4):460-5.
180. Driscoll PC. Solving the FYVE domain--PtdIns(3)P puzzle. Nat Struct Biol. 2001;8(4):287-90.
181. Leevers SJ, Vanhaesebroeck B, Waterfield MD. Signalling through phosphoinositide 3-kinases: the lipids take centre stage. Curr Opin Cell Biol. 1999;11(2):219-25.
182. Lindmo K, Stenmark H. Regulation of membrane traffic by phosphoinositide 3-kinases. J Cell Sci. 2006;119(Pt 4):605-14.
183. Zoncu R, Perera RM, Balkin DM, Pirruccello M, Toomre D, De Camilli P. A phosphoinositide switch controls the maturation and signaling properties of APPL endosomes. Cell. 2009;136(6):1110-21.
184. Kittler JT, Moss SJ. Neurotransmitter receptor trafficking and the regulation of synaptic strength. Traffic. 2001;2(7):437-48.
185. Mosesson Y, Mills GB, Yarden Y. Derailed endocytosis: an emerging feature of cancer. Nat Rev Cancer. 2008;8(11):835-50.
186. Raiborg C, Bache KG, Mehlum A, Stenmark H. Function of Hrs in endocytic trafficking and signalling. Biochem Soc Trans. 2001;29(Pt 4):472-5.
187. von Zastrow M. Role of endocytosis in signalling and regulation of G-protein-coupled receptors. Biochem Soc Trans. 2001;29(Pt 4):500-4.
188. Wiley HS, Burke PM. Regulation of receptor tyrosine kinase signaling by endocytic trafficking. Traffic. 2001;2(1):12-8.
189. Di Guglielmo GM, Le Roy C, Goodfellow AF, Wrana JL. Distinct endocytic pathways regulate TGF-beta receptor signalling and turnover. Nat Cell Biol. 2003;5(5):410-21.
190. Hayes S, Chawla A, Corvera S. TGF beta receptor internalization into EEA1-enriched early endosomes: role in signaling to Smad2. J Cell Biol. 2002;158(7):1239-49.
191. Miaczynska M, Christoforidis S, Giner A, Shevchenko A, Uttenweiler-Joseph S, Habermann B, et al. APPL proteins link Rab5 to nuclear signal transduction via an endosomal compartment. Cell. 2004;116(3):445-56.
192. Lin DC, Quevedo C, Brewer NE, Bell A, Testa JR, Grimes ML, et al. APPL1 associates with TrkA and GIPC1 and is required for nerve growth factor-mediated signal transduction. Mol Cell Biol. 2006;26(23):8928-41.
193. Mao X, Kikani CK, Riojas RA, Langlais P, Wang L, Ramos FJ, et al. APPL1 binds to adiponectin receptors and mediates adiponectin signalling and function. Nat Cell Biol. 2006;8(5):516-23.

194. Fritzius T, Burkard G, Haas E, Heinrich J, Schweneker M, Bosse M, et al. A WD-FYVE protein binds to the kinases Akt and PKCzeta/lambda. Biochem J. 2006;399(1):9-20.
195. Fritzius T, Frey AD, Schweneker M, Mayer D, Moelling K. WD-repeat-propeller-FYVE protein, ProF, binds VAMP2 and protein kinase Czeta. FEBS J. 2007;274(6):1552-66.
196. Franke TF. PI3K/Akt: getting it right matters. Oncogene. 2008;27(50):6473-88.
197. Hanada M, Feng J, Hemmings BA. Structure, regulation and function of PKB/AKT--a major therapeutic target. Biochim Biophys Acta. 2004;1697(1-2):3-16.
198. Easton RM, Cho H, Roovers K, Shineman DW, Mizrahi M, Forman MS, et al. Role for Akt3/protein kinase Bgamma in attainment of normal brain size. Mol Cell Biol. 2005;25(5):1869-78.
199. Jiang ZY, Zhou QL, Coleman KA, Chouinard M, Boese Q, Czech MP. Insulin signaling through Akt/protein kinase B analyzed by small interfering RNA-mediated gene silencing. Proc Natl Acad Sci U S A. 2003;100(13):7569-74.
200. Bellve KD, Leonard D, Standley C, Lifshitz LM, Tuft RA, Hayakawa A, et al. Plasma membrane domains specialized for clathrin-mediated endocytosis in primary cells. J Biol Chem. 2006;281(23):16139-46.
201. Evans DR, Swirsding KA, Taillon BE, Simons JF. "One plate/three-reporter" assay format for the detection and validation of yeast two-hybrid interactions. Biotechniques. 2004;37(5):840-3.
202. Fritzius T, Moelling K. Akt- and Foxo1-interacting WD-repeat-FYVE protein promotes adipogenesis. EMBO J. 2008;27(9):1399-410.
203. Brognard J, Sierecki E, Gao T, Newton AC. PHLPP and a second isoform, PHLPP2, differentially attenuate the amplitude of Akt signaling by regulating distinct Akt isoforms. Mol Cell. 2007;25(6):917-31.
204. Yan D, Guo L, Wang Y. Requirement of dendritic Akt degradation by the ubiquitin-proteasome system for neuronal polarity. J Cell Biol. 2006;174(3):415-24.
205. Medina EA, Afsari RR, Ravid T, Castillo SS, Erickson KL, Goldkorn T. Tumor necrosis factor-{alpha} decreases Akt protein levels in 3T3-L1 adipocytes via the caspase-dependent ubiquitination of Akt. Endocrinology. 2005;146(6):2726-35.
206. Xiang T, Ohashi A, Huang Y, Pandita TK, Ludwig T, Powell SN, et al. Negative Regulation of AKT Activation by BRCA1. Cancer Res. 2008;68(24):10040-4.
207. Janssen I, Heymsfield SB, Ross R. Low relative skeletal muscle mass (sarcopenia) in older persons is associated with functional impairment and physical disability. J Am Geriatr Soc. 2002;50(5):889-96.
208. Choi CS, Befroy DE, Codella R, Kim S, Reznick RM, Hwang YJ, et al. Paradoxical effects of increased expression of PGC-1alpha on muscle mitochondrial function and insulin-stimulated muscle glucose metabolism. Proc Natl Acad Sci U S A. 2008;105(50):19926-31.

209. Simpson JC, Griffiths G, Wessling-Resnick M, Fransen JA, Bennett H, Jones AT. A role for the small GTPase Rab21 in the early endocytic pathway. J Cell Sci. 2004;117(Pt 26):6297-311.
210. Somsel Rodman J, Wandinger-Ness A. Rab GTPases coordinate endocytosis. J Cell Sci. 2000;113 Pt 2:183-92.
211. Ekstrand MI, Falkenberg M, Rantanen A, Park CB, Gaspari M, Hultenby K, et al. Mitochondrial transcription factor A regulates mtDNA copy number in mammals. Hum Mol Genet. 2004;13(9):935-44.
212. Maniura-Weber K, Goffart S, Garstka HL, Montoya J, Wiesner RJ. Transient overexpression of mitochondrial transcription factor A (TFAM) is sufficient to stimulate mitochondrial DNA transcription, but not sufficient to increase mtDNA copy number in cultured cells. Nucleic Acids Res. 2004;32(20):6015-27.
213. Ylikallio E, Tyynismaa H, Tsutsui H, Ide T, Suomalainen A. High mitochondrial DNA copy number has detrimental effects in mice. Hum Mol Genet. 2010;19(13):2695-705.
214. Ikeuchi M, Matsusaka H, Kang D, Matsushima S, Ide T, Kubota T, et al. Overexpression of mitochondrial transcription factor a ameliorates mitochondrial deficiencies and cardiac failure after myocardial infarction. Circulation. 2005;112(5):683-90.
215. Hayashi Y, Yoshida M, Yamato M, Ide T, Wu Z, Ochi-Shindou M, et al. Reverse of age-dependent memory impairment and mitochondrial DNA damage in microglia by an overexpression of human mitochondrial transcription factor a in mice. J Neurosci. 2008;28(34):8624-34.
216. Suarez J, Hu Y, Makino A, Fricovsky E, Wang H, Dillmann WH. Alterations in mitochondrial function and cytosolic calcium induced by hyperglycemia are restored by mitochondrial transcription factor A in cardiomyocytes. Am J Physiol Cell Physiol. 2008;295(6):C1561-8.
217. Xu S, Zhong M, Zhang L, Wang Y, Zhou Z, Hao Y, et al. Overexpression of Tfam protects mitochondria against beta-amyloid-induced oxidative damage in SH-SY5Y cells. FEBS J. 2009;276(14):3800-9.
218. Hokari M, Kuroda S, Kinugawa S, Ide T, Tsutsui H, Iwasaki Y. Overexpression of mitochondrial transcription factor A (TFAM) ameliorates delayed neuronal death due to transient forebrain ischemia in mice. Neuropathology. 2010;30(4):401-7.
219. Pastukh V, Shokolenko I, Wang B, Wilson G, Alexeyev M. Human mitochondrial transcription factor A possesses multiple subcellular targeting signals. FEBS J. 2007;274(24):6488-99.
220. Dong X, Ghoshal K, Majumder S, Yadav SP, Jacob ST. Mitochondrial transcription factor A and its downstream targets are up-regulated in a rat hepatoma. J Biol Chem. 2002;277(45):43309-18.
221. Pietrowska M, Kolodziejczyk I, Widlak P. Mitochondrial transcription factor A is the major protein in rodent hepatocytes that recognizes DNA lesions induced by N-acetoxy-acetylaminofluorene. Acta Biochim Pol. 2006;53(4):777-82.

222. Kaufman BA, Durisic N, Mativetsky JM, Costantino S, Hancock MA, Grutter P, et al. The mitochondrial transcription factor TFAM coordinates the assembly of multiple DNA molecules into nucleoid-like structures. Mol Biol Cell. 2007;18(9):3225-36.
223. Frost SC, Lane MD. Evidence for the involvement of vicinal sulfhydryl groups in insulin-activated hexose transport by 3T3-L1 adipocytes. J Biol Chem. 1985;260(5):2646-52.
224. Ross SR, Graves RA, Greenstein A, Platt KA, Shyu HL, Mellovitz B, et al. A fat-specific enhancer is the primary determinant of gene expression for adipocyte P2 in vivo. Proc Natl Acad Sci U S A. 1990;87(24):9590-4.
225. Makowski L, Boord JB, Maeda K, Babaev VR, Uysal KT, Morgan MA, et al. Lack of macrophage fatty-acid-binding protein aP2 protects mice deficient in apolipoprotein E against atherosclerosis. Nat Med. 2001;7(6):699-705.
226. Gonzalez E, McGraw TE. The Akt kinases: isoform specificity in metabolism and cancer. Cell Cycle. 2009;8(16):2502-8.
227. Fayard E, Xue G, Parcellier A, Bozulic L, Hemmings BA. Protein Kinase B (PKB/Akt), a Key Mediator of the PI3K Signaling Pathway. Curr Top Microbiol Immunol. 2010.
228. Cross DA, Alessi DR, Cohen P, Andjelkovich M, Hemmings BA. Inhibition of glycogen synthase kinase-3 by insulin mediated by protein kinase B. Nature. 1995;378(6559):785-9.
229. Alessi DR, Caudwell FB, Andjelkovic M, Hemmings BA, Cohen P. Molecular basis for the substrate specificity of protein kinase B; comparison with MAPKAP kinase-1 and p70 S6 kinase. FEBS Lett. 1996;399(3):333-8.
230. Zhang H, Zha X, Tan Y, Hornbeck PV, Mastrangelo AJ, Alessi DR, et al. Phosphoprotein analysis using antibodies broadly reactive against phosphorylated motifs. J Biol Chem. 2002;277(42):39379-87.
231. Pecorari L, Marin O, Silvestri C, Candini O, Rossi E, Guerzoni C, et al. Elongation Factor 1 alpha interacts with phospho-Akt in breast cancer cells and regulates their proliferation, survival and motility. Mol Cancer. 2009;8:58.
232. Kielbassa K, Muller HJ, Meyer HE, Marks F, Gschwendt M. Protein kinase C delta-specific phosphorylation of the elongation factor eEF-alpha and an eEF-1 alpha peptide at threonine 431. J Biol Chem. 1995;270(11):6156-62.